

STELLINGEN

behorende bij het proefschrift

PILOT'S PERCEPTION AND CONTROL OF AIRCRAFT MOTIONS

1. De fixatietijden bij het bemonsteren van instrumenten ten behoeve van het uitvoeren van een complexe stuurtaak, zoals de nadering op instrumenten voor de landing, worden niet primair bepaald door de minimaal benodigde observatietijd voor het waarnemen van de betrokken variabelen, maar veel meer door de beperkte capaciteit van de menselijke informatieverwerking.

Dit proefschrift, hoofdstuk 5.

2. Hoewel uit onderzoek blijkt dat het evenwichtsorgaan een belangrijke bijdrage levert aan het waarnemen van de vliegtuigbeweging en aan de vliegtuigbesturing, is het niet raadzaam de methode, waarbij de leerlingvlieger geleerd wordt uitsluitend af te gaan op zijn visuele waarneming van de vliegtuigbeweging met behulp van de buitenwereld en de vlieginstrumenten, te veranderen.

Dit proefschrift, hoofdstukken 6, 7 en 8.

3. Daar de gezagvoerder de eindverantwoordelijkheid voor de veiligheid van de vluchtuitvoering draagt, is een verdere reductie van de omvang van de cockpitbemanning van verkeersvliegtuigen (gezagvoerder en eerste officier) af te raden.
4. Gezien de invloed van de statische en dynamische eigenschappen van het stuurorgaan op het menselijk regelgedrag, dienen deze, naast de dynamische eigenschappen van het te besturen systeem en het informatie presenterend systeem, eveneens bij de rapportage over onderzoek naar menselijk regelgedrag te worden vermeld.
5. Het ontbreken van voorschriften voor de bewegingsstimulatie van de vlieger tijdens vliegtuigsimulatie heeft er toe geleid dat de laatste 15 jaar geen wezenlijke onderzoek ter verbetering van de bewegingssimulatie is uitgevoerd.
6. Het realisme van vliegtuigsimulatie kan aanzienlijk worden verbeterd indien het instructor station buiten de kabine van de vluchtnabootser wordt geplaatst.
7. Het rapporteren door de cockpitbemanning over eigen gemaakte fouten in de vorm van een incident report, zoals in de Verenigde Staten wordt gepropageerd met het NASA Aviation Safety Reporting System, is voor de luchtvaart van wezenlijk belang voor de verdere verbetering van de vliegveiligheid, en verdient in de Europese Unie te worden nagevolgd.

8. Voor het welslagen van multidisciplinair onderzoek is het noodzakelijk dat de deelnemers uit de diverse disciplines gemotiveerd zijn om naar elkaar te luisteren. Tevens dienen zij overtuigd te zijn van de meerwaarde van het onderhavige multidisciplinaire onderzoek.
9. Haast is nooit een excuus om maximaal toegestane snelheden te overschrijden.
10. Voor de oplossing van het fileprobleem is, naast een aantal structurele maatregelen, een verkeersgeleidingssysteem noodzakelijk waarvan de naleving door de automobilist zonodig moet worden afgedwongen.

Ruud Hosman

Delft, 27 september 1996

PILOT'S PERCEPTION AND CONTROL OF AIRCRAFT MOTIONS

Ruud Hosman

PILOT'S PERCEPTION AND CONTROL OF AIRCRAFT
MOTIONS

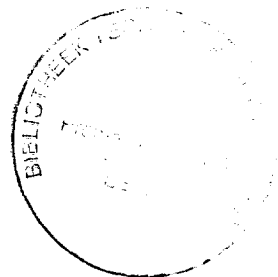
PROEFSCHRIFT

ter verkrijging van de graad van doctor
aan de Technische Universiteit Delft,
op gezag van de Rector Magnificus Prof. ir K.F. Wakker,
in het openbaar te verdedigen ten overstaan van een commissie,
door het College van Dekanen aangewezen,
op maandag 18 november 1996 te 16.00 uur

door

Rudolphus Johannes Anthonius Willibrordus HOSMAN
vliegtuigbouwkundig ingenieur

geboren te Utrecht



Dit proefschrift is goedgekeurd door de promotoren:

Prof. dr ir H.G. Stassen

Prof. ir F.J. Abbink

Samenstelling promotiecommissie:

Rector Magnificus, voorzitter

| | |
|---------------------------|--|
| Prof. dr ir H.G. Stassen, | Technische Universiteit Delft, promotor |
| Prof. ir F.J. Abbink, | Technische Universiteit Delft, promotor |
| Prof. T. B. Sheridan, | Massachusetts Institute of Technology |
| Prof. L.R. Young, | Massachusetts Institute of Technology |
| Prof. dr G.J.F. Smets, | Open Universiteit, Heerlen |
| Prof. dr G. Mulder, | Rijks Universiteit Groningen |
| Dr W. Bles, | T.N.O. Technische Menskunde, Soesterberg |

Published and distributed by:

Delftse Universitaire Pers

Mekelweg 4

2628 CD DELFT

The Netherlands

telephone: +31-15-2783254

Fax.: +31-15-2781661

CIP-GEGEVENS KONINKLIJKE BIBLIOTHEEK, DEN HAAG

Hosman, R.J.A.W.

Pilot's Perception and Control of Aircraft Motions. / R.J.A.W. Hosman

Delft: Delftse Universitaire Pers. -III.

Thesis Delft University of Technology. -With ref. -With Summary in Dutch.

ISBN: 90-407-1384-7

NUIG: 841

Keywords: Motion Perception, Simulation, Control Behavior

Copyright © 1996 by R.J.A.W. Hosman

All rights reserved. No part of the material protected by this copyright notice may be reproduced or utilized in any form or by any means, electronic or mechanical, including photocopying, recording or by any information storage and retrieval system, without permission from the publisher: Delftse Universitaire Pers, Mekelweg 4, 2628 CD DELFT, The Netherlands.

To my wife Pia

CONTENTS

| | page |
|---|------|
| CONTENTS | i |
| NOTATIONS | iii |
| 1. INTRODUCTION | 1 |
| 2. THE INFLUENCE OF PERCEIVED AIRCRAFT MOTION ON PILOT'S CONTROL BEHAVIOR | |
| 2.1 Introduction | 5 |
| 2.2 Tracking-task setup | 5 |
| 2.3 Literature review | 10 |
| 2.4 Summary and discussion. | 22 |
| 3. INFORMATION PROCESSING BY THE HUMAN OPERATOR | |
| 3.1 Introduction | 25 |
| 3.2 Information-processing | 25 |
| 3.3 Additive Factor Paradigm and dynamic systems | 28 |
| 3.4 Summary and conclusions | 32 |
| 4. THE STATIC AND DYNAMIC CHARACTERISTICS OF THE VISUAL AND VESTIBULAR SYSTEM | |
| 4.1 Introduction | 35 |
| 4.2 The visual system | 36 |
| 4.2.1 Introduction | 36 |
| 4.2.2 Motion sensors and the thresholds for motion perception. | 36 |
| 4.3 The vestibular system | 39 |
| 4.3.1 General description | 39 |
| 4.3.2 Dynamic models of the semi-circular canals and the otolith. | 43 |
| 5. VISUAL PERCEPTION OF AIRCRAFT ROLL ATTITUDE AND ROLL RATE | |
| 5.1 Introduction | 49 |
| 5.2 Experimental Test Procedure | 50 |
| 5.3 Experiments | 53 |
| 5.3.1 Experiment 1: The perception of roll attitude | 53 |
| 5.3.2 Experiment 2: The perception of roll rate | 54 |
| 5.3.3 Subjects and test procedure | 54 |

| | page |
|--|------|
| 5.4 Results | 55 |
| 5.4.1 Experiment 1, Roll attitude perception | 55 |
| 5.4.2 Experiment 2, Roll rate perception | 57 |
| 5.5 Discussion and conclusions | 61 |
| 6. PERCEPTION OF COCKPIT MOTION WITH THE VISUAL AND THE VESTIBULAR SYSTEM | |
| 6.1 Introduction | 65 |
| 6.2 Visual and vestibular perception of the step response stimulus. | 67 |
| 6.3 Experimental facility | 71 |
| 6.4 Experiments | 73 |
| 6.5 Subjects and training | 75 |
| 6.6 Results | 76 |
| 6.7 Discussion and conclusions | 84 |
| 7. TRACKING EXPERIMENT | |
| 7.1 Introduction | 87 |
| 7.2 Instrumentation and data reduction. | 88 |
| 7.2.2 Data reduction | 91 |
| 7.3 Subjects and experimental setup | 93 |
| 7.4 Results | 94 |
| 7.4.1 Performance | 94 |
| 7.4.2 Control behavior | 98 |
| 7.5 Influence of the task and the display configuration on pilot model parameters. | 100 |
| 7.6 Discussion and conclusions | 107 |
| 8. EVALUATION, DISCUSSION AND CONCLUSIONS | |
| 8.1 Introduction | 115 |
| 8.2 Evaluation of the experimental results | 116 |
| 8.3 The evaluation of the descriptive model | 121 |
| 8.4 Discussion and conclusions | 129 |
| 9. REFERENCES | 133 |
| APPENDIX I, Instrumentation | 139 |
| APPENDIX II, Overview of experimental results | 145 |
| SUMMARY | 155 |
| SAMENVATTING | 157 |
| ACKNOWLEDGEMENTS | 159 |
| CURRICULUM VITAE | 160 |

NOTATIONS

| | |
|----------------------------|---|
| A | system matrix |
| A_y | specific force along the Y axis |
| B | input matrix |
| C | display matrix |
| d | size of receptive field |
| e | error signal |
| e_{n_1} | stimulus magnitude |
| e_{n_2} | error value |
| e_φ | roll angle error |
| F_a | stick force for roll control |
| $H_{comp}(\omega)$ | frequency response function of the motion system compensation |
| $H_c(\omega)$ | frequency response function of the controlled system |
| $H_{e_\varphi, i}(\omega)$ | frequency response function relating roll angle error e_φ with forcing function i |
| $H_i(\omega)$ | frequency response function of the information processing |
| $H_m(\omega)$ | frequency response function of the simulator motion system |
| $H_p(\omega)$ | frequency response function of the human operator |
| $H_{oto}(\omega)$ | frequency response function of the otolith |
| $H_{scc}(\omega)$ | frequency response function of the semi-circular canals |
| $H_{vest}(\omega)$ | frequency response function of the vestibular system |
| $H_{\varphi, w}(\omega)$ | frequency response function relating roll angle φ with disturbance function w |
| i | forcing function |
| K_p | human operator gain |
| ΔO | response magnitude |

| | |
|------------------|--|
| R | sensory output |
| RT | reaction time |
| S | span bilocal detector |
| S_c | $= \sigma_e^2 / \sigma_i^2$, Score parameter |
| s_a | stick displacement for roll control |
| T_L | lead time constant of the simplified precision model |
| T_l | lag time constant of the simplified precision model |
| Δt | time advance |
| Δt_{exp} | exposure time |
| u | human operator control signal |
| V | stimulus velocity |
| V_c | critical stimulus velocity |
| w | disturbance function |
| x | system state |
| y | controlled system output signal |
| α | head input rotation |
| Δ | cupula spring stiffness |
| ϕ | roll angle |
| $\phi(\omega)$ | phase angle |
| ϕ_m | phase margin |
| $\Delta\phi$ | roll angle error |
| v_y | observation noise |
| v_m | motor noise |
| π | viscous damping of the endolymph |
| θ | moment of inertia of the endolymph |
| σ | standard deviation |
| τ | time delay |
| τ_u | adaptation time constant |
| τ_l | motion detector time delay, torsion pendulum time constant |
| τ_2 | neural transport delay, torsion pendulum time constant |
| τ_e | equivalent time delay |
| τ_i | information processing time delay |
| τ_L | neural time lead constant |

| | |
|------------|--|
| τ_N | neuromuscular time lag constant |
| ω_c | crossover frequency |
| ω_d | divergence frequency of an inverted pendulum |
| ξ | angular displacement of the endolymph |
| ζ | cupula deflection |

Subscripts

| | |
|------|--|
| att | attitude perception |
| C | central display |
| CM | central display and motion |
| CP | central and peripheral displays |
| CPM | central and peripheral displays and motion |
| CPR | central and right peripheral displays |
| CPS | central and peripheral displays in the simulator |
| Dist | disturbance task |
| Foll | target following task |
| PM | peripheral displays and motion |
| M | motion |
| rate | rate perception |
| P | peripheral displays |
| SCC | semi-circular canals |
| oto | otoliths |

1. INTRODUCTION

As long as pilots execute flight control, they need to be informed about the aircraft motion state. Whether they control the aircraft manually or automatically, they perceive the aircraft motions by stimulation of their senses. In aircraft control, this stimulation originates primarily from the environment, and the actual aircraft motions. A pilot's visual system is stimulated by the outside visual scene and the flight instruments, whereas his vestibular and proprioceptive system are stimulated by the aircraft specific forces and angular accelerations. In the day-to-day all-weather airline operation with limited accelerations, the pilot primarily depends on his flight instruments.

In civil transport aviation an important aspect of pilot training is instrument-flight training, which is nowadays performed in full-mission flight simulators. These simulators provide the pilot with visual, vestibular, and proprioceptive stimuli.

Due to economical and environmental pressure in civil aviation, the aim for the future is full simulation pilot training. This aim has already been reached for pilot type-conversion and type-recurrent training. For abinitio pilot training, on the contrary, the refinement of simulation technology has a long way to go. Extension of the application of flight simulation, however, requires a much broader understanding of a pilot's perception and control behavior in manual aircraft control.

Control performance and behavior of pilots in manual aircraft control have been the subject of research for a long time. After the first explorations during World War II, research on human control behavior evolved to the domain of Man-Machine Systems during the fifties and sixties. The need to solve the control problems of advanced fighter and transport jet aircraft, combined with the availability of linear control theory, led to the modeling of human operator behavior. A landmark report of McRuer et al. (1965) set forth the basic principles of human-operator adaptation to the control task. Considering his own experimental results and those from others, McRuer systematically laid down the rules for human operator dynamic behavior in control tasks. Although his research was initially limited to single-axis control tasks, the rule for human operator adaptation to the controlled system dynamics, as laid down in the crossover-model, turned out to have a much broader application. McRuer's Simplified-Precision-Model, used to describe the pilot's control behavior in the frequency domain together with the crossover-model, provides the tools to determine changes in control behavior due to changes in task variables and to analyze the consequences in closed-loop control.

In real aircraft control, however, the pilot's control task is not a single axis tracking task but a multi-axes multi-loop control task. Furthermore, the dynamic characteristics of the aircraft are of a higher order. Both the symmetric and asymmetric equations of motion are fourth order simultaneous differential equations. To make the aircraft control task performable for the

pilot, the task is configured as a nested multi-loop task from which the inner loop is an attitude-control and stabilization loop. The pilot's control task is either to follow flight path signals which constitute a target following task or to compensate for turbulence, disturbing the aircraft in the so-called disturbance task, or both. Finally, in addition to the presentation of the tracking error on the primary flight display, the pilot perceives the aircraft motions from the outside scene in the central and peripheral visual field and with the vestibular system. This all means that there is quite a difference between the laboratory single-axis compensatory tracking task with which the basic theory for manual control was developed and the multi-axes multi-loop real aircraft control task. It has been shown, however, that the closure of the inner attitude loop by the pilot determines the characteristic bandwidth of aircraft control and the closure of the outer loops. Therefore the present study on perception and control of aircraft motions will concentrate on attitude perception and control. As will be shown in this thesis pilot's perception and control of aircraft attitude can well be studied in a single axis tracking task with peripheral visual and motion feedback.

Around 1970, there was an important motive to stimulate research on the influence of motion feedback on pilot's control behavior. To extend the application of flight simulation in flight-crew training, more flight simulation realism was called for. In civil aviation the aim was to achieve zero flight hours type-conversion training. This was reached by the introduction of outside-world displays and six degrees of freedom motion systems.

The control of the simulator motion systems demanded a better understanding of the contribution of motion cues. Due to the simulator hardware, there is a number of differences between real and simulated flight. The most important of these are:

- The equations of motion of the simulated aircraft are solved by a digital computer with limited sample frequency and inherent time delay.
- The outside world is simulated by the display of a computer generated image with limited update frequency and computational time delay.
- The aircraft motions have to be simulated by proper control of the simulator motion system with its inherent dynamic characteristics and physical limitations.

These limitations cause two major problems, time delays and a mismatch between the visual cues and the motion cues. In the literature, these two problems are normally treated separately. The mismatch between the visual and vestibular stimulation posed an important question. How could the simulator motion system be controlled in order to provide the pilot with the required motion cues to perceive the real motions of the simulated aircraft? To solve that question, the aircraft motions have to be transformed to the reach of the dynamic characteristics and physical limitations of the motion system. The algorithms used have a direct influence on the simulated aircraft motions as perceived by the pilot. A solution was found by the application of 'washout filters' which are configured in such a way that the characteristic motion cues, specific forces and angular accelerations, are maintained. It must be clear that the ultimate solution is reached only if the aircraft motions, as perceived by the pilot in simulated flight, are equal to those perceived in actual flight. Pilot's motion perception, however, not only depends on the vestibular sensations but also on the visual sensations, and his internal representation of the aircraft dynamic characteristics.

An engineering approach to extend the knowledge of the influence of motion feedback on pilot's control behavior is to determine the changes in tracking performance and control behavior due to the addition of motion feedback. During the sixties and the seventies, this approach was applied by several institutes which provided objective data. A selection of publications presenting these data is discussed in Ch. 2 of this thesis. By fitting pilot models to the experimental data, the changes in characteristic model parameters due to the addition of

motion feedback could be established. This valuable experimental work, however, did not provide the required detailed information about the visual-vestibular motion perception process. An extension of the research reported was necessary to establish the influence of the visual and vestibular motion feedback on pilot's perception and control behavior.

From the beginning of the seventies, the Faculty of Aerospace Engineering of Delft University of Technology has had a research flight simulator at its disposal. This simulator was equipped with an outside-world display and a three-degrees-of-freedom motion system. The motion system was driven by electro-hydraulic actuators with hydrostatic bearings which provides almost rumble free simulator motions. After a study was made of the vestibular system, and the thresholds of motion perception were determined (Hosman and van der Vaart, 1978), an attempt to optimize the parameters of washout filters was performed (Hosman et al. 1979). This optimization was aimed at the minimization of the difference between the modeled vestibular sensory output in real and simulated flight. Although reasonable results were obtained, it became clear that the vestibular sensory output alone was not the right basis to optimize simulator motion system control. The ultimate goal of flight simulation is that pilot's perception of aircraft motions in simulated flight are equal to those in real flight. This can only be reached by optimizing the simulator motion system control under the condition that the perceived aircraft motions, based on the visual and vestibular cues in real and simulated flight, are equal. Such an optimization is only possible when the characteristics of the visual-vestibular motion perception process can be described in adequate detail.

Based on these considerations, it was decided to start an investigation on the contributions of the visual and the vestibular system to the perception process and the consequences for a pilot's control behavior. For this study a comparison of the specific characteristics of the visual and the vestibular system in motion perception was necessary. Given the rather moderate maneuvers with limited pitch and roll amplitudes in transport aviation, on one hand, and the limited possibilities of the available flight simulator, on the other hand, it was decided to concentrate the present study to the basic characteristics of the perception and control of the aircraft roll motions.

The tracking task was considered to be too complicated to determine the differences between the visual and vestibular contribution to the perception process. As mentioned above, changes in a subject's frequency response due to motion feedback can be determined from measurements in tracking tasks. It is, however, difficult to distinguish the contributions of the individual senses to the perception process from the overall frequency response. Therefore, it was decided to evaluate the visual and vestibular perception of motion by using stimulus-response tasks with well chosen roll stimuli. An important question was, however, if the results obtained from stimulus-response tasks could be applied to the closed-loop control task. Based on the literature on human information processing, the human operator has to be considered a single-channel information processor with limited capacity and input of multiple senses. If that model is correct, then there is no reason that it can not be applied to the closed-loop control task. Using this model, the stimulus-response tasks with discrete and dynamic stimuli were designed to investigate the contribution of the central or foveal visual and peripheral visual system on the perception of the aircraft roll angle and roll rate. In addition, dynamic stimuli were applied to establish the differences between the speed and accuracy of motion perception with the visual and/or the vestibular system. Beside these stimulus response experiments, a tracking task experiment was performed to obtain a data base on the influence of visual and/or vestibular motion feedback on pilot's tracking performance and control behavior.

The results of the stimulus-response experiments, together with the well-known characteristics of the visual and the vestibular system, provided the data to set up a descriptive multi-input single-channel information processor model. The validity of the descriptive model was evaluated with the frequency response data from tracking task data base. The experimental results and the descriptive model provided a solid knowledge of the influence of motion feedback on pilot's control behavior.

The aim of the present study is to develop and obtain knowledge of the influence of the visual and the vestibular stimulation on pilot's perception and control behavior in aircraft control. This knowledge must lead to a model with which the influence of the limitations of simulation on the simulator pilot's control behavior can be investigated and which can be applied to optimize the simulator motion system control algorithms.

The set up of the thesis is the following: In Ch. 2, a review of selected publications on the influence of visual and vestibular motion feedback on pilot's control behavior is presented. This review gives an overview of the influence of motion feedback on pilot's tracking behavior. The results of this review provide the information necessary to indicate the direction for the research plan.

In Ch. 3, an overview is presented of the information processing by the human operator. The human operator is considered to be a single-channel information processor with multi-sensory input. Considering the overview, a descriptive multi-input single-channel information processor model is chosen. This model is used to evaluate the experimental data obtained from the literature and the experiments described in Chs 5, 6, and 7. In Ch. 4, the functional and dynamic characteristics of the visual motion detectors and the vestibular system are discussed.

In Ch. 5, two experiments to determine the speed and accuracy of the visual perception of roll attitude and roll rate are described. Roll attitude perception from the central visual field and roll rate perception, both from the central and the peripheral visual field, are considered. In Ch. 6 three stimulus-response experiments are described to investigate the speed and accuracy of the estimation of the final magnitude of a dynamic input signal, a second-order step response. Based on the dynamic characteristics of the motion detectors in the visual system and the vestibular system, a pre-experimental evaluation was performed to establish the experimental conditions.

A tracking experiment to establish a data base on the influence of peripheral visual and vestibular motion feedback in control tasks is described in Ch. 7. In this experiment two roll tracking tasks, the target following task and the disturbance task, are used to investigate the contribution of central- and peripheral visual and vestibular motion perception on subject's control behavior.

Finally in Ch. 8 the experimental results of the preceding chapters are reviewed and evaluated by substituting the experimentally determined characteristic parameters in the descriptive model and by comparing the model with the measured subject's frequency response.

2. THE INFLUENCE OF PERCEIVED AIRCRAFT MOTION ON PILOT'S CONTROL BEHAVIOR

2.1 Introduction

The influence of aircraft motions on a pilot's control behavior has been subject to considerable study during the last twenty-five years. A review of this work in 1980 at the International Symposium on the Study of Motion Perception in Veldhoven, the Netherlands made clear that many questions remained to be answered. (Wertheim et al., 1981, 1982). In the flight-simulation community, there was still a motion-versus-no-motion controversy which originated primarily from the lack of sufficient knowledge about the role of motion perception in manual aircraft control.

Since the beginning of the seventies, civil aviation flight simulators for pilot training have been equipped with six degrees of freedom motion systems. This meant that, although the role of motion cues in aircraft motion perception was not completely understood, the simulation of aircraft motions was accepted as a necessity in the civil transport aviation community.

In military aviation, however, due to the much higher specific forces and rotational accelerations during maneuvering flight, the addition of cockpit motion to the simulation of fighter aircraft has been ignored. The last few years the attitude of the military-simulation community towards motion simulation is changing under the political pressure to decrease the actual flying hours in favor of flight simulation.

The restrictions of type- and recurrent training with flight simulation and an extensive study of the vestibular system led to the conclusion that at least a better understanding of motion perception was necessary.

A number of references have made clear that the addition of cockpit motion improve a subject's tracking performance. Most of these tracking tasks, however, were performed under rather restricted conditions, which differed considerably from the control tasks in actual flight. To further understanding of the reported experimental results, a literature review on the influence of motion simulation on a pilot's control behavior is presented in this chapter. Before the literature review is presented, however, relevant information on the tracking task and pilot control behavior is reviewed.

2.2 Tracking-task setup

In the last 45 years a large number of publications on a human operator control behavior has been published. Only a limited number of these publications are directed to the influence of

motion cues on human control behavior in vehicle control. Before these tracking experiments can be discussed, however, it is necessary to consider a number of aspects in performing them.

In a compensatory tracking task, the subject is asked to generate control inputs so that the error on the display remains as small as possible. In Fig. 2.1, the general layout of the closed loop for a manual single-loop compensatory tracking task is presented. It is the operator's task to make the output of the system $y(t)$ correspond with the reference signal $i(t)$, the forcing function.

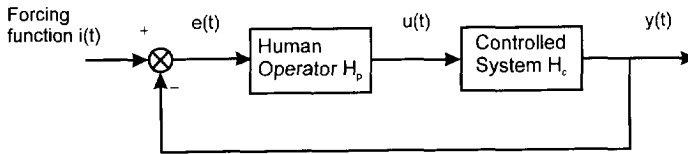


Figure 2.1 The single axis compensatory tracking or target following task.

On the basis of the error signal $e(t) = i(t) - y(t)$, the operator generates an output or control signal $u(t)$, with the aim to null the error signal $e(t)$. The operator will be labeled H_p and the controlled system H_c . In case of a description of the control behavior in the frequency domain $H_p(\omega)$ and $H_c(\omega)$ will be used respectively.

Two types of control tasks can be defined. A forcing function signal can be fed into the closed-loop at either of two points. As shown in Fig.2.1, the input forcing function $i(t)$ makes the output variable of the system to follow as an aircraft follows the leader in a formation flight. Hence this tracking task is called the **Target following task**. In Fig. 2.2, the system is disturbed by a forcing- or disturbance function, such as a gust disturbs an aircraft. This makes the tracking task a **Disturbance task**. For the single loop, as depicted in Fig. 2.1, the relation between the error signal $e(t)$ which has to be minimized by the pilot and the forcing function $i(t)$ is described by the transfer function in the target following task:

$$\frac{e(\omega)}{i(\omega)} = \frac{1}{1 + H_p(\omega)H_c(\omega)}. \quad (2.1)$$

In Eq. 2.2 the relation between the error signal $e(t)$ and the disturbance function $w(t)$ is described by the transfer function for the disturbance task:

$$\frac{e(\omega)}{w(\omega)} = \frac{-H_c(\omega)}{1 + H_p(\omega)H_c(\omega)}. \quad (2.2)$$

In a number of publications, the disturbance function is added to the output of the system. In that case the disturbance function is not filtered by the system dynamics and the transfer function between the input $w(t)$ and the error $e(t)$ is, except for a minus sign, equal to the negative of Eq. (2.1):

$$\frac{e(\omega)}{w(\omega)} = \frac{-1}{1 + H_p(\omega)H_c(\omega)}. \quad (2.3)$$

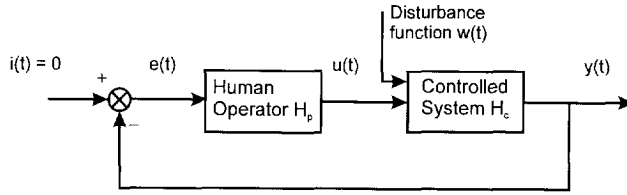
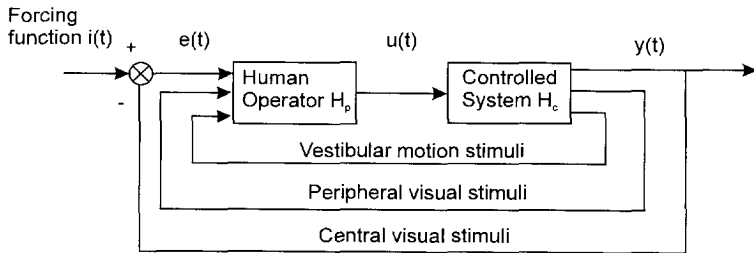


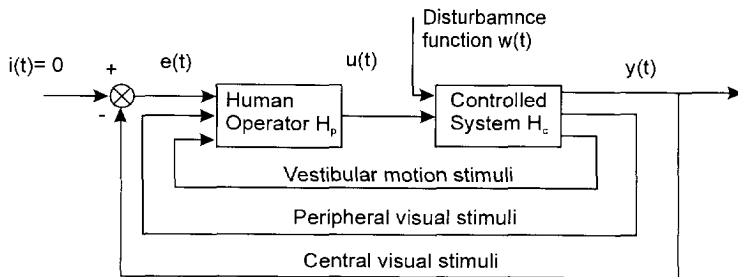
Figure 2.2 The disturbance task.

Apart from the changes in the frequency response, another important difference between the target following task and the disturbance task should be mentioned. In manual vehicle control, the human operator can additionally perceive the motion of the vehicle through his peripheral visual field and/or with his vestibular system, Fig. 2.3. In the case of the target following task, the central visual system senses only the error signal $e(t)$ which is the difference between the forcing function $i(t)$ and the vehicle output $y(t)$.

$$e(t) = i(t) - y(t). \quad (2.4)$$



a. Target following task



b. Disturbance task

Figure 2.3 Feedback of vehicle motion by the peripheral visual system and the vestibular system.

The vestibular system senses the actual vehicle output $y(t)$, i.e. the angular and/or linear acceleration of the vehicle output.

In the disturbance task, where $i(t) = 0$, the error signal $e(t)$ is:

$$e(t) = i(t) - y(t) = -y(t), \quad (2.5)$$

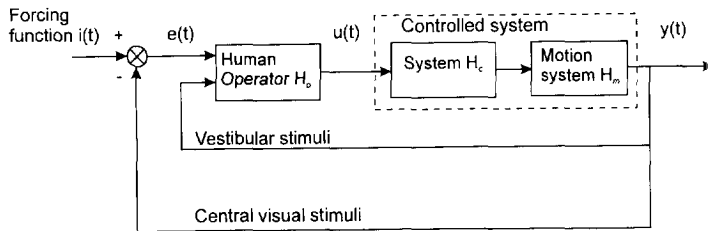
and both the visual system and the vestibular system perceive the vehicle output $y(t)$.

It will be shown in this chapter, that the effect of motion cues on the subject in the target following task is different from that in the disturbance task.

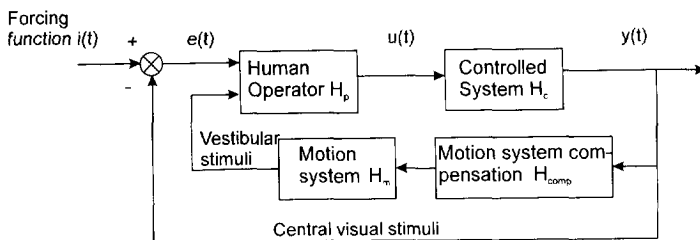
In actual flight, the outside visual- and vestibular motion stimuli are the direct result of the aircraft motion. In flight simulation, however, the visual and vestibular stimuli have to be generated by the visual display system and the simulator motion system. Both systems have their own dynamic characteristics. When tracking tasks are performed in a flight simulator to provide the subject with vestibular motion cues, the dynamic characteristics of both systems have to be taken into account. In that case, the motion system characteristics are incorporated in the closed control loop. Special care has to be taken when studying the influence of vestibular motion feedback on a subject's control behavior in a tracking task.

This study can be performed in two ways, Fig. 2.4. In both methods, visual feedback with or without vestibular motion feedback, the system dynamics controlled by the subject has to be equal. In the first method the system dynamics, as controlled by the subject, include the dynamic characteristics of the simulator motion system, $H_m(\omega)$. In the second method the motion system is compensated for its dynamic characteristics and the subject controls the system, $H_c(\omega)$.

In Fig. 2.4a the motion system dynamics are added to the system characteristics. The dynamic characteristics of the system, as controlled by the subject, incorporate the system and the motion-base dynamics. In Fig. 2.4b compensation for the motion system dynamics is applied.



a. Motion system dynamics included in the controlled system..



b. Motion system dynamics compensated.

Figure 2.4 Motion system dynamics in the target following task, included or compensated.

The compensation has to be chosen such that $H_{comp}(\omega)H_{motion}(\omega) = 1$ over the stimulated frequency range.

In tracking tasks, the subject uses a manipulator to generate a control input $u(t)$ to the system. The manipulators used for tracking-task experiments, as described in the literature, can vary from a control wheel, to center and side sticks, all with different kinds of dynamic characteristics. It has been shown by Hosman et al. (1988, 1990) that side-stick dynamics can have considerable influence on tracking performance and subject's dynamic control behavior. Therefore one should be careful in using tracking- task results from experiments with different experimental setup if no information on the dynamic and static characteristics of the manipulators used is presented.

As shown by McRuer (1965, 1974) system dynamics have a considerable influence on subject's tracking performance and dynamic control behavior. As will be shown in this thesis, peripheral visual and motion stimuli may also have an important influence on subject's behavior. To express the changes in tracking performance and control behavior, the following measures will be used: performance measures and pilot frequency response.

The influence of motion perception on tracking performance will be expressed by the standard deviation of the error signal $e(t)$. In the literature the error score parameter S_e is some times used which is defined by:

$$S_e = \sigma_e^2 / \sigma_i^2 \quad (2.6)$$

The subject's dynamic behavior will be described by the frequency response, $H_p(\omega)$ relating the subject's control signal $U(\omega)$ with the error signal $E(\omega)$ in the frequency domain:

$$H_p(\omega) = \frac{U(\omega)}{E(\omega)} \quad (2.7)$$

The control behavior and performance of the operator are, according to McRuer and Krendel (1974), influenced by four groups of variables:

Task variables; the dynamic characteristics of the controlled system H_c , characteristics of the forcing and disturbance functions and the characteristics of the display and the manipulator

Operator-centered variables; training, motivation, skill and fatigue.

Procedural variables; the experimental design, task of the operator, instructions, trade-off between objectives as effort and performance.

Environmental variables; ambient temperature, illumination, noise, etc.

From experience, it turns out that the control behavior of well-trained subjects, given certain task variables, is consistent and can easily be reproduced if the procedural and environmental variables are under control.

Based on extensive research and literature review, McRuer (1965) postulated a quasi- linear pilot model. The model describes human operator dynamic behavior in a single axis compensatory control task. The model consists of a linear describing function and remnant. This remnant constitutes the difference between the linear-correlated and total pilot output, and has a continuous and reasonably smooth spectrum. The most simple form of his model, the Simplified Precision Model, is given by:

$$H_p(\omega) = K_p \frac{1 + T_L j\omega}{1 + T_I j\omega} e^{-j\omega\tau}, \quad (2.8)$$

where: K_p = human operator gain;
 τ = reaction time delay;
 $\frac{1 + T_L j\omega}{1 + T_I j\omega}$ = equalization characteristics;

In Eq. (2.7) τ is the lumped parameter for the reaction time and neuromuscular system dynamics.

As McRuer found that in manual control tasks the open loop transfer function always showed the same characteristics, he postulated the crossover model:

$$H_p(\omega)H_c(\omega) = \frac{\omega_c e^{-j\omega\tau_c}}{j\omega}, \quad (2.9)$$

where ω_c is called the crossover frequency, that is the frequency where $|H_p(\omega)H_c(\omega)| = 1$.

For a closed-loop control system, it is necessary that a sufficiently large (positive) phase margin exists. For adequate stability it is necessary that at the crossover frequency the phase margin ϕ_m is:

$$\phi_m = \frac{\pi}{2} + \angle(H_p(\omega)H_c(\omega)) = \frac{\pi}{2} - \omega_c\tau_c > 0. \quad (2.10)$$

In the experiments to be described, the standard deviation of the error signal, the describing function $H_p(\omega)$ and the parameters of the fitted Simplified Precision Model will be used to study and to describe the changes in human closed loop control behavior. In addition to these parameters, the crossover frequency ω_c and the corresponding phase margin ϕ_m of the open loop transfer function, $H_p(\omega)H_c(\omega)$ are important parameters in the evaluation of the experimental results.

2.3 Literature review

A large number of investigations on the influence of motion perception on man-vehicle control were published the last decades. Bergeron (1970), Huang and Young (1981), Junker and Levison (1977), Junker and Repogle (1975), Junker and Price (1976), Levison (1976, 1977, 1978), Levison and Junker (1975, 1976, 1977, 1978), Levison and Zacharias (1978, 1980), Meiry (1965), Moriarty et. al. (1976), Neil and Smith (1970), Newell (1968, 1969), Newell and Smith (1969), Ringland and Stapleford (1972), Schroeder (1993), Seckel et. al. (1958), Shirley (1968), Shirley and Young (1968), Stapleford et al. (1969), Tomaske (1982), Young (1967), Zacharias (1977), Zacharias and Young (1967, 1981). Most of these publications feature the use of moving-base aircraft or car simulators. The amount of experimental data is impressive, but results are difficult to compare. This is mostly due to a

wide variety in simulated vehicle dynamics and simulator moving-base dynamics. There are also differences in type of motion to be controlled. Apart from motion simulation there may be further differences in the visual displays and in the error scores to be minimized by the subjects. Moreover subjects may range from naive non-pilots to experienced professional pilots. Experimental research on the influence of motion cues on a subject's tracking performance and dynamic behavior, relevant to the present study, has been performed at the following institutes:

- Man-Vehicle Laboratory of the Massachusetts Institute of Technology, MIT, by Meiry (1965), Young (1967), and Shirley and Young (1968).
- System Technology Inc., STI, by Stapleford et al. (1969) and Ringland et al. (1972).
- Aerospace Medical Research Laboratory, AMRL, at Wright-Patterson AFB and Bolt, Beranek and Newman, by Junker (1975, 1976), Levison (1976, 1977, 1978) and Moriarty et al. (1976)

In addition, there is a number of publications on the same topic by others that will be mentioned as far the results are important to this thesis. In this section, an overview of the selected research will be given.

Man Vehicle Laboratory, MIT

Meiry (1965) performed a study on the vestibular system related to human dynamic space orientation and manual control. He performed several tracking experiments to investigate the influence of vestibular-motion feedback on subject's control behavior, two of which are of direct importance.

The first was a target-following-task experiment, where the subject had to control the yaw angle of a simulator. The simulated dynamics of the controlled element were those of a single integrator, $K/j\omega$. By placing the subject's head in the axis of rotation of the simulator, centrifugal and tangential accelerations could be minimized. A two- degree-of-freedom research flight simulator, denoted as NE-2, was used. Although the approximated dynamic characteristics of the motion system were presented (flat gain up to 2 Hz and a time delay in yaw of 0.15 sec), it is not clear if the simulator motion control was compensated for this time delay. The manipulator was a lightweight, spring restrained side stick. The output was described as linear with stick displacement.

The results of the tracking experiment showed a decrease of the RMS of the tracking error when motion was added to the visual tracking error presentation. The score parameter, S_c , decreased from 0.075 to 0.050. The effective time delay, τ , in the fitted Simplified Precision Model decreased, due to the addition of motion, from 0.2 sec. to 0.1 sec. This resulted in an increase in the phase angle of the describing function $H_p(\omega)$ at the higher frequencies ($\omega > 1$ rad/sec) and in an equal magnitude, Fig. 2.5. Based on the details presented, the crossover frequency $\omega_c = 2.68$ rad/sec did not change and the phase margin ϕ_m increased from 34 to 50 degrees due to the addition of motion cues.

Vehicles always have second or higher order dynamic characteristics due to the fact that they have mass. Therefore a single integrator as controlled element is not representative for vehicle dynamics. In addition, simulator-motion systems have second- or higher- order system characteristics. Second-order systems mostly have difficulty in smoothly following a first order system response. Meiry's choice of the first order system dynamics, $H_c = K/j\omega$, in this experiment seems therefore inappropriate.

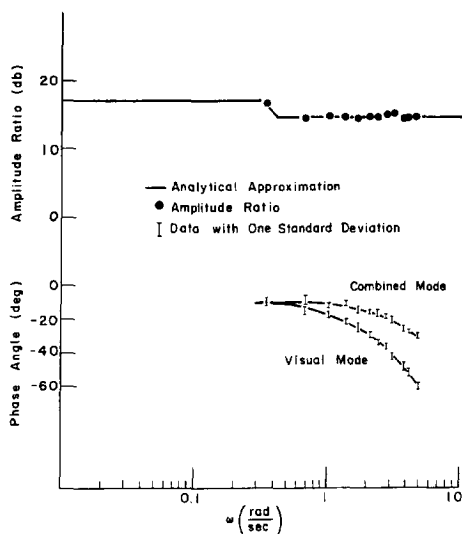


Figure 2.5 Describing function of the human operator in visual and combined mode in the horizontal rotation target following task controlling $H_c = K/j\omega$ (Meiry, 1965).

Meiry's second experiment concerned the control of an unstable roll system with the dynamics of an undamped, inverted pendulum. The transfer function of such a system is:

$$H_c(\omega) = \frac{A\omega_d}{(j\omega)^2 - \omega_d^2}. \quad (2.11)$$

In this particular experiment, the subject's control task was configured as a stabilization task. No forcing or disturbance function was used. The subject had to maintain the roll attitude as close as possible equal to zero.

For the experimental condition with only visual presentation of the roll angle, the subject was outside the simulator, seated 10 feet away from the cab controlling the cab roll angle. For the experimental condition with only cab motion presented, the subject was seated in the cab without any external reference. In case of the combined motion-visual experimental condition, the subject could see from inside the cab the horizontal and vertical reference lines on the laboratory wall facing the simulator.

Values of ω_d between 0.7 and 2.25 rad/sec were used in the experiment. Motion- system dynamics of the roll motion were described with a time delay of 0.1 sec, and were included in the control loop. The same manipulator was used as before.

The RMS error for the experimental conditions are presented in Fig. 2.6. From this figure it is clear that motion improved the stabilization considerably. The author summarizes his findings by "the vestibular sensors play a very significant part in providing rate information to the human operator in a closed loop system of vehicle orientation".

If the observation that "the vestibular sensors play a very significant part in providing rate information to the human operator" is correct, then the results of the first experiment of Meiry are even more remarkable. From the work of McCruer (1965, 1974) it is clear that the human operator controlling a first-order system does not have to generate lead, and there is no need to

perceive rate information. In Meiry's first experiment, however, addition of simulator motion to the visual presentation of the error signal improved the tracking performance and increased the phase angle of subject's describing function.

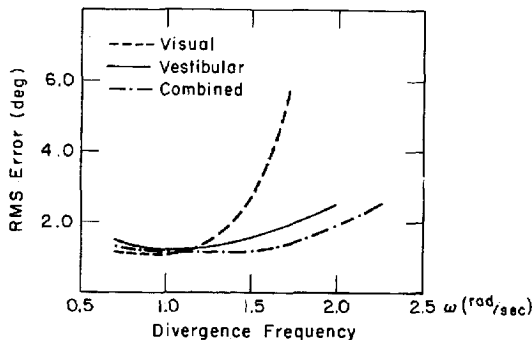


Figure 2.6 RMS error for control of the inverted pendulum (Meiry, 1965).

In an overview article, Young (1967) discussed four fixed- and moving-base experiments at the MIT Man-Vehicle Laboratory. He reported among others on the results of Meiry's experiment with the inverted pendulum. In addition, he also presented an extension of that experiment, in collaboration with Grabiell, on labyrinthine defective subjects with various vestibular disorders. The results suggested, that although tactile and other non-vestibular cues are of some value in conjunction with visual cues, it is primarily the vestibular system contribution that allows the pilot to improve his performance.

In the conclusions of the paper, Young accentuates the importance of motion cues for the control of marginally stable and unstable vehicle dynamics. These vehicles may require more lead compensation than is comfortably generated by pilots on the basis of the instruments alone. Consequently, the rate-sensing elements of the vestibular system prove valuable in giving early indications of attitude changes.

An extensive series of roll-disturbance tasks were performed by Shirley and Young (1968). They used a number of system dynamics, ranging from the easy to control single integrator via stable and unstable second-order to stable third-order dynamics. The NE-2 research Flight Simulator was used in the roll configuration (flat gain and 0.1 sec. time delay). The motion-system time delay was incorporated in the visual-error display, to synchronize the visual- and vestibular-motion presentation of the tracking error. The disturbance input, consisting of a sum of sinusoids, was added to the system output. The input frequencies ranged from 0.141 up to 7.66 rad/s with a rectangular cutoff frequency of 2.18 rad/s. Tracking tasks were performed with only visual presentation of the tracking error, with only vestibular-motion inputs, and with both combined visual- and vestibular-motion inputs.

The main conclusion of Shirley and Young was, that the addition of roll-motion cues to the visual cues in the disturbance-task experiment causes the human operator "to modify his control behavior in two ways. He generates additional phase lead at frequencies above 3 rad/sec and he increases his gain over all or part of the frequency range between 0.1 and 10 rad/sec.", Fig. 2.7.

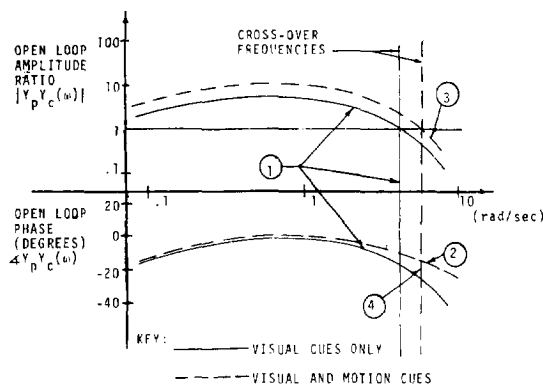


Figure 2.7 Schematic indication of how the human operator modifies his control behavior when roll-motion cues are added to visual cues in a single axis disturbance task. 1. Open-loop dynamics of the man-vehicle system with visual cues only; 2. The addition of roll-motion cues permits the human operator to generate additional phase lead; and hence 3. additional gain; 4. without loss of system closed loop stability. The crossover frequency is raised (Shirley and Young, 1968).

The performance data show a considerable decrease, 18 % for $H_c(\omega) = Ke^{-0.1j\omega} / (j\omega)^2$, in the score parameter due to the addition of motion feedback to the visual presented error signal.

System Technology, Inc.

Stapleford et al. (1969) performed a series of tracking experiments with central visual and vestibular-motion inputs, using the NASA Ames Six-Degree-of-Freedom Simulator. For these investigations, a roll-tracking task was used. In his experiments, he used a large number of conditions to investigate the influence of system dynamics, the influence of roll-washout filters and lateral-position washout, as well as equalization motion. By using both forcing-function and disturbance-function inputs, he was able to separate and identify the subject's dynamic behavior due to visual and motion feedback, Fig. 2.8. In the closed-loop control task, both the forcing function $i(t)$ and the disturbance function $w(t)$ were inserted. Stapleford showed that this configuration provides the opportunity to determine both the describing functions $H_{p,visual}(\omega)$ and $H_{p,motion}(\omega)$.

The results show that when motion cues are present, the visual feedback gain at low frequency is increased, and less lead is used in the visual path, i.e., the high frequency phase lags are larger. With the lead information supplied by the motion cues, the operator does not need to supply as much visual lead as he does for the case of a fixed base, Fig. 2.9. He can also increase his gain and achieve a higher crossover frequency because his effective time delay is reduced.

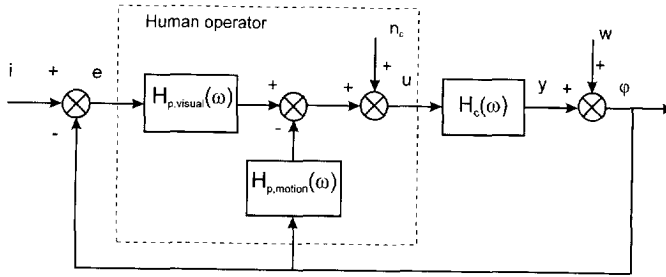


Figure 2.8 Effective loop structure for two input configuration (Stapleford et al., 1969).

For Stapleford's experiment the results of the disturbance tasks are of most interest. The controlled element dynamics were of the form:

$$H_c(\omega) = \frac{K_c}{j\omega(j\omega + a)}, \quad (2.12)$$

with the parameter a equal to 0, 1 or 10 sec⁻¹.

In Fig. 2.8 the layout of the control loop, as used in the experiments, is presented. Independent of the controlled element dynamics and washout dynamics, the following conclusions could be drawn from the results.

1. The error variance was considerably reduced by the addition of vestibular motion cues. For $K/j\omega^2$ system dynamics the score parameter decreased from $S_c = 0.65$ to 0.25.
2. Reductions of pilot phase lag when motion cues are added. The phase change is roughly equivalent to a time delay reduction of 0.1 to 0.2 seconds.
3. With less phase lag, the pilot can and does increase his mid frequency gain and increases his crossover frequency ω_c . For $K/j\omega^2$ system dynamics ω_c increased from 2.5 to 3.4 rad/sec at a constant phase margin ϕ_m .

The results of the experiment presented here cannot be directly compared with the results of the other experiments described in this chapter. In the STI experiment, subjects react on the forcing function primarily using visual perceived information, while they react at the same time on the disturbance function by the vestibularly-perceived information.

Aerospace Medical Research Laboratory, AMRL

Finally, a long-term study of the effects of motion perception on the human operator, performed at the Aerospace Medical Research Laboratory, AMRL, at Wright Patterson AFB, is of interest. This study included both peripheral-visual motion cues and simulator moving-base motion cues for roll-axis tracking tasks. A large number of experiments was performed to investigate:

1. The influence of peripheral-field displays on subject's tracking performance and dynamic behavior in target following tasks for so called 'easy' and 'difficult' to control system dynamics (Moriarty et al., 1976).
2. The influence of cockpit motion on subject's tracking performance and dynamic behavior in target following tasks for the same easy and difficult to control system dynamics (Levison, 1976)

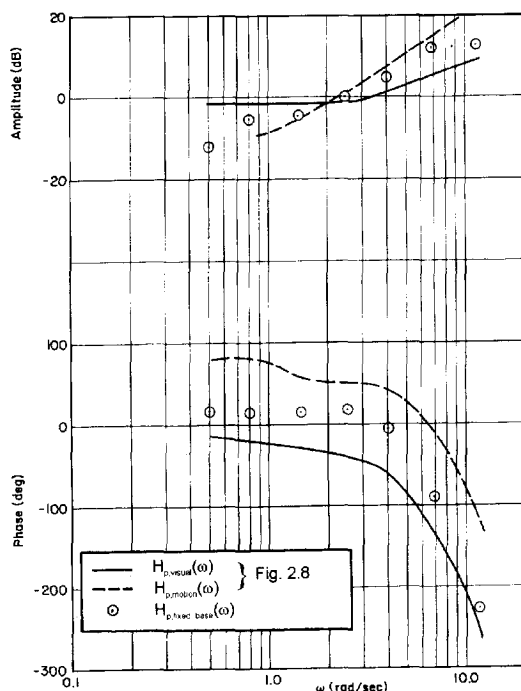


Figure 2.9 Visual and motion feed backs for $H_c(\omega) = K / (j\omega)^2$ for one subject (Stapleford et al., 1969).

1. Comparison between a peripheral visual- and vestibular motion information on manual tracking about the roll axis (Junker and Price, 1976).
2. The influence of cockpit motion on subject's tracking performance and dynamic behavior in following and disturbance tasks (Levison and Junker, 1977), (Levison, 1978).

AMRL Experiments 1 and 2

The first two experiments, 1 and 2, were configured as target following tasks. In both the experiments, the same two controlled-system dynamics were used as well as a force stick as manipulator, mounted on the right side of the subject, and a central display (simulated artificial horizon). The controlled task was configured as a roll control task. Task I, "Easy" dynamics, had a transfer function of:

$$H_c(\omega) = \frac{135}{j\omega(j\omega + 1)(j\omega + 10)} \quad (2.13)$$

In the reported crossover region, $\omega_c = 1.7$ to 2.2 rad/sec, the system characteristics are approximately equal to those of a double integrator, $K/(j\omega)^2$.

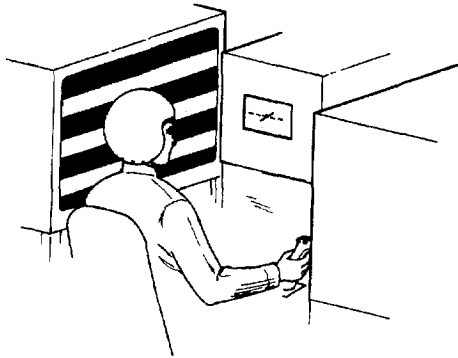


Figure 2.10 Placement of peripheral and central displays (Junker et al., 1976).

Task II, "Difficult" dynamics, had a transfer function of

$$H_c(\omega) = \frac{63.75}{(j\omega)^2(j\omega + 0.5)(j\omega + 10)} \quad (2.14)$$

The system dynamics of this system are approximately equal to those of $K/(j\omega)^3$ in the crossover region, $\omega_c = 1.4$ to 1.6 rad/sec.

The peripheral display consisted of two TV monitors, placed at the right and left side of the subject. They presented alternately black and white horizontal bars, 2.75 inch wide, Fig. 2.10. This peripheral display presented roll rate by vertically moving the horizontal bars on the monitors.

To generate vestibular roll motion, an electrical driven, one axis, roll-motion simulator, called Roll Axis Tracking Simulator, RATS, was used. Compensation for motion-system dynamics was configured as shown in Fig. 2.11 and 2.4a.

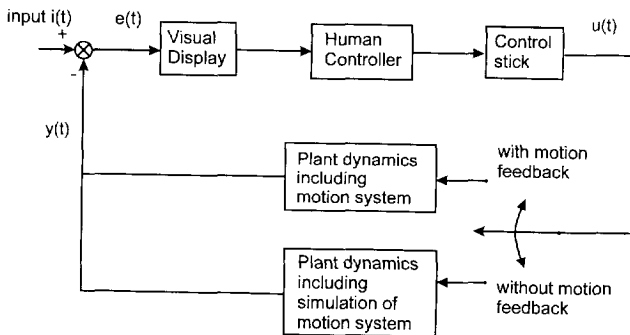


Figure 2.11 Block diagram of the tracking task (Levison 1976).

A forcing function with a bandwidth of 1.25 rad/sec and a RMS of 20 degrees as used for the easy plant and a bandwidth of 0.5 rad/sec and a RMS of 40 degrees for the difficult plant. Both forcing functions consisted of 12 sinusoids and had a second order fall off.

The results of the first two experiments are summarized in Table 1.

Table 1. Influence of peripheral display (Moriarty et al. 1976) and motion (Levison 1976) on the target following task.

| Display Configuration | Task I, Easy dynamics | | | Task II, Difficult dynamics | | |
|-----------------------------|---|-----------------------|---------------------|-----------------------------|-----------------------|---------------------|
| | Score S_e | ω_c rad/sec | ϕ_m degrees | Score S_e | ω_c rad/sec | ϕ_m degrees |
| First Experiment | Central display, no motion | | | | | |
| without peripheral displays | 0.49 | 2.21 | 47 | 1.17 | 1.4 | 22 |
| with peripheral displays | 0.48 | 2.04 | 57 | 0.45 | 1.4 | 38 |
| Second Experiment | Central display, no peripheral displays | | | | | |
| without motion | 0.42 | 1.74 | 67 | 0.56 | 1.57 | 31 |
| with motion | 0.42 | 1.74 | 67 | 0.24 | 1.57 | 44 |

Moriarty et al. (1976) concluded from the results of the first experiment that the influence of the peripheral display on subject's performance and dynamic behavior is only marginal for the easy plant (task I) but significant for the difficult plant (task II). The improvements in case of the task II are primarily: low-frequency lead and better tracking performance. From the data extracted from Moriarty et al.(1976) and presented in Table 1, clearly the changes in the score parameter S_e and phase margin ϕ_m are the same for both tasks, but the largest for task II. The crossover frequency ω_c is hardly changed.

The results of the second AMRL experiment, described by Levison (1976), show that motion cues increase subject's low-frequency lead. Tracking error score S_e was significantly reduced in the case of the difficult plant dynamics (task II, Table 1). The data in Table 1. correspond with these findings. The results of these two experiments do not correspond completely with each other or with the literature.

For both task I and task II, the results with only the central display, Table 1, should be approximately equal. In fact the differences are rather large. In the experiments of Moriarty et al.(1976) and Levison (1976) the task variables were equal. The differences in crossover frequency and phase margin may be a result due to changes in the operator-centered-, the procedural- and the environmental variables of the two experiments.

Compared to the data of a tracking experiment, presented by McRuer et al. (1965) the crossover frequencies and phase margins differ considerably. The crossover frequency ω_c is low compared to the 3.35 rad/sec. and the phase margin ϕ_m is larger than the 15 degrees as found by McRuer. In addition, in the AMRL experiments a force stick was used which normally gives better performance and less phase lag compared to a displacement stick. McRuer used in his experiments a displacement stick with mass, spring damper characteristics.

The results of these experiments may be influenced by the relative high power of the forcing functions relative to the low break frequencies of the controlled elements in both tasks.

AMRL Experiment 3

In the third experiment, described by Junker and Price (1976), a direct comparison of the influence of peripheral displays and vestibular motion during a target following task is made.

In this single experiment, a controlled system with third-order system dynamics, including the motion-base characteristics, was used.

$$H_c(\omega) = \frac{14}{(j\omega)^2 (2j\omega + 1)} \quad (2.15)$$

The experiment was performed with the Roll Axis Tracking Simulator (RATS) at AMRL. The same peripheral display and force stick were used as in the two experiments described previously.

The results of the third experiment confirm those of the two previously described experiments. Compared to the central display configuration, approximately the same performance improvement as expressed by the score parameter S_c was obtained by the peripheral visual cues and the vestibular motion cues. In both cases, a low frequency phase lead was found, although the additional phase lead due to vestibular motion stimulation was slightly larger than for the peripheral visual input, Fig. 2.12. System crossover frequency ω_c was 1.5 rad/sec for the vestibular motion case and slightly lower for the static and peripheral-visual-input cases. The motion case resulted in the largest phase margin ($\phi_m = 44$ deg.) with a slightly reduced value for the peripheral visual case ($\phi_m = 37$ deg.) and more reduced for the central visual-input-only configuration ($\phi_m = 27$ deg.).

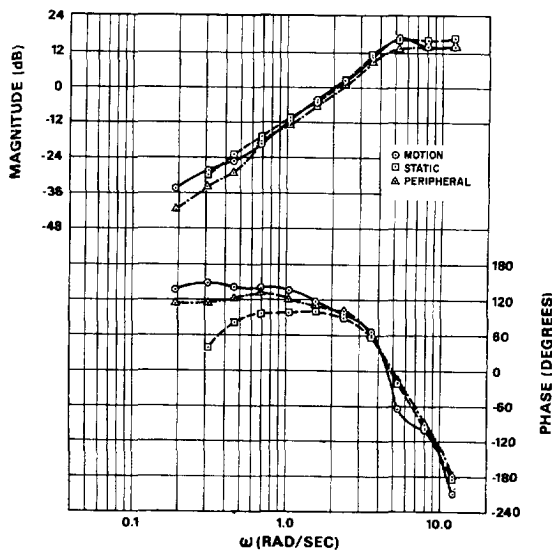


Figure 2.12 . Human operator describing function for three display configurations, static (central display), peripheral (central and peripheral displays) and motion (central display and motion) (Junker et al., 1976).

AMRL Experiment 4

In Levison and Junker (1977) and Levison (1978) a fourth experiment is described. It was aimed at studying the influence of motion cues on a subject's tracking performance and control behavior in the target following task and the disturbance task. This experiment was performed using approximately the same experimental setup as before.

The roll-axis motion capability of the Multi-Axis Tracking Simulator of the AMRL was used to generate the roll motion. A central display was used to generate an artificial horizon image. A force stick was installed at the right-hand side of a single-pilot cockpit. The combined control plant and motion system dynamics had the transfer function:

$$\frac{\varphi(\omega)}{F_a(\omega)} = \frac{10}{j\omega} \cdot \frac{5}{(j\omega + 5)} \cdot \frac{20}{(j\omega + 20)} \cdot e^{-j0.095\omega}, \quad (2.16)$$

where $\varphi(\omega)$ was the roll angle in degrees, and $F_a(\omega)$ was the control force in pounds.

According to the authors, for $\omega < 3$ rad/sec the system characteristics can be approximated by a single integrator $K/j\omega$ combined with a time delay $\tau = 0.095$ sec.

Both forcing and disturbance-function inputs were constructed from 13 sinusoids. The input signals had break frequencies of 1 rad/sec for the target following task and 2 rad/sec for the disturbance task with second-order fall off. Input amplitude was adjusted to a RMS forcing-function input of 10 degrees and a RMS disturbance-function input of 14 degrees.

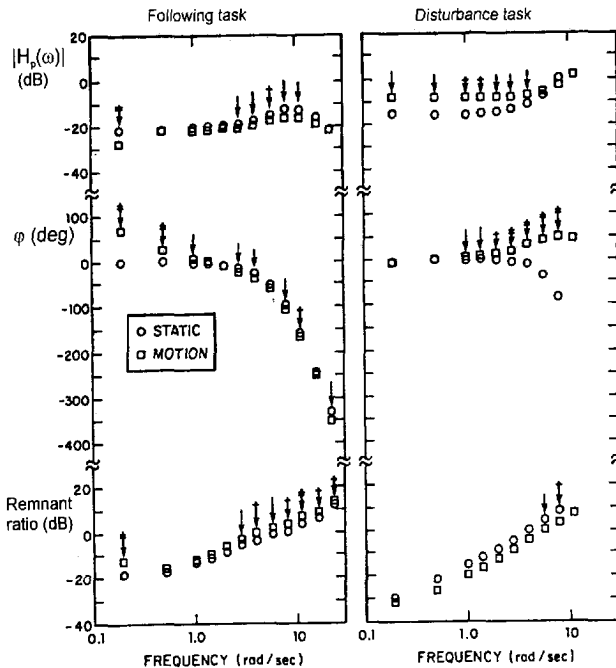


Figure 2.13 Effect of motion cues on human operator frequency response. Average of six subjects (Levison, 1978).

Table 2. Effect of motion cues on tracking score, crossover frequency and phase margin, Levison and Junker (1977) and Levison (1978).

| Display Configuration | Target following task | | | Disturbance task | | |
|-----------------------|-----------------------|--------------------|------------------|------------------|--------------------|------------------|
| | Score S_c | ω_c rad/sec | ϕ_m degrees | Score S_c | ω_c rad/sec | ϕ_m degrees |
| without motion | 0.50 | 0.93 | 71 | 0.40 | 1.70 | 56 |
| with motion | 0.47 | 0.80 | 90 | 0.18 | 3.49 | 55 |

Subjects were trained for four experimental conditions (the target-following and disturbance tasks both with and without motion). Training was continued until time- invariant performance was obtained.

The same parameters as used in Table 1 are presented for this experiment in Table 2.

The influence of motion cues on tracking performance in the target following task is very small, whereas there is a strong tracking improvement in the disturbance task. The results of the measured subject's describing functions are plotted in Fig. 2.13.

According to Levison and Junker, there is a low-frequency lead in the subject's describing function in the case of the target following task, which corresponds with the increase in phase margin as shown in Table 2. In the disturbance task, an increase in the subject's describing function magnitude at low- frequency and a high- frequency lead was found. This led to an increase in the crossover frequency, and a performance improvement.

2.4 Summary and discussion.

In single-axis target following and disturbance tasks, the influence of adding peripheral-visual and vestibular-motion feedback can be summarized as:

1. In the case of first-order system dynamics, an influence of vestibular-motion cues may be found on the subject's tracking performance and dynamic behavior in both the target following task and disturbance task. If the system dynamics are of the second or higher order, peripheral-visual and vestibular-motion cues have an influence in both the target following task and disturbance task .
2. The changes in the subject's dynamic behavior for the target following task and disturbance task are different. In the case of the target following task, the subject increases his low frequency lead, which increases the phase margin at an approximately constant crossover frequency. In the case of the disturbance task, the subject increases his high frequency lead. This enables the subject to increase his gain and the crossover frequency at an approximately constant phase margin.
3. In the case of the disturbance task, the time delay τ of the fitted pilot model (Eq. 2.8) is decreased by 0.1 to 0.15 sec due to the addition of motion cues.

The results of the described experiments unambiguously show improvements in subject's tracking performance and dynamic behavior in "difficult" tracking tasks. The origin of these improvements may result from the peripheral-visual and vestibular stimuli. It is not clear, however, how they cause the improvements. Some authors argue that the additional rate information, which is provided by the peripheral-visual and/or vestibular-motion stimuli,

enables the subjects to generate more lead compensation. This agrees partly with the results of the experiments discussed, as in the disturbance task where high frequency lead is generated by the subjects. In the target following task, however, subjects generate low frequency lead, which cannot be explained directly by the generation of lead compensation.

If, however, peripheral-visual and vestibular-motion stimuli provide the subject with rate information, then there is no decisive reason why these stimuli should have only an insignificant influence in the case of control of a second order system, as shown in some of the experiments (tracking experiments at AMRL) described in the literature. One possible reason why these experiments do not demonstrate a positive influence of motion, may be deduced by the fact that the results of these experimental tracking tasks with $K/(j\omega)^2$ system dynamics, do not correspond with those published by McRuer (1965). McRuer found in target following tasks without motion stimuli, a high value of the crossover frequency, $\omega_c = 3.25$ rad/sec. He also found a phase margin, depending on the forcing function bandwidth ϕ_m , between 15 and 40 degrees. In the AMRL study the corresponding values were, $\omega_c = 0.93$ rad/sec and $\phi_m = 71$ degrees. This means that the task variables (i.e. forcing function, manipulator characteristics, display format, etc.) and the operator-centered variables (i.e. subject's training, motivation, skill, etc.) in the experiments of McRuer were probably of a factor in obtaining the best possible performance.

All experiments discussed so far were performed under laboratory conditions and it is not clear if the results obtained may be extrapolated to the flight environment. Thus the question remains if, under actual flight conditions, motion cues can improve the performance in the manual control of second-order like systems, and to what extent.

Another question which arises as a result of the previous review is how the interaction between the peripheral-visual and vestibular-motion takes place in the perception process. In actual flight, the central-and peripheral-visual and vestibular stimuli are normally available to the pilot at the same time and the pilot obtains one percept (conscious perception of the task relevant components of the aircraft state) of the aircraft movements. If these stimuli enhance each other in the perception process, then this is of interest for further investigation.

Where the improvements in performance and control behavior were caused only by changes in the display configurations, addition of peripheral-visual or vestibular stimuli, it may be concluded that the improvements result from a refined perception of the first derivative of the controlled variable. This improvement may be obtained into two ways.

Firstly, due to the addition of peripheral-visual and or vestibular stimuli, redundant information is made available to the subject, thus improving the accuracy of the motion perception process.

Secondly, due to differences in the dynamic characteristics of the vestibular system and the peripheral visual system, on the one hand, and those of the central (foveal) visual system, on the other, the perception process changes and/or improves. The result of the improved perception enables the subject to change and improve his control behavior. This improvement may result from a shorter perception latency.

This possibility is more likely, given the results of the experiments discussed. Stapleford (1969) assumed that when in a control situation both visual and vestibular stimuli are fed back to the subject, the subject's output is the sum of the output of the two information processing channels, the visual channel and the vestibular channel, Fig. 2.8. This assumption is correct as long as the subject's behavior may be considered as linear. Zacharias and Young (1977), Repperger and Junker (1977), van der Vaart and Hosman (1987) used this assumption in analyzing results from tracking tasks with visual and motion inputs.

In the following chapters an investigation of the visual and the vestibular perception of motion stimuli will be described. In addition, the influence of the visual and vestibular motion perception on the subject's performance and dynamic behavior will be established in tracking tasks. By considering the results obtained a descriptive pilot model will be evaluated.

3. INFORMATION PROCESSING BY THE HUMAN OPERATOR

3.1 Introduction

In the preceding chapter, it has been shown that the tracking performance and the dynamic control behavior of a subject in executing compensatory-tracking tasks are influenced by the feedback of peripheral-visual and simulator-motion cues. Especially simulator-motion feedback has a positive influence both in the disturbance task and in the target-following task. From measurements taken during tracking tasks, a subject's control performance and frequency response can be obtained to establish the changes in control behavior due to changes in motion feedback. In addition, the model parameters of a human-operator model: the Simplified-Precision Model, the Crossover Model (McRuer et al., 1965, 1967) and the Optimal-Control Model (Kleinman et al., 1971), may be estimated to express the changes in operator control behavior. Changes in model parameters, however, do not improve per se the understanding of the functional changes in the information processing between the subject's input and output.

A practical method to study the functional changes in the information processing is the "Additive Factors Paradigm" as proposed by Sternberg (1969). With this method, a number of individual independent stages in the information processing have been recognized. In addition, it has been shown that the total information-processing time or reaction time is the sum of the processing times of the individual stages which are dependent on the task factors. The Additive Factors Paradigm, however, has been shown to be valid for static-task conditions.

Vehicle or aircraft control may be considered as a stochastic linear regulator problem. That class of control problems may be solved by the combination of the solution of the stochastic optimal-regulator problem and the optimal-reconstruction problem. This solution is known as the separation principle, Kwakernaak and Sivan (1972). Thus the stochastic linear-control problem of controlling the aircraft can be solved in two stages, Kok and Stassen (1980). Now, if the separation principle is likewise applicable to the manual aircraft control by the human pilot then the perception process of the 'observer' does not influence the 'controller' generating the control signal. By analogy, results of an experimental analysis of the perception process under static task conditions and based on Sternberg's Additive Factors Paradigm may be applied to the dynamic control task condition.

In this chapter it will be shown that such an approach is acceptable.

3.2 Information-processing

The publication of Shannon and Weaver's (1949) *Mathematical Theory of Communication* inspired many researchers in psychology to develop a vision on human information processing. In this vision, the human is considered as an information-processing channel. The major contribution of information theory has been the acceptance of information as a commodity that can be quantified, manipulated and transmitted.

Within the framework of information theory, the amount of information per item could vary considerably as for instance for digits, words, concepts, etc. Miller (1956) introduced the notion of a 'chunk'. These chunks were described as composite units that result from organizing or recoding of a group or system state.

The capacity of the information-processing channel is limited. This implies that only a limited amount of information (bits) can be processed per unit of time (s). The maximum capacity of the information-processing channel was determined experimentally at approximately 2.5 bits/s. This means that it takes an amount of time to put through a certain amount of information.

Hick (1952) and Heyman (1953) found that the reaction time in stimulus-response tasks increases linearly as a function of the information content of the stimulus. The Hick-Heyman law asserts that:

$$RT = a + b I(x), \quad (3.1)$$

where a and b are parameters and $I(x)$ the information content in bits. This law appeared to have considerable generality. Fitts (1954) reasoned that the execution of movements should obey the same rules of other information-processing tasks. He showed that the amount of information contained in the conduct of a specific movement should be a function of distance or amplitude and the accuracy of movement. His law states that:

$$MT = \log A/(W/2), \quad (3.2)$$

where:
 MT = movement time,
 A = amplitude,
 W = width of the target.

The limited capacity of the information-processing channel was closer examined and several short comings of the simple one-input one-output single channel became clear. Single-bottleneck views supported an information-flow model that consisted of several processing mechanisms, one of which is more constrained than the others.

Welford (1967) showed that, due to the observation that the information-processing channel is a single channel, subsequent decisions are delayed till the subject has dealt with the preceding decision. Welford's main thesis was that performance is limited by the operation of a single-channel decision mechanism. This mechanism can handle only one signal or chunk at a time.

Other studies were devoted to the parallel input of stimuli. Results of experiments showed that partial processing of parallel stimuli was possible. The main contention of this finding was that encoding and intake of information are not so demanding and can be handled in parallel. The system becomes single channeled and limited once the process of evaluating and selection of responses has begun.

From these studies, it became clear that the information processing by a single channel had to be viewed as a processing in a series of steps, or information-processing stages. Each component had to be viewed as a functional entity playing an identifiable role in the information-processing. The processing of a stage has to be completed before the next stage can proceed. Two stages have already been mentioned; the decision stage and the perception stage. The total number of stages depends on the requirements of the particular task. The need to analyze the architecture of the complete information-processing system provided the motivation for the development of new analysis tools.

The main experimental quantity in the analysis of the series of stages is the total duration of the information-processing, the reaction time, RT . This can be used in the framework of the Additive Factors Paradigm analysis method proposed by Sternberg (1969). Donders (1868) suggested that by manipulating the task variables and measuring the resulting change in reaction time, the individual stages could be established. Sternberg incorporated this rationale into a framework of information-processing. He developed a formal procedure to detect and assign the processing stages of the human information processing. In this procedure the individual stages are considered to be static systems. The general idea, Fig. 3.1, is that the effects of factors affecting different stages on the mean RT will be independent and additive, because stage durations are additive. In contrast, two factors, G and H , influencing the same stage (stage b) will usually show interactive effects on the RT .

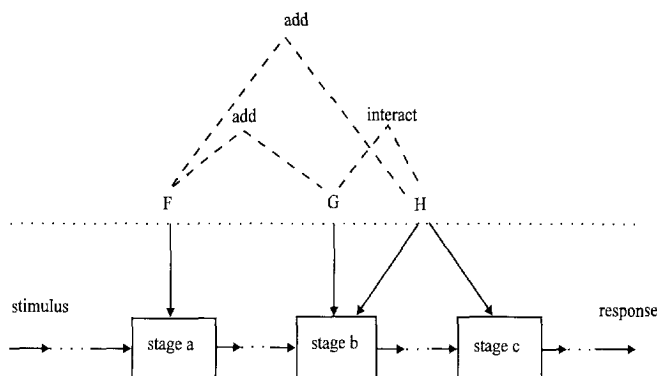


Figure 3.1 Example of an arrangement of stages (a , b and c) and factors (F , G and H). Below the horizontal line three hypothetical stages between stimulus and response are shown. Horizontal arrows represent inputs and outputs of stages; time proceeds from left to right. Dots indicate the possibility of other stages in a string in which the hypothetical stages are embedded. Arrows are drawn from factors to the stages assumed to be influenced by those factors. Above the line are indicated the relations among effects of the factors on the mean RT that are expected from the arrangement. (Sternberg 1969).

Thus if RT is the total reaction time of the information processing between the stimulus and the response, then:

$$RT = (RT_a + RT_b + \dots),$$

where:

$$RT_a = \text{function } (F),$$

and

$$RT_b = \text{function}(G, H). \quad (3.3)$$

When a factor, affecting the information-processing task of a stage, changes at t_0 , Fig. 3.2, then the total reaction time RT for a static system will be:

$$RT(t:t_0) = (RT_a(t:t_0) + RT_b(t:t_0) + \dots). \quad (3.4)$$

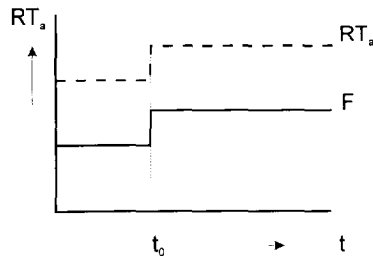


Figure 3.2 The change of the response time of stage a due to a change in the factor F at t_0 for a static system.

Considering the single channel characteristic of human information processing, and the multiple input due to the individual senses, a general model of the information processing is presented in Fig. 3.3.

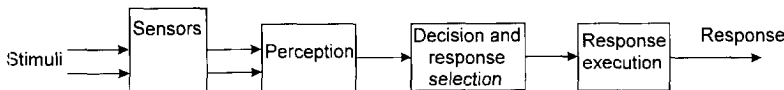


Figure 3.3 A model of the information-processing.

In the model of Fig. 3.3, four stages are considered (Wickens and Flach, 1988; Gopher and Donchin, 1986): the sensors which convert the input stimulus to a neuro signal, the perception process, the decision and response selection, and the response execution. Such a model is primarily based on the results of stimulus response experiments and the application of the Additive Factors Paradigm. Therefore, this kind of model only describes the reaction time, RT , between the initiation of the stimulus and the response. The question is, however, if experimental results obtained based on such a model can be applied to the dynamic environment of vehicle/aircraft control, and how they may be related to the control engineering models describing human control behavior.

3.3 Additive Factor Paradigm and dynamic systems

The most extended human-operator model is the Optimal Control Model, OCM, which is formulated in terms of optimal control theory. It provides the opportunity to describe the human

operator as a multi-input, multi-output processor. The OCM is based on the assumption that the well-trained, well-motivated human operator behaves in an optimal manner, subject to his inherent limitations and to the requirements of the control task (Kleinman et al. 1971). The inherent limitations of the human operator are modeled by:

- a single pure time delay τ , representing the information-processing time delay
 - observation noise v_o , representing the operator's perception uncertainty
 - motor noise v_m , representing the operator's uncertainty in generating his control output
 - neuromuscular time lag τ_N representing the operator's neuromuscular system dynamics
- Furthermore, it has been assumed that the operator has a complete understanding of:
- the dynamic characteristics of the system to be controlled
 - the statistical properties of the system disturbances
 - the task to be performed

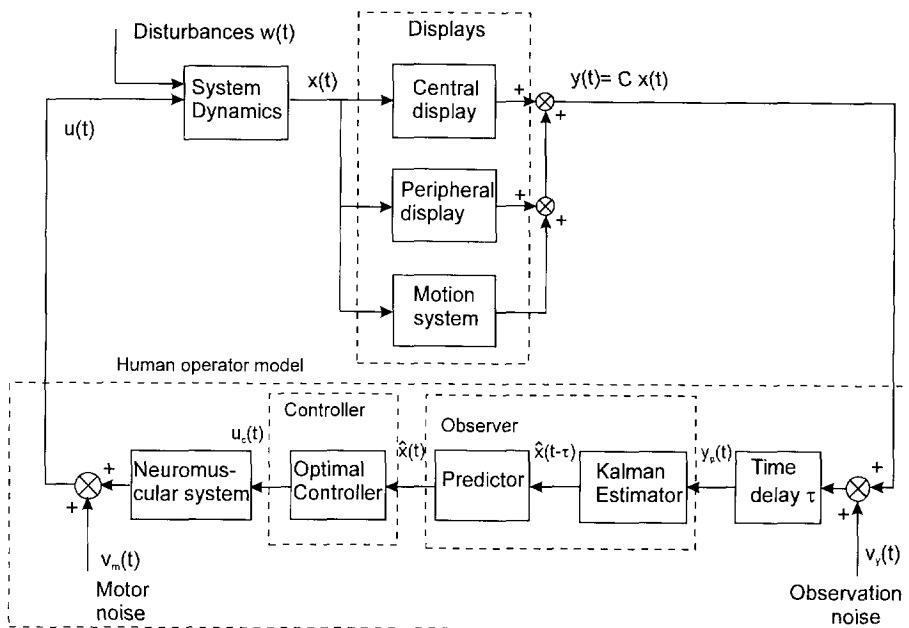


Figure 3.4 Structure of the Optimal Control Model. Modified after Levison (1978).

The model, Fig. 3.4, is based on the optimal solution of the stochastic linear regulator problem. This solution is realized by cascading an optimal state estimator and an optimal controller based on the separation theorem. The optimal state estimator or observer is a combination of a Kalman filter and a optimal predictor, which provide an optimal estimate of the system state $\hat{x}(t)$. The controller transfers the system state estimate to the optimal control signal $u(t)$.

The difference between the model of the information-processing, Fig. 3.3, and the OCM, Fig. 3.4, is that the OCM consists of two stages while the information-processing model consists of four stages. The OCM observer provides an estimate of the system state which corresponds

with the output of the perception stage. The output of the OCM controller corresponds with the response of the information-processing model.

White (1983) has shown that in the case of Supervisory Control a commonality between the two models exists. This correspondence is based on the separation principle applicable to the observer-controller solution of the OCM. A full description of the derivation of the OCM can be found in Kleinman et al.(1971a,1971b).

In the observer and controller the linear system to be controlled by the control signal is described by:

$$\dot{x}(t) = Ax(t) + Bu(t) + w(t). \quad (3.5)$$

The system outputs $y_i(t)$ of the system are linear combinations of the system state variables:

$$y(t) = Cx(t). \quad (3.6)$$

To take into account the human inherent limitations, the system output $y(t)$ is corrupted with observation noise. The observation noise signals $v_{y_i}(t)$ are zero-mean, Gaussian white noise processes with auto covariances V_{y_i} , and the observer perceives the delayed system output :

$$y_p(t) = y(t - \tau) + v_y(t - \tau). \quad (3.7)$$

An optimal estimate of delayed state $\hat{x}(t - \tau)$ is found by the Kalman filter by minimizing:

$$E \{e^T(t)e(t)\},$$

where

$$e(t) = x(t - \tau) - \hat{x}(t - \tau). \quad (3.8)$$

The controller minimizes the cost functional:

$$J(u) = E \left\{ \sum_{i=1}^{i=m} (Qx^2 + Ru_c^2) \right\}, \quad (3.9)$$

where the optimal control signal u_c is:

$$u_c(t) = -\hat{k}\hat{x}(t). \quad (3.10)$$

The human operator is not able to execute control movements perfectly, and has not a precise knowledge of his actual output. In order to represent these effects, the model output is disturbed by motor noise $v_u(t)$. Thus the model output becomes:

$$u(t) + \tau_a \dot{u}(t) = u_c(t) + v_u(t), \quad (3.11)$$

and this motor noise is a zero-mean, Gaussian white noise with auto covariance V_u .

In Table 3, the model parameters effecting the observer and the controller of the OCM are presented. Both the controller and the observer have some parameters in common and some parameters effecting only one of both. The same holds for the Observer Controller Decision

Table 3. Parameters of the Optimal Control Model and the Observer Controller Decision Model effecting the controller and observer of the models.

| Model parameters | Optimal Control Model | | Observer Controller Decision Model | |
|---------------------------|-----------------------|-----------------|------------------------------------|------------|
| | Controller | Observer | Controller | Observer |
| Task | Q, R | | Q, R | |
| Display | | C | | C |
| Delays and time constants | τ_n | τ | | |
| Control | B | B | B | B |
| System | A | A | A | A |
| Disturbance | | V_w, V_y, V_u | | V_w, V_y |

Model, OCDM, which is a discrete derivative of the OCM for the Supervisory Control Task (Kok en van Wijk, 1978, White, 1983). A decision-making mechanism was introduced to model the selection of output variables to be observed and the instant in time of the observation for improving state estimation. The decision mechanism was also required to model the interference by means of setpoint control actions. In a steady state supervisory control task, the human operator task can therefore be summarized as keeping the output variables within specified limitations by means of setpoint control actions. In addition, the OCDM is considered a reduced version of the OCM in the sense that the neuromuscular system is neglected, and no motor noise is added to the control signal. Only the observation noise is considered. Considering the large time constants dominating the industrial systems to be supervised, the relative small neuromuscular time constant and the perceptual time delay are omitted. Therefore, the predictor is not required to compensate for the perceptual time delay and the observer reduces to a Kalman filter.

White postulated that if the separation theorem is valid for the human controller and/or supervisor, then changing parameters affecting either the observer or the controller would change the human-operator observation or control behavior, respectively. Changing a parameter affecting both the observer and the controller would change both the human-

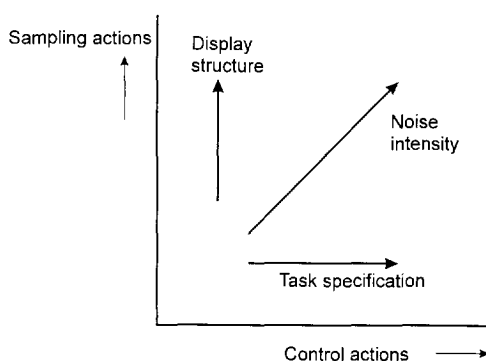


Figure 3.5 Graphical representation of the postulated effects of different variables on directly measurable quantities (White, 1983).

operator observation and control behavior. This is expressed graphically in Fig. 3.5. To prove the possible validity of the separation theorem for the human operator, White performed an experimental study on the human supervisor in process control.

The advantage of using the supervisory control task for this evaluation was that the changes in observation and control behavior could simply be assumed to be expressed in a change in subject's observation sample frequency and control action frequency.

White showed that changing the display structure influenced only the observation behavior as expressed by the sample frequency. Changing the system noise intensity influenced both the observation and control behavior. Although some changes in control behavior of individual subjects could be established, no significant change in control behavior due to task changes could be demonstrated. Therefore, White concludes that the separation theorem is valid for the human operator in a supervisory-control task.

The general acceptance of the separation theorem for supervisory control of dynamic systems by the human operator is supported by the work of White (1983). This allows Sternberg's Additive Factors Paradigm to have a much broader application to the analysis of the information-processing sequence for static and dynamic tasks. In addition, results obtained from the analysis of the information processing in static tasks may be applied to the processing in dynamic tasks.

3.4 Summary and conclusions

The results of Ch.2 showed that the display configuration (the combination of central- and peripheral displays and cockpit motion) has a considerable influence on subject's tracking performance and dynamic-control behavior in the tracking task. Although, the changes in behavior can be measured, it is not clear how they are affected. Further research is necessary to understand the functional influence of the display configuration on subject's behavior.

According to the preceding review, the human operator may be considered as a single-channel information processor with a multi-sensor input, Fig. 3.3. The information is processed by this single channel in a number of stages. In the first perception stage, the multi-sensor output is combined to one percept which may be multi-dimensional. The separate stages of the information processing are performed in series. The total duration of the information-processing is the sum of the durations of the individual stages.

The information-processing stages have been identified by using the Additive Factors Paradigm in static stimulus-response tasks and consequently the results are valid for this type of tasks. The question remains if the single-channel model is likewise valid for the dynamic task conditions of the control task. The answer to this question is not clear.

The control of an aircraft or vehicle may be considered as a stochastic linear regulator problem which can be solved by using the separation principle. The solution, which is obtained, consists of the combination of an optimal observer and optimal controller. It has been shown that in the case of supervisory control, the separation principle also holds for the behavior of the human supervisor. Considering these findings, it is likely that in the dynamic environment of a supervisory-control task the human supervisor processes the information in at least two stages: the observer stage and the controller stage.

Based on the preceding considerations the following working hypothesis will be used throughout this thesis:

There is no difference between the information-processing in static tasks and dynamic control tasks.

This hypothesis is enforced by the following observations:

- During the execution of a dynamic control task, the human operator processes the required information using a single information-processing channel with multi- sensor input.
- The multi-sensor output is processed in the perception process to one single percept which may be multi-dimensional
- Results of static, stimulus-response tasks are applicable to the information-processing in a dynamic control task.

In the following chapters, the validity of the working hypotheses has to be evaluated. This will be performed in Ch. 8 where the experimental results of stimulus-response experiments and of the tracking tasks experiment will be used to set up a descriptive model which describes the influence of the visual and vestibular motion perception on pilot's control behavior.

4. THE STATIC AND DYNAMIC CHARACTERISTICS OF THE VISUAL AND VESTIBULAR SYSTEM

4.1 Introduction

In Ch. 2, it was shown that in tracking tasks the addition of motion feedback has a positive influence on the tracking performance, and results in changes in dynamic behavior of the human operator. The conclusions of the literature review in Chapter 2 clearly demonstrate that both the peripheral-visual motion cues and the vestibular motion cues have, in principle, the same positive influence.

In the preceding chapter it has been shown that the senses form the first stage of the information processing by the human operator. In this chapter the senses that provide the human operator with the essential information necessary to perceive the vehicle or aircraft motions will be discussed. The models describing the dynamic behavior of these senses will be presented. These models will be used to evaluate the results of the experiments described in the Chapters 5 and 6. Finally these models will be used to set up a descriptive pilot model in Chapter 8.

In vehicle control, the human operator has to perceive the state of the vehicle motions. The senses perceiving vehicle motions are the visual system and the vestibular system. In addition, the proprioceptive system and the skin receptors are sensitive to changes in specific force acting on the body. The function of the visual system in motion perception is quite clear. Under normal conditions, the human operator is capable of controlling the vehicle based on visual information only.

When the vehicle with the human operator moves, the proprioceptive and vestibular output will be strongly related. Under normal operating conditions the human operator is not able to distinguish between proprioceptive and vestibular cues. They fuse to one percept. In the perception process, the proprioceptive and vestibular sensations are weighted depending on their reliability. For the present study, however, it has to be decided whether the proprioceptive system has to be taken into account.

Young (1967) argues, that based on experiments with normal and labyrinthine-defective subjects, that the contribution of the vestibular system to motion perception is much more important than the contribution of the proprioceptive system. Young's findings are supported by the results of an experiment to determine thresholds of motion perception (Hosman and van der Vaart, 1978), performed in the research flight simulator of the Delft University of Technology. It was shown that the threshold magnitudes depend on stimulus input frequency and correspond perfectly with the magnitudes of the dynamic models of the vestibular system components. This can be interpreted that even at very small motion stimuli the vestibular system, in comparison with the proprioceptive system, dominates the motion perception.

With the consideration of these facts, the proprioceptive system will not be taken into account for the present study. Hence, in the following chapters it is assumed that motion is perceived by the visual and the vestibular system. Therefore, a description of these senses is presented in this chapter. Although they are well described in the literature, a recapitulation of those aspects, necessary as a background for the experimental work described later in this thesis, is presented. Visual system components, such as the motion sensitive neural circuits and their dynamic characteristics will be described. Vestibular system components, the semi-circular canals and the otoliths and their dynamic models will be discussed.

4.2 The visual system

4.2.1 Introduction

Of all senses the visual system is the most versatile. The human is able to decide where to direct his eyes. Therefore, he is able to decide what he is looking for in his central visual field. In addition, the peripheral visual field provides the human observer with information about changes in his environment.

In the perception of self-motion, both the central or foveal visual field and the peripheral-visual field play their part. In the central-visual field the observer perceives precise information about objects and their motion whereas the observer obtains more general information on movement in the environment from the peripheral field. The human operator controlling a vehicle makes use of the capabilities of the visual system to perceive the state of the vehicle.

The visual system is a universal system capable of perceiving many different aspects of our environment under a large range of environmental conditions. It has been described extensively in the literature. This section will be focused on the special characteristics, which are related to the perception of self motion. A short description of the motion perception system and its dynamic characteristics will be presented.

4.2.2 Motion sensors and the thresholds for motion perception.

In the visual system, many types of detectors exist which are based on a receptor field on the retina and a neural network in the visual cortex detecting a specific stimulus. The "on center" and "off center" ganglion cells and their receptive fields in the retina are the basic receptors. These provide the input for the complex detectors located in the visual cortex. Hubel (1988) and van de Grind (1988) describe the motion sensitive detectors and their characteristics. For this thesis a schematic description of the principle of this detector is sufficient.

In Fig. 4.1, a schematic of the motion detector is presented. A wide range of detectors in the visual cortex are connected to receptive fields on the retina. The so-called 'bilocal' motion detector is one of these detectors and is connected to two receptive fields on the retina. The size of the receptive field in the motion sensitive direction is denoted by d and the span of the detector by S . If a stimulus, the projection of a moving object, passes both receptive fields from left to right than the receptor field F1 and thereafter receptor field F2 will be activated. The detector will be activated only if the delayed response of field F1, by a time delay τ ,

coincides at the comparator C at the same moment with the response of receptive field F2. This means that a particular motion detector is sensitive only for one velocity V :

$$V = \frac{S}{\tau_1}. \quad (4.1)$$

Thus a particular motion detector in the visual cortex is sensitive for one velocity and one direction. To make the perception of movement in the whole visual field possible, receptive fields on the retina are wired to a very large number of motion detectors, each sensitive for their own velocity direction and velocity magnitude.

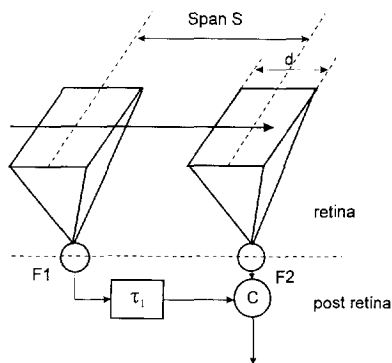


Figure 4.1 The principle of the motion detector of the visual system (van de Grind, 1988).

The detectors are placed in columns in the visual cortex, changing in direction sensitivity and/or velocity-magnitude sensitivity from detector to detector and from column to column. The question arises whether the visual system is also able to perceive acceleration and whether there are acceleration detectors in the visual system. By remapping the column outputs of the motion analysis system, accelerations or decelerations could be determined. This would be possible by comparing the velocity V_i of one column with V_j of another column by using a similar bilocal detector. There is, however, no evidence for remapping of the available information to detect acceleration (van de Grind, 1988).

In van de Grind et al. (1986), experiments are described to determine the relation between the span S of the motion detectors, the stimulus velocity V and lateral eccentricity E in the peripheral field. The results for the span S of one subject are presented in Fig. 4.2. The figure shows two specific characteristics. There is a minimum span, S_{min} which increases with increasing lateral eccentricity E in the peripheral field. (3 min of arc in the fovea up to 1 degree in the peripheral field) Secondly, the curves approach an asymptote (dashed line) corresponding with a constant minimum time delay τ_1 . The asymptote is independent of the eccentricity E and described by:

$$S = V \cdot \tau_1. \quad (4.2)$$

For each eccentricity there is a critical stimulus velocity V_c where for $V < V_c$ the span $S = S_{min}$. For $V > V_c$ the span S corresponds with Eq. 4.2. The value of the minimum time delay τ_1 varies between 45 to 85 msec depending on the individual subject.

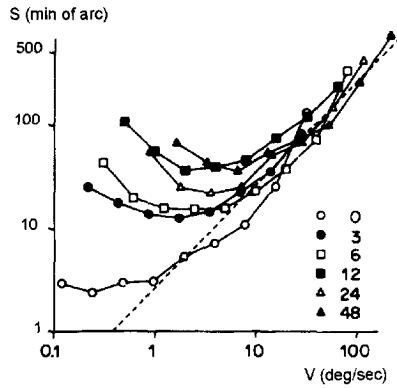


Figure 4.2 The span S in minutes of arc as a function of the field velocity V expressed in deg/sec. Different symbols are used for different lateral eccentricities E , as indicated in the lower right-hand corner. The dashed line represent the relation that would hold if all bilocal detectors in a given subject would have the same constant time delay τ_i . (van de Grind et al., 1986).

From the data obtained, the authors conclude that the motion detectors can be roughly divided into two groups separated by a critical velocity V_c . This critical velocity depends on the lateral eccentricity. One group has a constant time delay τ_i and is sensitive for the higher velocities. The span of the motion detector increases with velocity, see eq. (4.2). A second group with constant minimum span S_{min} is sensitive for low velocities. The time delay of this group can vary, increasing with decreasing velocity.

$$\tau_i = S_{min}/V \quad (4.3)$$

Depending on these thresholds, and the minimum span of the motion detectors in the fovea, the maximum values of the detector time delay τ_i are 1 - 5 sec.

To perceive the velocity of a stimulus with the velocity detector it is necessary that the projection of the stimulus on the retina pass through the span of the detector. The time required equals $\tau_i = S/V$. Thus the working principle of the detector causes that with the perception of motion/velocity a certain time delay τ_i is involved. This motion detector time delay is not equal for all detectors. If the velocity $V \geq V_c$ then τ_i has a constant value of approximately 65 ms. At velocities smaller than V_c , the time delay τ_i increases with the inverse of the velocity.

In addition to the time delay, τ_i , motion perception is further delayed by a second delay, τ_2 , due to the neural transmission from the retina to the visual cortex and the processing of information during the perception of motion. The relation between stimulus velocity and perceived velocity can be described by a function:

$$H_{velocity} = Ke^{-j\omega(\tau_1 + \tau_2)} \quad (4.4)$$

The gain, K , is normally assumed to be equal to 1. The magnitude of the second time delay, τ_2 , can not be measured directly. The total time delay, $(\tau_1 + \tau_2)$, contributes to the effective time delay, τ_e , of the human operator as expressed in the crossover model of McRuer (1965, 1969).

Harter and Aine (1984) have shown that the time delay, τ_2 , for perception of motion in the peripheral visual field is approximately 60 ms. shorter than for the central visual field. This is caused by a faster neural pathway to the visual cortex for the peripheral visual stimuli.

In the next chapter, two experiments are described which determine the speed and accuracy of the visual perception of aircraft attitude and angular rate from central and peripheral displays. It will be shown that the motion detector characteristics discussed influence the perception speed.

4.3 The vestibular system

4.3.1 General description

The vestibular system is located in the inner ear. The organ consists of two different sensory systems: the semi-circular canals sensitive to angular acceleration and the otoliths sensitive to specific force. The system of the semi-circular canals consists of three circular canals in approximately three orthogonal planes and the otoliths consists of two sac-like swellings, the utricle and saccule, Fig. 4.3. The semi-circular canals and the otoliths are interconnected and filled with a fluid, the endolymph.

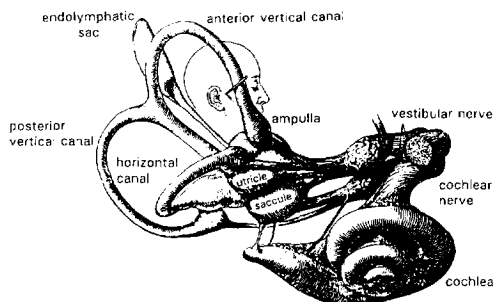


Figure 4.3 The structure of the inner ear (Hardy, 1934).

The two systems are normally treated separately although there is a similarity in the conversion of the input rotational- or linear-acceleration to the neural output, the afferent firing rate.

The semi-circular canals

Both the ends of each of the fluid-filled semi-circular ducts are continuous with the utricle. Each duct bears an enlargement called the ampulla. The epithelium of the duct in part of the ampulla is thickened and contains the sensitive haircells; the thickened zone containing the haircells, is called the ampullary crest or crista, Fig. 4.4. The crista is covered with a

gelatinous capsule called the cupula that stretches from the crista to the roof of the ampulla. When the head undergoes an angular acceleration, the reaction to the momentum to accelerate the fluid causes a pressure differential over the cupula. The resulting distortion of the cupula elicits a receptor potential in the haircells of the crista and alters the level of activity of the primary neurons in the eighth-nerve fibers innervating them. It is generally assumed that, unless extremely large angular accelerations occur, the cupula always seals the ampulla. The semi-circular canals are almost insensitive for linear acceleration due to an equal specific mass of the cupula and the endolymph.

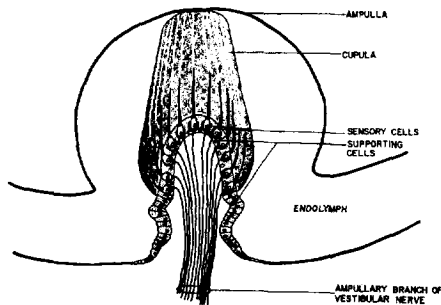


Figure 4.4 Simplified diagram of the ampulla in the plane of the semi-circular canal. The hairs of the sensory cells pass into fine canals in the gelatinous cupula which surrounds the crista (Peters, 1969).

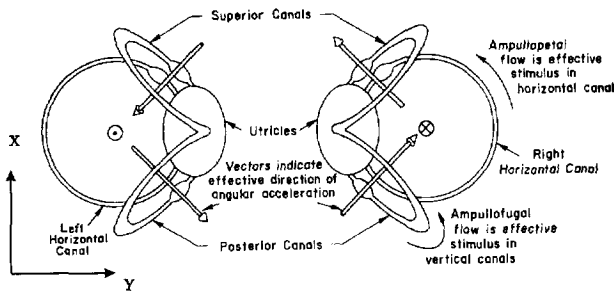


Figure 4.5 The approximate orientation of the semi-circular canal (Peters, 1969).

The three semi-circular canals lie in three approximately orthogonal planes. The planes of the vertical canals in the left and the right ear make an angle of 45 degrees with the lateral Y axis, Fig. 4.5. For each canal there is another coplanar canal in the opposite ear. The horizontal canal makes an angle of 30 degrees with the horizontal XOY plane. The diameter of the canals is about 6 mm and the canals have a width of 0.24 mm, Fig. 4.6.

The otoliths

There are two otolith systems in each inner ear. One is the utricle, the common base of the semi-circular canals, and the other is the saccule, a bean like downward extension of the utricle. A portion of the floor of the utricle and the saccule is thickened and contains specialized receptor cells, the vestibular haircells. These zones, termed maculae, are the

principal receptor regions of the otoliths. Each macula is covered with a gelatinous substance

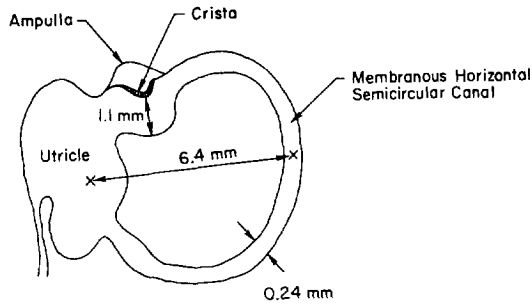


Figure 4.6 Average dimensions of the membranous horizontal semi-circular canal (Peters, 1969).

in which crystals of calcium carbonate, called statoconia, are embedded, Fig.4.7. The macula of the utricle lies partly in the horizontal plane when the head is bend forward by approximately 30 degrees, so the statoconia rest upon it. The macula of the saccule is oriented vertically when the head is in its normal attitude. The specific density of the statoconia is 2.71, much higher than the specific density of the endolymph, which is reported to be 1.003.

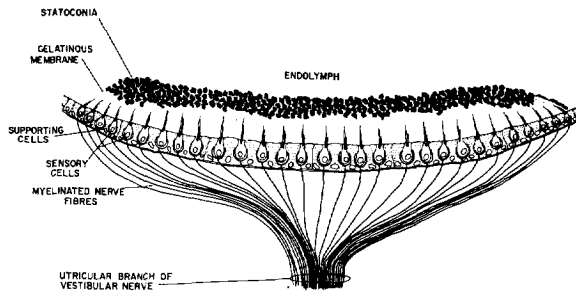


Figure 4.7 Simplified diagram of a vertical section through the utricular macula, (Peters, 1969).

Specific forces parallel to the plane of the macula will cause the statoconia to shear the gelatinous layer, and bend the hairs or cilia of the sensitive hair cells. This bending of the cilia will alter the firing rate of the afferent neurons. The average plane of the utricular macula is approximately parallel to the horizontal canals. The saccular macula is roughly parallel to the Z-axis. The polarization of the haircells on the maculae gradually changes from place to place. On the dividing line, the striola, the polarization changes 180 degrees, Fig. 4.8. Given the wide range of polarization of the haircells on the maculae of the utricles, and the saccules specific forces along three orthogonal axes can be perceived.

Two basically different types of haircells in the maculae and in the cristae of the semi-circular canals are to be distinguished. Vestibular hair cells are restricted to the crista of the semi-circular canals and to the maculae of the saccule and the utricle. Haircells are separated from one other by supporting cells, to which they are joined at their apical surfaces by tight junctions. On the upper surface of the haircell a number of hairs, called stereocilia, and a single kinocilium extend, Fig. 4.9. In the semi-circular canals these hairs project into the

overlying cupula, whereas at the maculae they project in the gelatinous layer covering the macula. The kinocilium is always found on one side of the hair bundle.

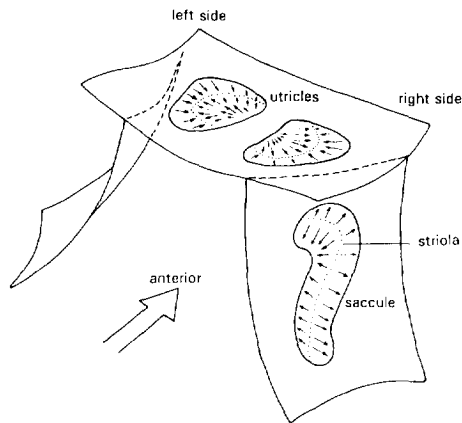


Figure 4.8 Schematic representation of the polarization of the sensory haircells on the saccular and utricular macula, (Malcolm and Melvill Jones, 1970).

This gives each hair cell its morphological axis, or polarization. The axis can be defined as running from the smallest stereocilium to the kinocilium. Bending of the hairs to the kinocilium leads to a depolarization of the haircell and an increase in the firing rate of the afferent fibers in the eighth nerve.

All the haircells in the crista have the same polarization, while the polarization of the haircells on the macula change with their position. The distinction of the two different classes of haircells mentioned above, has been well established. The most important difference in the so called type I and type II cell lies in the innervation with afferent fibers, Fig. 4.9. The cell body

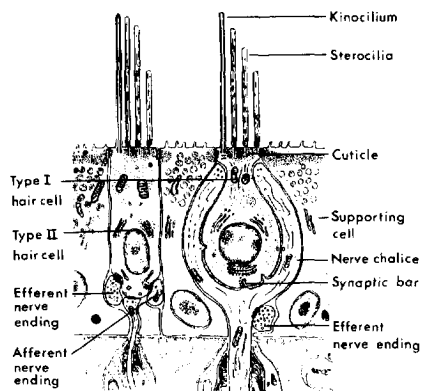


Figure 4.9 Schematic drawing of the two types of sensory haircells in the mammalian labyrinth showing the fine structural organization of the type I and type II cells and their innervation (Wersäll and Bagger-Sjöbäck).

of the type I cell is spherical, enclosed by the ending of one thick afferent fiber. The firing rate of the afferent neuron is irregular and correlated with the bending and the change, or first derivative, of the bending of the cilia. The afferent neurons are called irregular cells.

Type II cells have a cylindrically-formed cell body innervated by a number of thin afferent nerve fibers. The dendrites of the afferent neurons innervate with several type II cells. The firing rate of the afferent neurons has a regular character, and correlates with the bending of the cilia. The type II cells are called regular cells.

Advanced techniques have made the recording of the response of the afferent neurons possible, and the discharge rate due to linear or angular accelerations can now also be experimentally determined. Experiments on several species have demonstrated the functional difference of the two types of haircells. See, for example Kornhuber (1971), Fernandez and Goldberg (1976) and Goldberg and Fernandez (1971).

In summary, the vestibular system is capable of perceiving rotational acceleration and specific forces along three orthogonal axis. Due to the characteristics of the type I and II haircells, both hair bending and its first derivative influence the vestibular output.

4.3.2 Dynamic models of the semi-circular canals and the otoliths.

The semi-circular canals

Given the mass, spring, damper characteristics of the semi-circular canals (moment of inertia of the endolymph and the cupula, the viscous damping of the endolymph, and the spring stiffness of the cupula) Steinhausen (1931) proposed a dynamic model. The parameters of the overdamped-torsion-pendulum model were first identified by van Egmond, Groen and Jonkees (1949). The angular displacement of the endolymph $\xi(t)$ was related to the input angular acceleration of the head $\ddot{\alpha}(t)$ by the differential equation:

$$\theta \frac{d^2 \xi(t)}{dt^2} + \pi \frac{d\xi(t)}{dt} + \Delta \xi(t) = \theta \ddot{\alpha}(t), \quad (4.5)$$

where:

θ = the moment of inertia of the endolymph;

π = the viscous damping of the endolymph;

Δ = the spring stiffness of the cupula.

Since the cupula deflection is approximately proportional to the angular displacement of the endolymph the transfer function between the cupula deflection $\zeta(t)$ and the input angular acceleration $\alpha(t)$ can be formulated as:

$$\frac{\zeta(\omega)}{\alpha(\omega)} = \frac{K}{(1 + \tau_1 j\omega)(1 + \tau_2 j\omega)}, \quad (4.6)$$

where: $\tau_1 = 10$ s and $\tau_2 = 0.1$ s, (van Egmond et al., 1949).

These parameters were determined by van Egmond et al. (1949) based on subjective verbal responses of well-trained subjects to stimuli generated with a rotating chair and a torsion swing.

The technique to measure the neural discharge rate (impulses/sec, ips) of primary neurons in the vestibular nerve, mentioned in the previous section, made the determination of the transfer

functions of the semi-circular canals possible. Fernandez and Goldberg (1971) measured the transfer function describing the relation between input angular acceleration and output discharge rate of the squirrel monkey :

$$H_{SCC}(\omega) = \frac{j\omega\tau_a}{(1 + j\omega\tau_a)(1 + j\omega\tau_1)(1 + j\omega\tau_2)}, \quad (4.7)$$

where:

τ_a = adaptation time constant ; τ_1, τ_2 = time constants of the
 τ_L = neural lead term; overdamped torsion pendulum.

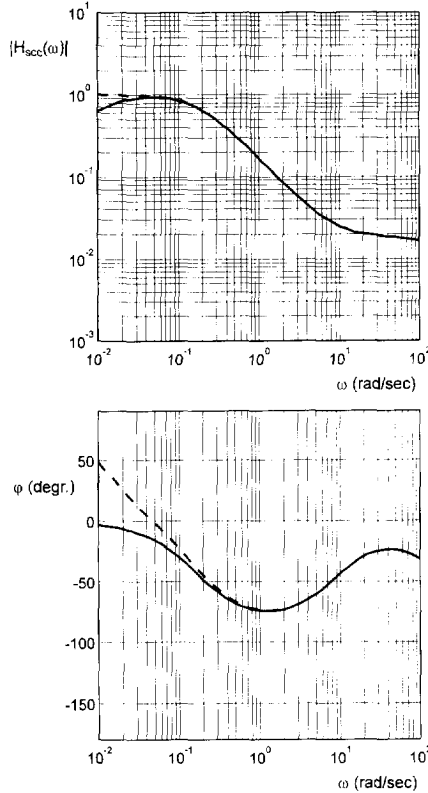


Figure 4.10 Bode plot of the transfer function of the semi-circular canals, Eq. 4.7. Dashed line includes the adaptation term.

The adaptation term has been established by many researchers and is important for long-duration or very low-frequency stimuli. The adaptation time constant $\tau_a \cong 80$ s. In tracking tasks, the bandwidth of interest lies approximately between 0.1 and 20 rad/sec. Hence the adaptation term in the model of the semi-circular canals may be neglected and Eq. 4.7 reduces to:

$$H_{SCC}(\omega) = \frac{K(1 + j\omega\tau_L)}{(1 + j\omega\tau_1)(1 + j\omega\tau_2)}. \quad (4.8)$$

Table 4. The parameters of the model for the semi-circular canals, Eq. 4.8.

| | |
|----------|--------------------------|
| K | 2 ips/°/sec ² |
| τ_L | 0.11 s |
| τ_1 | 5.9 s |
| τ_2 | 0.005 s |

For the squirrel monkey the lead time constant, τ_L , has been determined by Fernandez et al. (1971) at 0.49 s. The parameters for the human semi-circular canal model used in this thesis are presented in Table 4. They are based on data from the literature, and research at Delft University of Technology, (Hosman and van der Vaart, 1978).

In Fig. 4.10 the Bode plot of the transfer function of the semi-circular canals according to Eq. (4.7) is presented.

Dynamic model for the otoliths

By considering their physical structure, the otoliths can be modeled as an accelerometer with overdamped mass-spring-dashpot characteristics, as described by the differential equation:

$$\ddot{x}_s(t) + \frac{r}{m} \dot{x}_s(t) + \frac{k}{m} x_s(t) = \ddot{x}_m(t), \quad (4.9)$$

where:

- m = mass of the statoconia;
- x_s = displacement of the statoconia relative to the macula;
- x_m = displacement of the macula (equal to head displacement);
- r = viscous damping coefficient;
- k = spring stiffness of the gelatinous layer.

Due to the overdamped characteristics of the otoliths ($\beta > 1$), such a system has a transfer function:

$$H_{oto}(\omega) = \frac{K}{(1 + \tau_1 j\omega)(1 + \tau_2 j\omega)}, \quad (4.10)$$

Since this model was established, it has been very difficult to identify its parameters. The main reason is the lack of adequate experimental installations to generate the necessary linear acceleration stimuli. The counterparts to the torsion swing and rotating chair, as used for the stimulation of the semi-circular canals, are the parallel swing and the sled. In particular, the sled, a car smoothly running on a rail system, is the best experimental tool for generating acceleration stimuli if an accurate acceleration control is available, and the acceleration noise is below threshold values.

Based on different arguments, researchers concluded that the numerator of Eq. (4.10) should be extended with a first-order term in order to describe the transfer of the statoconia displacement to afferent output:

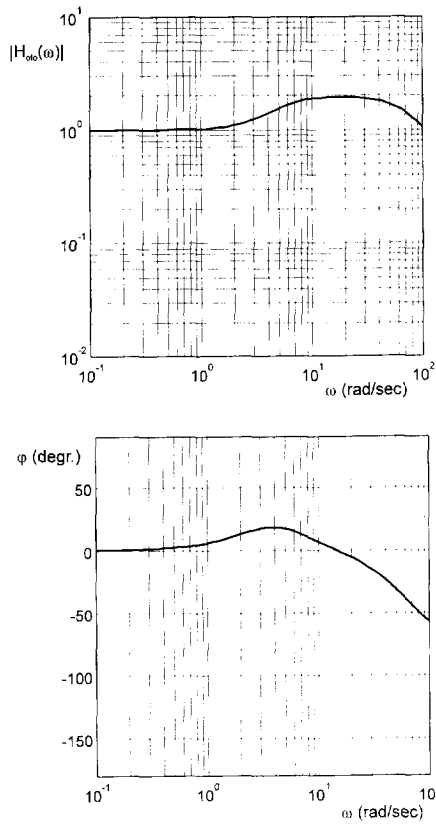


Figure 4.11 Bode plot of the transfer function of the otoliths, Eq. 4.11.

$$H_{oto}(\omega) = \frac{K(1 + \tau_n j\omega)}{(1 + \tau_1 j\omega)(1 + \tau_2 j\omega)}, \quad (4.11)$$

with: τ_n = neural lead term

No agreement could be obtained on the magnitude of the time constant τ_n , by considering the results of experimental research as described in the literature (Hosman and van der Vaart, 1978).

In 1976, Fernandez and Goldberg published the results from tests with squirrel monkeys, wherein the relation between input linear acceleration and output discharge rate of the corresponding primary neurons in the vestibular nerve was measured. The following model was matched to the measured transfer functions:

$$H_{oto}(\omega) = K \frac{1 + j\omega K_a \tau_a}{1 + j\omega \tau_a} \cdot \frac{1 + K_v (j\omega \tau_v)^{K_v}}{1 + j\omega \tau_m}. \quad (4.12)$$

Table 5. The parameters of the model of the otoliths.

| | |
|----------|----------------------------|
| K | 3.4 ips/m/sec ² |
| τ_n | 1 s |
| τ_1 | 0.5 s |
| τ_2 | 0.016s |

The first term of this equation is the adaptation term, whereas the denominator of the second term corresponds to a simplified description of the second order mass-spring-dashpot characteristics. The numerator of the second term describes the influence of the type I and type II cells, section 4.3.1. For both the regular and irregular cells the model parameters were presented (Fernandez and Goldberg, 1976). The model of Eq. (4.12), however, is not easy to use due to the broken exponential power K_v in the second numerator term. Therefore, the simplified model according to Eq. (4.11) will be used in this thesis. The model parameters are presented in Table 5. In Fig. 4.11 the Bode plot of the otoliths transfer function defined by Eq. 4.11 is presented.

5. VISUAL PERCEPTION OF AIRCRAFT ROLL ATTITUDE AND ROLL RATE

5.1 Introduction

From the discussion in Ch. 2, it was concluded that further research on the perception of aircraft motion by the pilot from the central- and peripheral visual field and cockpit motion was necessary, in order to obtain a better understanding of the changes in control behavior. In Ch. 3, it was shown that perception may be considered as multi- input single-output process, which is the first stage of the single information- processing channel. Changes in the response time of the information-processing channel result from factors affecting one or more of its stages. Clearly the most appropriate experimental task to investigate the complex motion-perception process is the stimulus-response task.

As has been shown in Ch. 4, the static and dynamic characteristics of the visual and vestibular systems are quite different. The same also holds for the apparatus to present visual and inertial stimuli to the subjects.

Electronic displays are much easier to manipulate when used to present motion stimuli than motion systems, such as rotating rooms, linear sleds and those used in flight simulation. The presentation of stimuli on electronic displays can be switched on and off at any desired instant and the velocity of the moving stimulus can be changed instantly. In contrast only the input acceleration of motion systems can be changed relatively fast, depending on the dynamic characteristics of the driving actuator. Due to these basic differences it was decided to first study visual motion perception using central and peripheral electronic displays. With these two displays the perception of roll attitude and roll rate were investigated. An experiment to determine the influence of inertial motion stimuli will be described in the next chapter.

Two experiments were designed and performed to determine the perception accuracy and reaction times of subjects who were to give accurate estimates of discrete visual stimuli. In Experiment I, discrete values of roll angle were presented foveally or in the central visual field. In Experiment II, discrete values of roll rate were presented foveally and/or peripherally. To investigate the influence of stimulus duration on perception accuracy and reaction time, the exposure times of the presented stimuli were systematically varied in both experiments.

Two important requirements in the selection of an output device for the subjects to answer to the stimuli in the two experiments must be mentioned. The first one is that the output signal generated should be suitable to measure the reaction time to the stimulus. Not only the value of the reaction time is important, but also its repeatability independent of stimulus magnitude and task conditions. The second is that the subject should be able to provide an estimate of the perceived stimulus with adequate accuracy. A special designed digital keyboard was the most appropriate solution to meet these requirements. Depressing a key marks the reaction time

while the key selected determines the estimated stimulus magnitude. With the digital keyboard quick and accurate reactions can be obtained.

In a number of experimental configurations, the displays were blanked after the exposure of the stimulus during the predetermined exposure time. In other configurations the displays were, immediately after the stimulus exposure, masked by displaying high frequency random motion. This masking was done to investigate whether there would exist, for attitude and/or rate perception, a so-called 'iconic memory' as established by Sperling (1963). Finally, for each display configuration an experimental condition, where the exposure time was equal to the reaction time, was added to the experiments.

The independent experimental variables of both the experiments were: Roll attitude or roll rate magnitude, the preselected exposure time, and the masking or blanking condition after stimulus exposure. For Experiment II, the display configuration (Central-, Peripheral- and Central and Peripheral displays combined) was added as an independent variable. The main dependent variables were perceived roll attitude or roll rate and the reaction time.

The question has to be raised whether changes in the reaction time due to changes in display configuration and exposure time should be attributed to the perception stage of the information processing channel alone. Firstly, it should be noted that the later stages of the information processing were not changed in the present experiments. Further, as discussed in Ch. 3, Sternberg (1969) argued that the effects of disturbances on individual stages of the information processing on the reaction time are additive. Thus, if the perception process in the present experiments needs a longer or shorter time interval, the reaction time should correspondingly be longer or shorter, and there is no need to expect any interaction with the decision or response stage of information processing.

Apart from possibly obtaining explanations for the results of the tracking experiments described in Ch. 2 and Ch. 7, it was hoped that reliable data on perception accuracy, minimum required exposure times and reaction times could be used to verify some assumptions underlying current mathematical models of the pilot's control behavior.

5.2 Experimental Test Procedure

As mentioned earlier, a stimulus-response technique was chosen to obtain information about perception accuracy, as well as reaction time of the roll attitude ϕ and the roll rate $\dot{\phi}$. All measurements were performed in a low noise room where, in front of the subject's seat, a central display was mounted in an instrument panel. This display simulated an artificial horizon, Fig. 5.1. The artificial horizon symbol was presented on the CRT with an update rate of 250 times a second. Such an update rate is, according to the limitations of the visual system, more than sufficient to perceive a moving image on the stroboscopic display as a real moving object.

Two black and white TV monitors with an interlaced field were used to present peripheral stimuli to the subjects. These monitors displayed a moveable checkerboard pattern, Fig. 5.2. The refresh and update rate of the pattern on the TV monitors was 30 times a second. When flicker has to be avoided, the higher refresh and update rate of the North American TV system (30 Hz) is, according to Rolfe and Staples (1986), preferable above the European TV system (25 Hz).

Subjects gave their response through a digital keyboard, Fig. 5.3. The relative position of the central and peripheral displays, the keyboard and the eye reference point are presented in Appendix 1.

During the experiments each run consisted of 100 presentations at fixed time intervals. The stimulus (roll attitude or roll rate) was displayed to the subject for a limited duration, Δt_{exp} . The sequence during one interval was as follows, Fig. 5.4.

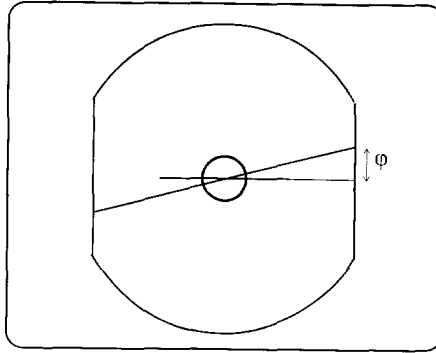


Figure 5.1 The CRT display with the presentation of the roll angle φ on the simulated artificial horizon.

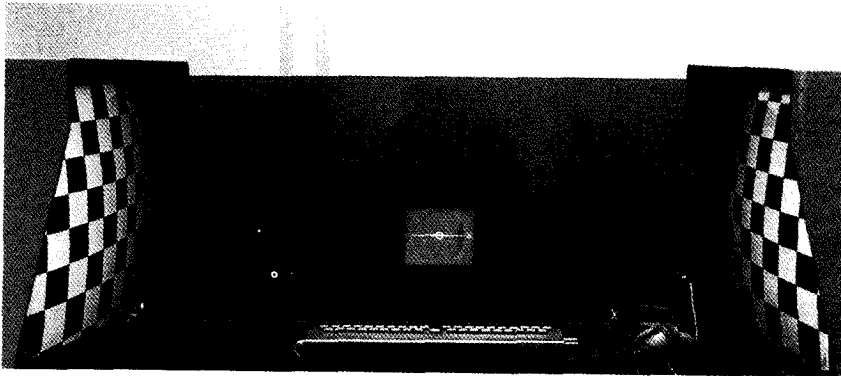


Figure 5.2 Overview of the experimental facility with the central display, peripheral display and the keyboard.

At the beginning of an interval, a new value e_{n_1} of the stimulus was presented, the event being marked by an audio tone in the subject's headset. After observation of the stimulus magnitude, the subject was required to respond by pressing the corresponding key of the keyboard, Fig. 5.3. The response magnitude is designated by ΔO_n . Immediately after the response the error value e_{n_2} was shown on the displays, thus giving the subject an immediate knowledge of the result. The relation between the stimulus magnitude e_{n_1} , the error value e_{n_2} and the response magnitude ΔO_n is:

$$\Delta O_n = e_{n_1} - e_{n_2} . \quad (5.1)$$

The exposure time Δt_{exp} could be varied and was set either at a constant value by the experimenter prior to each run, or was extended until the response of the subject. In the first condition, the stimulus e_{n_1} was made to disappear at the end of the preset exposure time.

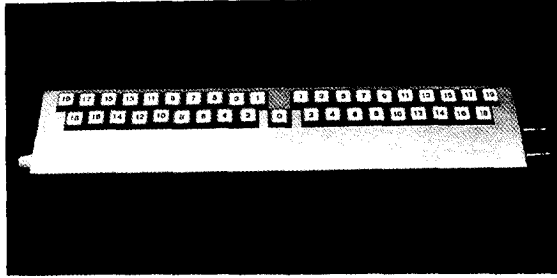


Figure 5.3 The digital keyboard.

Subjects were then required to give responses only after the termination of the exposure, while responses during the exposure time were neglected by the computer program. Termination of the exposure could be programmed in either two ways. Apart from simply 'blanking' the display, an additional feature of the test facility was that immediately after exposure, the central display and the peripheral display could be masked.

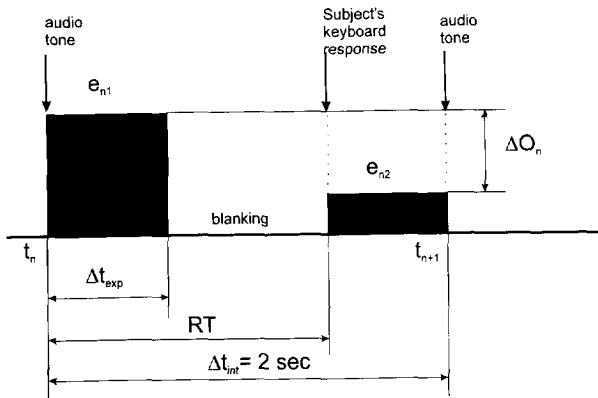


Figure 5.4 Sequence of one interval of a test run.

The central display was masked by a horizontal line randomly moving up and down. This was controlled by a wide band, 5 Hz, zero mean noise signal. The peripheral displays were masked by making the checkerboard pattern move randomly up and down by the same random signal.

At the start of the next interval, a new value of the stimulus was generated by adding a quantified sample i_n of a noise signal to the latest (n-1) value of the error value e_{n_2} :

$$e_{n_1} = e_{(n-1)_2} + i_n . \quad (5.2)$$

The standard deviation of the noise signal from which the sample i_n was taken, and the scaling of the display was chosen such that the number of discrete values and the practical range of i_n , e_{n_1} , e_{n_2} , ΔO_n during the experiments remained within the range and number of keys on the keyboard device. The 21 different values of the stimulus corresponded with the keys (zero ± 10) of the keyboard. The distribution of the stimulus was normal.

During each run, the variables i_n , e_{n_1} , e_{n_2} , ΔO_n and the subject's reaction time, RT, were recorded. After the run, the following values were calculated: the number of times a stimulus value j was shown, $n s_j$, the sum of observation errors per stimulus value j , $n e_j$, the mean value and variance of i_n , e_{n_1} , e_{n_2} , ΔO_n , the reaction time RT and a score parameter Sc defined by:

$$Sc = \sigma_{e_{n_2}}^2 / \sigma_{e_{n_1}}^2, \quad (2.6)$$

indicating a dimension less performance index.

5.3 Experiments

5.3.1 Experiment 1: The perception of roll attitude

In the experiment concerning the perception of the roll attitude, the central display was used to present the roll attitude on a simulated artificial horizon, Fig. 5.1. The parameters chosen were the range of the roll attitude φ , and the particular exposure times Δt_{exp} . The interval time of one sequence was determined at 2 s.

To keep the displayed roll attitude within the range representative for normal transport aircraft operation (± 30 degrees), the standard deviation of the stimulus roll attitude was chosen at $\sigma_\varphi = 10$ degrees. The range of keys to be used on the keyboard was set at ± 10 degrees, corresponding with ± 30 degrees of roll attitude on the central display.

The choice of exposure time Δt_{exp} , was based on the following considerations. Sperling (1963) demonstrated that a number of letters could be read correctly within an exposure duration ≥ 50 ms. During some preliminary tests with the present experimental setup, it turned out that reasonably accurate estimates of the roll attitude could be made at exposure times down to 20 ms.

From the research on pilot scanning behavior it is known that 'dwell times' on primary flight instruments such as the artificial horizon, are in the range of 400 to 800 ms, which is rather long compared to the short exposure time just mentioned.

Considering these results the range of the exposure times tested was chosen to include the short exposure times from Sperling as well as the larger dwell times. The largest exposure time was made equal to the subject's reaction time by disabling the exposure-duration mode of the controlling computer program. The lowest exposure time was set at 40 ms which is 10 times the display refresh interval. Five exposure times were chosen: $\Delta t_{exp} = 40, 60, 80, 100$ ms, and a period equal to the reaction time RT.

From Sperling (1963) it is known that the perception of characters deteriorates if, immediate after the exposure, a stationary image consisting of random dots (visual noise) is exposed.

This procedure called 'masking' destroys the image in the short-term visual store or iconic memory. To investigate the influence of the iconic memory on the perception process, it was decided to add masking to the experimental conditions. As discussed in Sect. 5.2, masking was achieved by displaying a randomly vertically moving horizontal line immediately after the stimulus exposure. The exposure times for the masking condition were the same as those with blanking.

5.3.2 Experiment 2: The perception of roll rate

Three display configurations were used to investigate the perception of roll rate. Central display only (C), Peripheral displays only (P) and Central and Peripheral displays combined (CP). The interval time was set at 2 seconds, as used in Experiment 1. The range of roll rate presented was again chosen to be representative for normal airline operation ($\dot{\phi} = \pm 25$ degrees/s). The standard deviation of the stimuli was set at $\sigma_{\dot{\phi}} = 8$ degrees/s. As before, the range of keys to be used on the keyboard was set at ± 10 corresponding with ± 25 degrees/s on the display.

To set the range of exposure times to be studied, a preliminary experiment was run, (Hosman and van der Vaart, 1982). In that experiment exposure times between 0.2 and 0.5 s were used. Furthermore, pre-experimental evaluation showed that by using exposure times between 0.1 and 0.4 s the roll rate perception process and thus the score parameter S_c could be influenced over a wide range for all three display configurations. With the update rate of the peripheral displays of 30 Hz, the three frames during the exposure time of 0.1 s were considered as a minimum for the present tests. As in experiment 1, the longest exposure time was chosen equal to the subject's reaction time, the others were set at 100, 150, 200, 300 and 400 ms. In this way 18 experimental conditions were obtained; 3 display configurations (C, P and CP) and 6 exposure times.

The question was raised whether for rate perception there would also exist a short-term sensory store or iconic memory. Therefore, the experiment was extended with the masking feature. This added another 15 conditions to the experiment for a total number of 33.

5.3.3 Subjects and test procedure

Experiment 1

Two subjects, both qualified airline transport pilots, participated in the experiment. They were instructed to respond primarily as accurate as possible and secondly as fast as possible to the presented stimuli. They were required to fixate on the central display after answering to a stimulus on the keyboard, but were free to look at the keyboard to respond to the stimulus.

Apart from the immediate feedback of the remaining error after each keyboard response, subjects were informed of the score parameter S_c , and their mean reaction time after each run. The experience gained by executing experiments with subjects in our laboratory shows that in stimulus-response perception tasks as well as in tracking tasks, subjects reach the best performance when they are informed about their experimental results. During the training, subjects are informed about the general and best performance of all subjects participating in the experiment. During the execution of the experiment they are informed only about their own performance. In this way, subjects are encouraged to maintain their performance during the experiment at the level of the best performance during the training.

Subjects were trained until a steady level of performance was reached. For the first experiment, 180 training runs were performed. The final experiment was accomplished in a series of 5 morning sessions for each subject. All 9 experimental conditions were presented in a random order during one morning session. 90 runs were made for this experiment (2 subjects, 9 conditions, and 5 replications).

Experiment 2

Three subjects, two of which took part in Experiment 1, and a staff-member pilot of the Netherlands Department of Civil Aviation, participated in this experiment. The instructions were basically the same as in Experiment 1.

Over 400 training runs were performed before adequate steady performance of the subjects was reached. The total number of experimental conditions was 33.

The experiment was performed during morning sessions. Each subject performed all experimental configurations 5 times. The number of sessions differed over the subjects due to the large number of experimental conditions and depending on subject's availability. A total of 495 runs (3 subjects, 33 conditions, and 5 replications) were made to complete the experiment.

In the sense of Experimental Design, both experiments were set up as a Randomized Factorial Design. The experimental configurations were considered to be fixed independent variables when applying the ANOVA on the output variables. The subjects, however, represent a random sample from a population of subjects. Therefore, the influence of the subjects had to be considered as a random variable in the ANOVA. Hence, the ANOVA has to be based on the mixed effects model (Hays, 1963 and Kirk, 1968). A summary of the ANOVA results, the statistical significance of the influence of the independent variables and their interactions on the dependent variables, will be presented.

5.4 Results

5.4.1 Experiment 1, Roll attitude perception

The mean and standard deviation of the main output variables, the score S_c , and the reaction time RT are presented in Figs 5.5 and 5.6. The experimental condition with the exposure time equal to the reaction time was considered as the standard condition. In the case of blanking the performance parameter, S_c , is hardly affected by the exposure time Δt_{exp} . Masking affected the performance at the smaller exposure times.

There is no significant influence of masking, and exposure time on the reaction time RT , Fig. 5.6. The subjects have a significant different mean reaction time. The interaction between subjects and exposure time on the reaction time RT is significant. An overview of the results of the analysis of variance, ANOVA, is presented in Table 6.

In Fig. 5.7, the mean of the absolute error $e_{n_2} = \Delta\phi$ of the standard condition as a function of stimulus magnitude is presented. The error magnitude increases with stimulus magnitude, roll angle ϕ . An overview of the experimental data is presented in Appendix 1.

Table 6. Results of the ANOVA for roll attitude perception.

| Main effects | S_c | RT |
|---|-------|----|
| Exposure time $\Delta t \text{ exp}$ | * | - |
| Blanking-Masking | - | - |
| Subjects | - | ** |
| Replications | - | * |
| Interactions: | | |
| $\Delta t \text{ exp} \times S$ | - | ** |
| B-M $\times S$ | - | - |
| $\Delta t \text{ exp} \times \text{B-M}$ | * | - |
| $\Delta t \text{ exp} \times \text{B-M} \times S$ | - | - |

$\alpha < 0.05$ *
 $\alpha < 0.01$ **

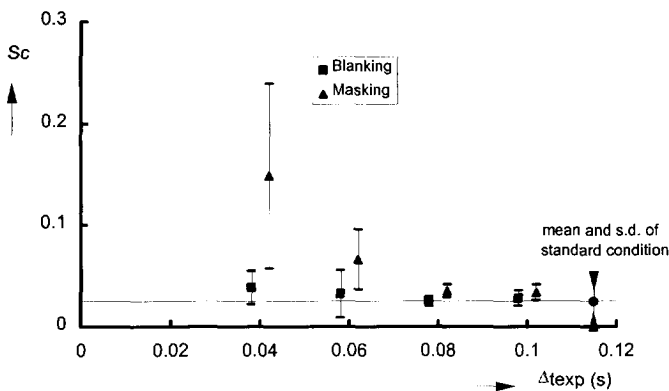


Figure 5.5 Score parameter for roll attitude perception.

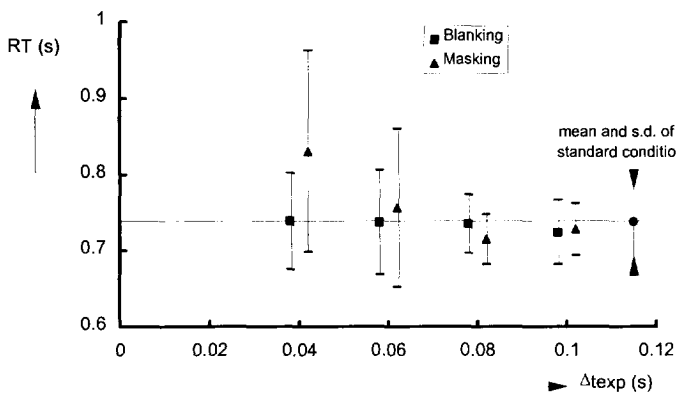


Figure 5.6 Reaction time for roll attitude perception.

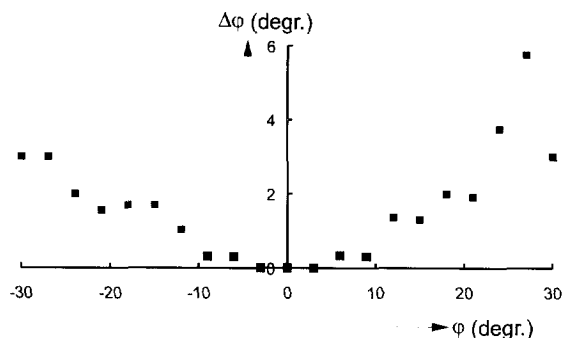


Figure 5.7 Mean absolute perception error $\Delta\phi$ as a function of stimulus roll angle ϕ , standard condition $\Delta t_{exp} = RT$.

5.4.2 Experiment 2, Roll rate perception

The score parameter for roll rate perception is presented in Figs 5.8 and 5.9 for the blanking and the masking condition respectively. Rate perception from the central display with the exposure time Δt_{exp} equal to the reaction time RT is considered as the standard condition.

There is a clear difference between the score S_c for roll rate perception from the central display (C), the peripheral displays (P), and the combined central and peripheral displays (CP), Fig. 5.8. From the peripheral displays a more accurate roll rate perception is obtained, especially at the short exposure times.

The exposure time Δt_{exp} has a strong influence on the score parameter for all three display configurations. Roll rate perception from the central display needs a much longer exposure time, 0.3 seconds, to reach the final accuracy than from the peripheral displays, 0.15 seconds. In addition, the required exposure times to perceive roll rate are much longer than to perceive roll angle in Experiment 1, Fig. 5.5.

Masking influences the roll rate perception at the small exposure times ($\Delta t_{exp} = 0.1, 0.15$ and 0.2 s.). In the case of the combined display configuration, CP, subjects apparently are not able to derive any additional information from the peripheral displays at $\Delta t_{exp} = 0.1$ s.

As a result of the characteristics of the motion detectors of the visual system, as discussed in Ch. 4, there is a minimum exposure time for each stimulus magnitude necessary to pass through the span of the bilocal detector, Fig. 4.1. When the stimulus does not pass the span it will have an adverse influence on the perception accuracy. Given the minimum span of the motion detectors, the dimensions and velocity of the stimuli on the displays, and the positions of the displays relative to the eye reference point, this indeed may cause a decrease in the perception accuracy at low values of the exposure time.

For the central display the smallest stimulus of 2.5 deg/s roll rate needs an exposure time of 250 ms to pass through the span of the bilocal detector. This quite well confirms the decrease in score S_c with increasing exposure time as shown in Fig. 5.8. For the peripheral displays this minimum exposure time is approximately 265 ms. The data presented by van de Grind et al. (1986) were based on two subjects only and have to be considered as an indication for the span of the bilocal detector in the foveal and peripheral visual field. Thus the geometry of the

experimental setup together with the bilocal detector characteristics may be considered to cause the increase in the score parameter as a function of the decreasing exposure time Δt_{exp} .

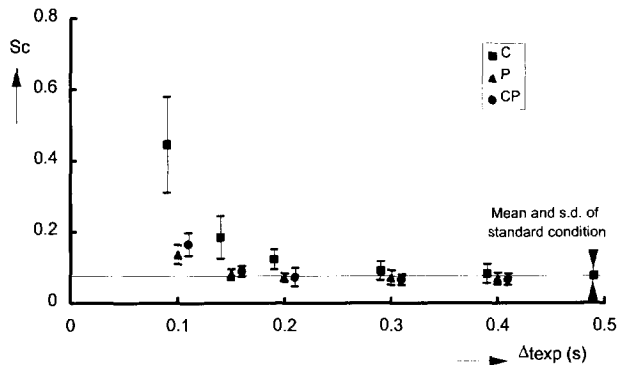


Figure 5.8 Score parameter S_c for blanking after stimulus exposure as a function of exposure time Δt_{exp} and display configuration.

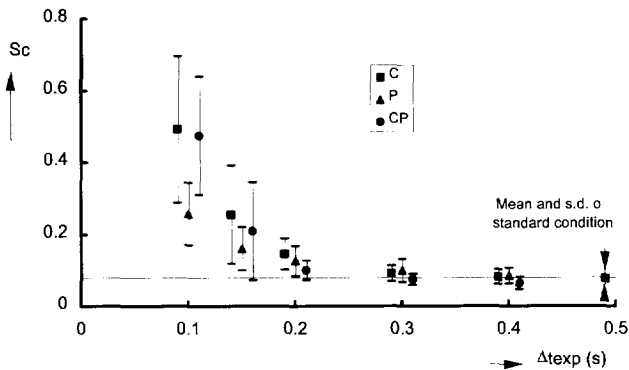


Figure 5.9 Score parameter S_c for masking after stimulus exposure as a function of exposure time Δt_{exp} and display configuration.

In Table 7, an overview of the results of the ANOVA for the score S_c and the reaction time RT are presented. The main effects, Subjects, Display Configurations and Exposure Time, have a significant influence on the score S_c . Masking as a main effect has no influence at all, but the interactions between masking and exposure time and masking and display configurations may have a significant influence. The significant interactions between subjects and exposure time, display configuration and masking show that the subjects react different on these main effects.

Table 7. Results of the ANOVA on the score parameter S_c and the reaction time RT.

| Main effects | S_c | RT |
|--------------------------------|-------|----|
| Subjects | ** | ** |
| Exposure time Δt_{exp} | ** | - |
| Display Configuration | * | * |
| Blanking-Masking | - | - |
| Replications | * | - |
| Interactions: | | |
| Δt_{exp} , S | ** | ** |
| DC, S | ** | ** |
| BM, S | ** | ** |
| Δt_{exp} , DC | ** | - |
| Δt_{exp} , BM | * | * |
| DC, BM | * | - |
| Δt_{exp} , DC, S | ** | ** |
| Δt_{exp} , BM, S | ** | - |
| DC, BM, S | - | - |
| Δt_{exp} , DC, BM | ** | - |
| Δt_{exp} , DC, BM, S | * | - |

$\alpha < 0.05$ *

$\alpha < 0.01$ **

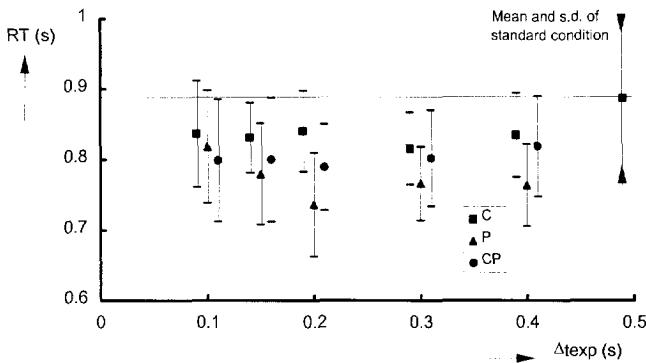


Figure 5.10 Reaction time to roll rate stimuli with blanking after stimulus exposure as a function of exposure time and display configuration.

In the Figs 5.10 and 5.11 the reaction times RT are shown as a function of exposure time and display configurations. The mean values of the reaction times are shorter than for the standard condition. The reaction times for rate perception from the central display are longer than for the conditions with the peripheral displays, P, and the central and peripheral displays, CP. In the Table 8 the mean reaction times for $\Delta t_{exp} = 0.3$ and 0.4 s are presented.

According to the ANOVA, there is a significant difference between the reaction times of the subjects. The display configurations may have a significant influence on the reaction time. Further analyses show that the reaction time for the peripheral displays is significantly shorter than for the two other display configurations. Masking does not have a general influence on the reaction time.

Table 8. Mean reaction times for $\Delta t_{exp} = 0.3$ and 0.4 s.

| Display Configuration | Blanking RT (s) | Masking RT (s) |
|---------------------------------|--------------------|-------------------|
| Central display | 0.82 | 0.84 |
| Peripheral displays | 0.76 | 0.73 |
| Central and Peripheral displays | 0.81 | 0.79 |

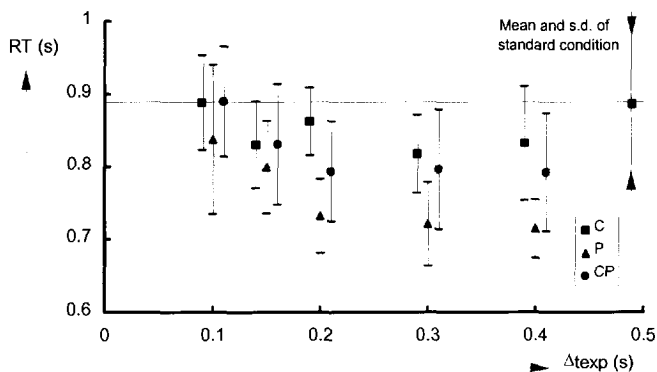


Figure 5.11 Reaction time to roll rate stimuli with masking after stimulus exposure as a function of exposure time and display configuration.

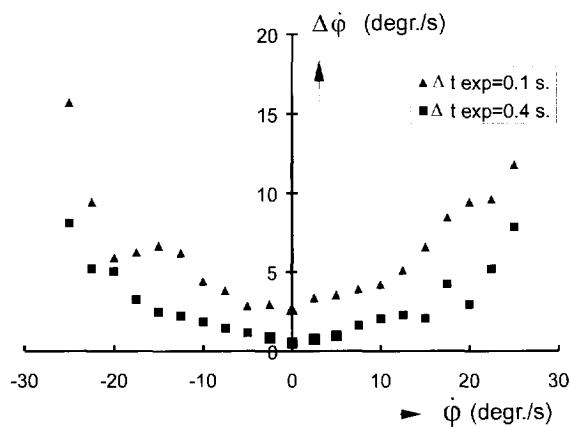


Figure 5.12 Mean absolute error of perceived roll rate as a function of stimulus roll rate. Central display, blanking.

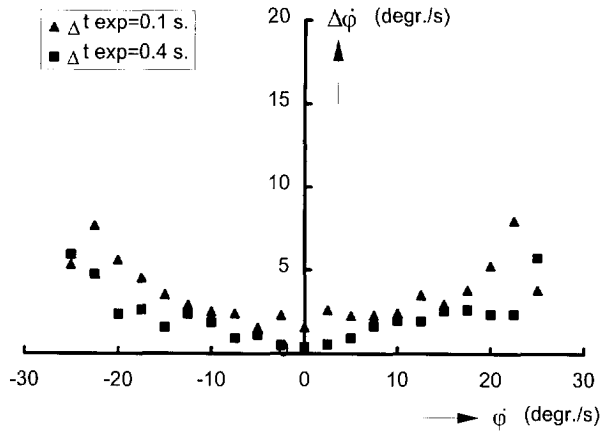


Figure 5.13 Mean absolute error of perceived roll rate as a function of stimulus roll rate. Central and Peripheral display, blanking.

In Figs 5.12 and 5.13, some examples are presented of the mean absolute error of the perceived roll rate, $\Delta\dot{\phi}$, plotted as a function of stimulus roll rate $\dot{\phi}$ for the display configurations C and CP and exposure time $\Delta t_{exp} = 0.1$ and 0.4 s. The perception error is increasing with stimulus magnitude, the roll rate. Decreasing exposure times Δt_{exp} tend to shift these curves upwards to larger values of $\Delta\dot{\phi}$.

An overview of the experimental data is presented in Appendix 1.

5.5 Discussion and conclusions

Experiment 1, Roll attitude perception

Roll attitude can be perceived after an exposure time of 40 ms. The reaction time is approximately 0.73 s. From the results it is evident that the perception accuracy expressed by the score S_c and the reaction time RT is not influenced by the exposure time Δt_{exp} when the display is blanked after stimulus exposure. Masking has an influence on both parameters only for the shortest exposure times, $\Delta t_{exp} = 0.04$ and 0.06 s.

From the results it appears that the reaction time increases when the uncertainty about the perceived stimulus increases. This is, in particular, evident where a high error score at $\Delta t_{exp} = 0.04$ s, combined with a large spread due to masking, reflects such a high uncertainty. This situation indeed corresponds with longer reaction times, Figs 5.5 and 5.6. This result is confirmed by Vickers and Packer (1982).

Experiment 2, Roll rate perception

From the results it appears that the roll rate can be perceived from the central display almost as accurately as from the peripheral displays. The perception accuracy of the combined central-peripheral configuration, CP, is better than for the individual display configurations, C and P, in the case of longer exposure times, $\Delta t_{exp} > 0.2$ s. For these exposure times, where the

full span of the motion detectors have been passed through by the stimuli, the subject's were able to improve their perception accuracy by using the central and the peripheral information. The reaction times for the peripheral displays, RT_p , and the central and peripheral displays, RT_{CP} , are shorter than the reaction times for the central display, RT_C . The difference in reaction time for peripheral- and central visual stimuli is approximately $RT_p - RT_C = 60$ ms. This magnitude corresponds quite well with the data published by Harter and Aine (1984). In addition a shorter exposure time suffices for accurate roll rate perception when the peripheral displays are involved. As suggested in the introduction, it indeed appears that the change in reaction time results from a change in the perception stage of the information processing due to changes in display configuration.

The influence of masking on the perception process seems rather complicated. The score parameter increases for the shorter exposure times and roll rate perception becomes less accurate. The score for central and peripheral displays, CP, tends to the score of the central display, C, only. This is in contrast to the result for blanking.

Differences in roll attitude and roll rate perception

The results reveal a number of differences in the perception of roll attitude and roll rate, all tending to the conclusion that rate perception is a more difficult task than attitude perception especially when only the central display is used.

Firstly, attitude perception can be done at much shorter exposure time (typical value being 0.05 s.) than roll rate perception (exposure times in the order of 0.30 s.). More- over, reaction times for roll rate perception from the central display are significantly longer (100 to 150 ms.) than for attitude perception. The greater difficulty of roll rate perception is also reflected by the performance in the standard conditions as expressed by the score parameter (0.024 for attitude perception and 0.077 for rate perception, both for the central display only).

All these differences are to be attributed to differences in the perception stage only, as the experimental task structure and output device were exactly the same in both experiments.

Some classic, well-documented results from visual tracking tasks with a central display only can be explained by the above distinctions between roll attitude and roll rate perception. It has long been shown by McRuer et al. (1965,1969) that measured transfer functions for subjects controlling a single, or double integrator in a target following task, can well be approximated by:

$$H_{p_1}(\omega) = K_p e^{-j\omega\tau_1}; \quad (5.3)$$

$$H_{p_2}(\omega) = K_p (1 + T_L j\omega) e^{-j\omega\tau_2} \cong K_p j\omega e^{-j\omega\tau_2}, \quad (5.4)$$

where, in the case of a forcing function bandwidth of 1.5 rad/sec, $\tau_1 = 0.24$ s and $\tau_2 = 0.38$ s, Fig. 7.11.

Evidently, Eq. (5.3), a subject controlling a single integrator, will primarily observe the presented error signal itself, whereas a subject controlling a double integrator, Eq.(5.4), will observe the time derivative as the *primary* variable. Remembering the difference between continuous tracking and stimulus response type observation tasks, together with the approximative nature of Eqs (5.3) and (5.4), the difference in experimentally obtained time constants $\tau_2 - \tau_1 = 0.14$ s can well be explained by the response times for rate perception, which were found to be about 0.10 to 0.15 s longer than for attitude perception.

From the results presented it is concluded that:

- Roll attitude perception is more accurate than roll rate perception.
- The reaction time for roll attitude perception is shorter than for roll rate perception.
- The exposure time needed for an accurate roll rate perception is much longer than for attitude perception.
- The perception stage for roll rate perception from the peripheral visual field has a shorter duration than that from the central visual field.
- The perception of roll rate from the peripheral visual field and the central visual field are different processes.

6. PERCEPTION OF COCKPIT MOTION WITH THE VISUAL AND THE VESTIBULAR SYSTEM

6.1 Introduction

The aim of the experiments described in this chapter is to obtain a better understanding of the visual-vestibular perception of vehicle or aircraft motions by the pilot. As shown in Ch. 4, there is a relatively good knowledge about the visual system and the dynamic characteristics of the components of the vestibular system, the semi-circular canals and the otoliths. There is, however, little understanding on how the vestibular output contributes to the notion of motion perception. This is an implication of the very complex interaction between the visual and vestibular system to support essential functions as perception and control of self motion, stabilization and control of eye movements, and posture control.

As shown in Ch. 3, control information is processed consciously by the human operator through a single information processing channel. The total duration of the processing depends on the sum of durations of the individual stages of this process. By using the Additive Factors Paradigm as the analysis tool (Sternberg, 1969), it is possible to obtain knowledge about the different stages of the information processing and/or about changes in individual stages due to the different task factors and their variations, Section 3.2. This knowledge, however, is obtained by comparing results. Hence, this method does not provide absolute data. Thus, if the additive factor method is used to study the vestibular motion perception, the results have to be compared with an alternative motion perception mode: the visual motion perception. In this chapter, stimulus response experiments will be described to study the speed and accuracy of motion perception with the vestibular system in relation to the motion perception with the visual system.

As already mentioned in the introduction of Ch. 5, there is not only a fundamental difference between the dynamic characteristics of the visual- and the vestibular system, but also between the systems available to stimulate the visual- and vestibular system: electronic displays and motion systems. In contradiction to electronic displays, simulator motion systems have mass and dynamic characteristics. The choice of the motion-input to the subject is limited by the characteristics of the simulator motion system. It is not possible to present or manipulate attitude, rate and acceleration independently, since these variables are related with each other by the equations of motion of the simulator motion system.

The motion stimuli used to evaluate the visual-vestibular interaction in the present research had to be representative for aircraft motions in response to the pilot's control actions. The attitude of an aircraft is controlled by the inner-loop attitude control. In normal aircraft control the pilot controls the aircraft state by small attitude changes. The symmetric and asymmetric motions of an aircraft are described by two sets of four first order simultaneous equations. These equations reduce to second order equations describing the short term response of the

aircraft attitude to the pilot's control inputs. After some evaluation, the step response of a second-order system with a natural frequency in the range of the aircraft dynamic characteristics (symmetric short period mode and asymmetric roll control) and good damping was chosen as the roll input stimulus to the subjects. Combinations of the central- and peripheral displays and cockpit motion were used to present the stimulus to the subjects in the experiments. After stimulus onset, the subject was asked to predict the final magnitude of the step response and to answer by pressing the corresponding key on the keyboard, Sects 6.2 and 6.3. Subject's response corrected the initial input to the second-order system and the resulting output was displayed thus presenting a direct feedback of the remaining perception error to the subject.

In Fig. 6.1, the visual and vestibular pathways for the stimulus-response task are shown. When the step input at point A is known then the time course of the roll angle, roll rate and roll accelerations at point B can be determined. By compensating the control of the simulator motion system for its dynamic characteristics and by avoiding

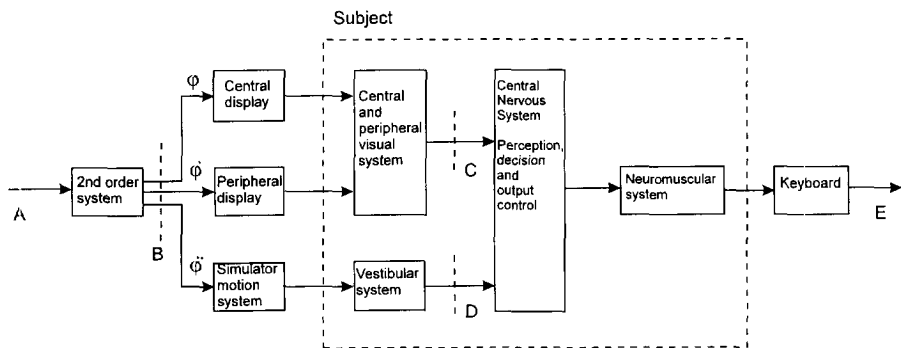


Figure 6.1 The visual and vestibular pathway for stimulus information in the stimulus response experiment.

unnecessary time delays, these time courses can be displayed to the subject hardly undistorted. When the dynamic characteristics of the visual and the vestibular system are known, the sensory output at the points C and D can be derived by simulation. They may be considered as motion sensations or sensory outputs. The sensory outputs are the neural inputs to the final perception process in the central nervous system. Comparison of these inputs with the subject's response on the keyboard (perceived step magnitude and reaction time) at E, provide the information on how the different stimuli interact in the perception process. This approach is the procedure applied to obtain information on how the visual- and vestibular stimuli influence the perception process.

In the previous chapter, the visual perception of roll attitude and roll rate has been investigated. The results obtained are valid for the visual perception of steady roll- attitude and roll-rate stimuli. Due to the characteristics of the vestibular system and the motion systems to generate the stimuli, a dynamic stimulus has to be used to stimulate the visual and the vestibular system. The second-order system step response, which will be used as the stimulus, provides a constantly changing roll attitude, roll rate, and roll acceleration. The subject has to estimate the final magnitude from this stimulus. The first question which arises is whether the results of the experiments in the previous chapter correspond with or may be extrapolated to the visual perception of the dynamic stimulus. The second question is whether

the differences between the dynamic characteristics of the visual and the vestibular systems influence the speed and accuracy of the motion perception. The third question is whether the interaction between the sensor dynamics, on the one hand, and the dynamic characteristics of the stimulus generating second-order system, on the other hand, interact on the perception process. If that should be the case then the experimental results depend on the motion generating dynamics: the vehicle or aircraft dynamics.

To obtain the answers to the above questions, three experiments were designed. The first experiment was directed to the visual perception of the stimulus and the estimation of the step magnitude by using the central and the peripheral displays. From this experiment, the minimum required exposure time to obtain an accurate magnitude perception was determined. In addition, the difference between the perception of motion by the central- and peripheral visual system for dynamic stimuli was evaluated.

The second experiment was directed to the differences in perception accuracy and reaction time as a function of the display configuration. This experiment was performed with the same second-order system characteristics, as in the first experiment. The results of this experiment demonstrated a strong influence of the vestibular system on the speed of perception.

The third experiment was designed to extend the results of the second experiment and to demonstrate the influence of the vehicle dynamics on motion perception. In addition, the results prove that the strong influence of the vestibular system on the reaction time clearly results from the dynamic characteristics of the semi-circular canals.

In this chapter, the visual and vestibular response to the stimulus will be evaluated by simulation in Sect. 6.2. Then the experimental facility and the experiments will be described in Sections 6.3 and 6.4. After the subjects and test procedures are described, in Sect. 6.5, the results will be presented in Sect. 6.6. The chapter concludes with a discussion and conclusions.

6.2 Visual and vestibular perception of the step response stimulus.

In Ch. 4, the visual and vestibular system have been described in their function as motion sensors. As discussed in the previous section, to investigate the differences between the motion perception with the visual and vestibular system, a second-order system step response will be used as the input in a stimulus-response experiment. The response of the basic second-order system with $\omega_n = 2$ rad/sec and $\zeta = 0.7$ is presented in Fig. 6.2.

The advantage of the step response as a stimulus is that after some time a steady roll attitude is reached. The task of the subject was to estimate the final steady value of the roll angle. As shown in Fig. 6.2, the roll acceleration starts at an initial value ($4^\circ/\text{sec}^2$ for a 1 degree step input). The roll attitude, roll rate, and roll acceleration stimulate the central and peripheral visual system and the semi-circular canals. In addition, the roll acceleration causes an initial lateral linear acceleration of the subject's head when the subject's head is out of the axis of rotation. For larger step inputs this acceleration is above threshold and will be sensed by the otoliths. It is therefore necessary not only to look at the semi-circular canal output but also at the otoliths output.

Considering the models described in Ch. 4, the response of the visual- and vestibular system to the stimulus will be evaluated first by a computer simulation.

The perception of motion in the visual field with the bilocal motion detector, Sect. 4.2, can be described by the transfer function:

$$H_{\text{velocity}}(\omega) = Ke^{-j\omega(\tau_1 + \tau_2)} \quad (4.4)$$

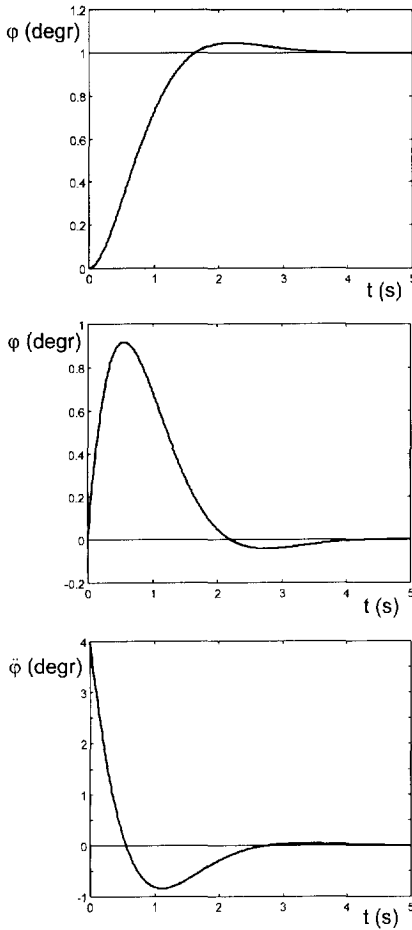


Fig. 6.2 Attitude, rate and acceleration of a second-order system step response.

In this transfer function K is assumed to be equal to 1, τ_1 ($= 0.065$ s) is a characteristic of the bilocal motion detector and τ_2 equals the sum of the neural processing time and transmission time from the retina to the visual cortex. Based on the data of Tynan and Sekuler (1982), and Ball and Sekuler (1980), van den Berg and van de Grind (1989) have shown, that when motion has to be perceived from a visual stimulus the reaction time RT is:

$$RT = RT_0 + S/V, \quad (6.1)$$

where RT_0 is the minimum reaction time which incorporates τ_2 , S is the span of the bilocal detector and V is the stimulus velocity. The minimum reaction time RT_0 reported is 185 msec and $S/V = \tau_1$. The minimum value of $\tau_1 = 65$ msec, Sect. 4.2.2. Thus the minimum reaction time to motion stimuli is 250 msec which is part of the total time between the start of the stimulus until the reaction of the subject.

The results of the motion perception experiment, described in Ch. 5, show that the reaction time for roll rate perception is 100 to 150 msec longer than for roll attitude perception. McRuer et al. (1965, 1969) described tracking experiments with controlled elements with first and second order dynamic characteristics. He concluded that the time delay τ in the Simplified Precision Model increased by 140 msec when changing the controlled system dynamics

from a first-order to a second-order system. This means that the change from attitude perception to rate perception in the tracking task increases the effective time delay by 140 msec. In Ch. 5 it was shown that the above-mentioned data corresponded quite well. Considering these data, the total time delay in the transfer function of Eq. (4.4) is assumed to have a value of at least 150 msec. In Fig. 6.3, the response of the visual motion sensor to the step response stimulus is presented together with the stimulus roll rate $\dot{\phi}$.

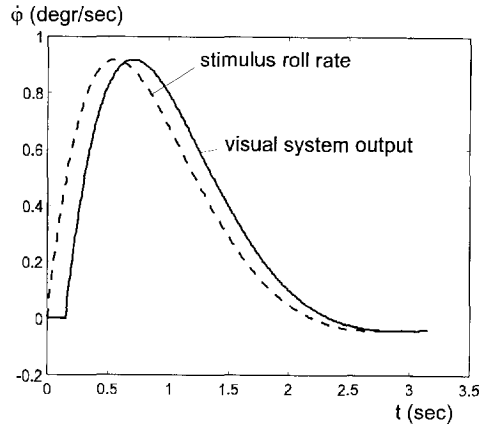


Fig. 6.3 The stimulus roll rate and the visually perceived roll rate.

Strictly speaking, the vestibular system is sensitive only to input angular acceleration and specific force. The output of this organ may be expressed as changes in output firing rate (impulses per second, ips), or more general as sensory output.

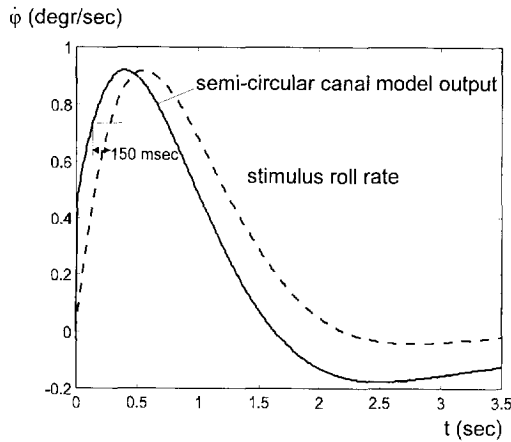


Figure 6.4 The simulated semi-circular canal response to the stimulus angular rate. The response leads the stimulus rate by approximately 150 msec.

As discussed in Ch. 4, the transfer function relating input angular acceleration with the semi-circular canal output firing rate is:

$$H_{sc}(\omega) = \frac{K(1 + j\omega\tau_L)}{(1 + j\omega\tau_1)(1 + j\omega\tau_2)}, \quad (4.8)$$

where:

τ_L = neural lead term;

τ_1 and τ_2 are time constants of the overdamped torsion pendulum.

The output of the semi-circular canals is strongly related to the angular rate. This is a result of the integrating character in the frequency range between 0.1 and 10 rad/sec as shown by the bode plot of the semi-circular model in Fig. 4.10. The second-order system roll rate $\dot{\phi}$ and the semi-circular canals response is, after scaling to approximately the same magnitude, compared in Fig. 6.4. The semi-circular canal response leads the stimulus angular rate by approximately 150 msec.

When comparing the output of the semi-circular canals with the visual perceived roll rate, Figs 6.3 and 6.4, clearly the vestibular output advances the visual output by approximately 300 msec. This time advance Δt suggests an important advantage of vestibular motion perception when compared to visual motion perception.

During the roll step the subject will perceive a specific force A_y along the lateral Y axis with the otoliths. The subject was seated in the simulator cockpit in the right hand seat with his head a distance $l = 0.8$ m above the simulator cockpit longitudinal axis.

When the cockpit moves according to the step response, the subject's head will be accelerated due to the roll acceleration. In addition, when the cockpit rotates to a roll angle ϕ the component of the gravitational force g along the lateral axis will act on the otoliths. The total specific force resulting along the lateral Y axis then is:

$$A_y(t) = \ddot{\phi}(t) \cdot l - g \cdot \sin \phi(t) = f\{\phi(t)\}. \quad (6.2)$$

where: l = the distance of the subject's head above the rotational axis
 g = gravitational force

According to Ch. 4, the transfer function of the otoliths model describing the relation between otoliths input specific force and output firing rate is:

$$H_{oto}(\omega) = \frac{K(1 + \tau_n j\omega)}{(1 + \tau_1 j\omega)(1 + \tau_2 j\omega)} \quad (4.11)$$

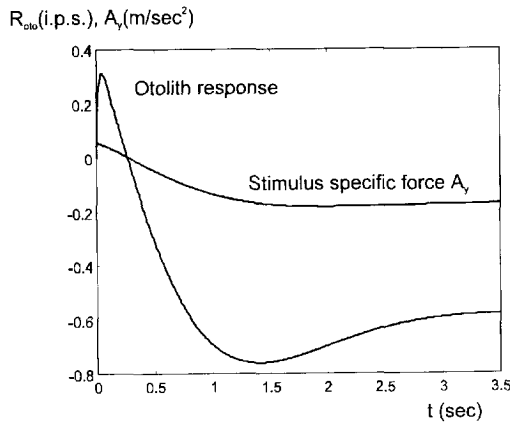


Figure 6.5 The simulated stimulus input specific force A_y and the otoliths response.

In Fig. 6.5, a computer simulation of the specific force A_y and the otoliths firing rate due to a roll step input of 1 degree is shown.

The stimulus at the start of a 1 degree step input is approximately equal to the threshold for specific force (Hosman and van der Vaart, 1978). Thus, for larger step inputs, the resulting specific force may be perceived by the subject. There is, however, no direct relation between the time course of A_y and the rotational rate, Fig. 6.2. It is, therefore, not expected that the perception of the lateral specific force A_y helps the subject to estimate the step magnitude. Possibly at the initiation of the step, the subject perceives a (strong) alerting cue due to the onset of A_y .

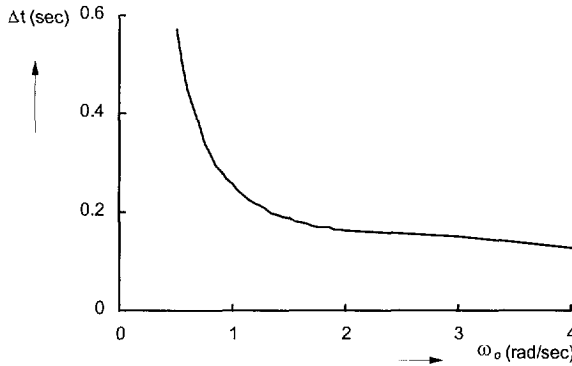


Figure 6.6 The time advance Δt of the semi-circular canal output relative to the roll rate $\dot{\phi}$ as a function of the natural frequency ω_0 of the second-order system.

To examine the influence of the natural frequency ω_0 of the second-order system on the time advance Δt of the semi-circular canal output relative to the stimulus rate, the time advance was computed as a function of ω_0 , Fig. 6.4. The results are plotted in Fig. 6.6. This figure clearly demonstrates that the advantage of the vestibular motion perception relative to the visual motion perception improves, when the natural frequency of the second-order system decreases. This means that the advance of the vestibular system in motion perception is larger for slower moving vehicles. The only restriction is that the vestibular input acceleration must exceed the sensation threshold.

6.3 Experimental facility

The three experiments on the perception of cockpit motion were performed in the flight simulator of the Faculty of Aerospace Engineering. The instrumentation used to present the stimuli, the central and the peripheral displays, were the same as before in Ch. 5. The motion system of the simulator was a three degrees of freedom (pitch, roll and heave) motion system (den Hollander, 1977). The keyboard, used in the experiments of Ch. 5, was applied to generate the subject's output. Appendix 1 gives a description of the instrumentation and the motion system compensation. During the measurement runs the subjects placed the keyboard on their knees, Fig. 6.7. Experiments I and II were controlled with a EAI 100 hybrid

computer. Experiment III was controlled by the Encore 8087 digital computer combined with the EAI 640 analog computer.

The step response of the second-order system was generated by the analog part of the hybrid computer. The maximum step magnitude of 12 degrees was well within the limitations of the motion system. The sequence of one stimulus interval is presented in Fig. 6.8. At the beginning of the n-th interval a new step input ϕ_{i_n} was given to the system. This event was marked by an audio tone.



Figure 6.7 Overview of the experimental station in the flight simulator with the subject, the central and peripheral displays and the keyboard.

The system outputs ϕ , $\dot{\phi}$ and $\ddot{\phi}$ were presented by the central and peripheral displays and the motion system, thus presenting the second-order system response as the stimulus to the subject. Depending on the experiment, different display configurations were used. After observing the stimulus onset, the subject was asked to estimate the final step magnitude and to respond by pressing the appropriate key on the keyboard.

The response magnitude is designated by ϕ_p . After the keyboard response the input step magnitude ϕ_i of the system changed to remaining error $\Delta\phi$:

$$\Delta\phi_n = \phi_{i_n} - \phi_{p_n} \quad (6.3)$$

To inform the subject about the error value $\Delta\phi_n$ and next to bring the simulator motion system back to the initial condition, the system response to $\Delta\phi_n$ is first displayed. Next, the system input is reset to zero and the displays blanked as the simulator is rolled back to the zero roll angle. The total interval time depended on the natural frequency ω_0 of the second-order system and varied from 7 to 12 seconds.

During each run the variables ϕ_{i_n} , $\Delta\phi_n$, ϕ_{p_n} and the subject's reaction time RT_n were recorded and stored for subsequent analysis. In the analysis of the results the mean value of the error $\overline{\Delta\phi}$, the error standard deviation $\sigma_{\Delta\phi}$, the mean reaction time RT and the σ_{RT} were computed

for each run. The $\sigma_{\Delta\varphi}$ and the RT were used as the dependent variables to be analyzed with the ANOVA.

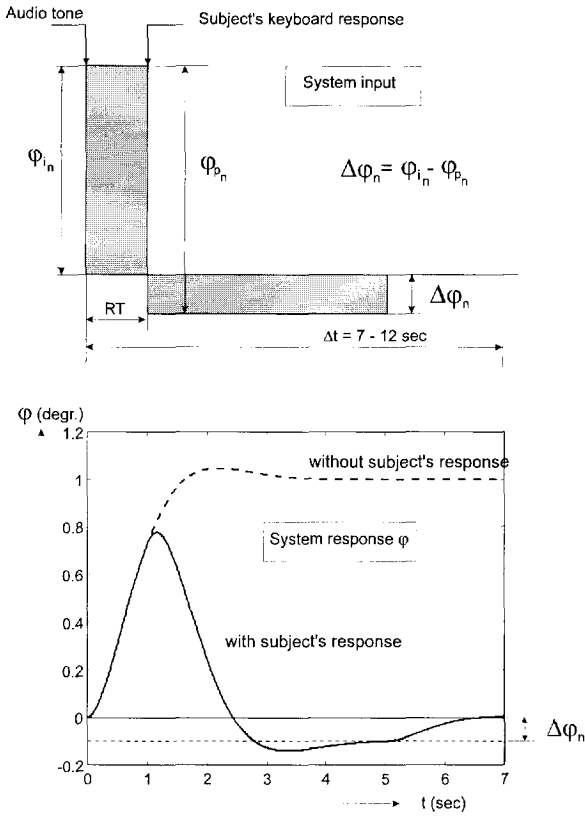


Figure 6.8 Sequence of one interval of a test run.

6.4 Experiments

As already mentioned, the aim of the experiments described was to investigate the accuracy and speed with which subjects can perceive simulator motion by observing the artificial horizon on the central display, the outside world simulated by the peripheral displays and cockpit motion.

In Ch. 5, two experiments were described where the perception of roll attitude and roll rate was investigated by using discrete stimuli presented on the central and/or the peripheral displays. In the experiments described in this chapter, the motion system of the simulator was involved to stimulate the vestibular system. Discrete stimuli were no longer possible due to the limitations of the simulator motion system.

To obtain the required results and to have the possibility to correlate the results of Ch. 5 with the results of the experiments with motion stimuli, the following three experiments were designed and executed.

The actual sequence in which the experiments were performed is different from the sequence in which they are presented here. Experiment II was performed in advance of Experiment I.

Experiment I

Experiment I was designed to investigate the visual perception of the step response stimulus. The roll attitude and roll rate were presented to the subject on the central display, the peripheral displays or both. To understand how the subject's estimate of the step magnitude improves while the time advances, the stimulus was presented for a limited exposure time Δt_{exp} as in the experiments of Ch. 5. After exposure the displays were blanked until the subject responded on the keyboard.

The perception accuracy and speed were investigated for the following display configurations: Central display (C), the Peripheral displays (P) and the combination of the central and peripheral displays (CP).

The second-order system used to generate the step response stimulus did have a natural frequency $\omega_0 = 2$ rad/sec and a damping $\zeta = 0.7$.

The step magnitudes used in the experiment were 0, ± 2 , ± 4 , ± 6 , ± 8 , ± 10 and ± 12 degrees. During one measurement run, 5 replications of these 13 magnitudes were presented in random order. In this way a uniform distribution of the stimulus magnitude resulted. This distribution was chosen so that all stimulus magnitudes would be evaluated with an equal number of replications. After some evaluation five exposure times 0.2, 0.3, 0.4, 0.6 and 0.8 seconds were selected. Each subject performed the fifteen runs 5 times.

Experiment II

In this experiment the estimation of the step magnitude due to the stimulation of the visual and the vestibular system was investigated. The step response was presented to the subject by using the central and peripheral displays and simulator motion.

All seven combinations of the Central display (C), the Peripheral display (P) and Motion (M) were used. The step magnitudes of Experiment I were used again. The measurement runs were the same as before. Exposure of the stimulus was continued till the subject responded on the keyboard. After the subject's response, the system responded to the new input, the remaining error $\Delta\phi$. Each subject performed the seven runs 5 times.

Experiment III

The aim of experiment III was to verify the predicted change of the time advance Δt as a function of the time course of the stimulus. In Sect. 6.2, the time advance Δt was predicted, according to the visual and vestibular models, to increase with decreasing natural frequency ω_0 of the second-order system. By changing the natural frequency of the second-order system the reaction times of the subjects would change depending on the display configuration C, P or M. Thus, if appropriate experimental conditions would be incorporated in the experiment, the relation between the time advance Δt and the natural frequency could be evaluated experimentally.

From Fig. 6.6 it is clear that the natural frequency range of the second-order system between 0.5 and 2 rad/sec is the most interesting due to the increase of Δt with decreasing ω_0 . In addition, the natural frequency of the pitch and roll modes of a wide range of aircraft is in this frequency range. This makes this frequency region even more interesting.

The initial magnitude of the angular acceleration as a response to the second order step response depends on the step magnitude A multiplied by the natural frequency squared, $A\omega_0^2$. At values of the natural frequency $\omega_0 < 1$ rad/sec and small step magnitudes the stimulus angular acceleration may fall within the range of threshold values for motion perception. The vestibular output firing rate depends on the stimulus time course and the dynamic characteristics of the vestibular system. A stimulus can only be sensed if the output firing rate exceeds a certain threshold. It turned out that the lowest natural frequency of the second-order system that could be used in the experiment was 0.65 rad/sec. For the smallest step magnitude of 2 degrees the vestibular output reaches about the threshold of motion perception. For that particular stimulus a perception uncertainty may be experienced when the stimulus is presented to the subject only with the motion system. The highest natural frequency $\omega_0 = 2$ rad/sec was equal to that used in the Experiments I and II. A third natural frequency was chosen at 1 rad/sec.

To present the stimulus to the subject, the same three display systems were available as before: the central display C, the peripheral displays P, and the simulator motion system M. These three display configurations were used in the experiment. In addition the combination of the central display and simulator motion CM was included.

The step magnitudes i_n used in the experiment were 0, ± 2 , ± 4 , ± 6 , ± 8 , ± 10 and ± 12 degrees. During each run 5 replications of these 13 magnitudes were applied in random order. To prevent that the subjects would too easily estimate the largest stimulus magnitudes, the perception error of the preceding stimulus $\Delta\phi_{n-1}$ was added to i_n :

$$\phi_{i_n} = i_n + \Delta\phi_{n-1}. \quad (6.4)$$

Hence, step magnitudes ± 14 and ± 16 degrees happened only a few times each run. The duration of each run depended on the natural frequency of the second-order system and ranged from 10 to 17 minutes. Each subject performed all 12 experimental configurations 5 times.

6.5 Subjects and training

Subjects were instructed to respond, primarily, as accurately as possible, and secondly, as quickly as possible to the presented stimuli. They were not required to fixate their eyes continually on the central display but were free to look at the keyboard when responding. For all experimental conditions, they were asked to fixate their eyes on the central display after their keyboard response was made before the next stimulus was presented. In addition to the feedback of the error after each keyboard response was made, subjects were informed about their performance, the error standard deviation, $\sigma_{\Delta\phi}$, and the mean reaction time, RT , after each run, Sect. 5.3.3.

Experiment I

Two subjects, both university staff members and qualified jet transport pilots, volunteered for the experiment. They were both familiar with this kind of task because they had participated in the experiments of Ch. 5 and Experiment II of this chapter. They were trained until a steady performance was reached. With the evaluation of the step response stimulus and the final training, approximately 100 runs were performed before the final experiment was started.

Five exposure times were incorporated in the experiment, 0.2, 0.3, 0.4, 0.6 and 0.8 seconds. Each display configuration (C, P and CP) was combined with the 5 exposure times and repeated 5 times by each subject. The number of measurement runs in the experiment was $3 \cdot 5 \cdot 2 \cdot 5 = 150$.

Experiment II

The same two subjects of Experiment I participated in this experiment. For preliminary evaluation and training 150 runs were made. After the steady level of performance was achieved the experiment was carried out during morning sessions. Measurement runs with all display configurations (C, P, M, CP, CM, PM and CPM) were performed and repeated 5 times by each subject. The number of runs in Experiment II was $7 \cdot 2 \cdot 5 = 70$.

Experiment III

Two subjects participated in this experiment. One was a student with a private pilot license. The other was a staff member who had already participated in the earlier experiments. During the training it turned out that the subjects had difficulty switching from a measurement run with one natural frequency ω_0 to a run with another natural frequency. Therefore, it was decided to perform the experiment in three blocks, one block for each natural frequency ω_0 . Within these blocks the four display configurations (C, P, M and CM) were randomized. For training 160 training runs were performed. After steady performance was reached all three blocks of the experiment were run during morning sessions. The subjects performed 5 replications of all experimental conditions: 3 natural frequencies and 4 display configurations. A total number of $4 \cdot 3 \cdot 2 \cdot 5 = 120$ measurement runs was performed to complete the experiment.

In the sense of Experimental Design, the experiments were set up as a Randomized Factorial Design. The experimental configurations were considered to be fixed independent variables when applying the ANOVA on the output variables. The subjects, however, represent a random sample from a population of subjects. Therefore, the influence of the subjects had to be considered as a random variable in the ANOVA. Hence, the ANOVA has to be based on the mixed effects model (Hays, 1963 and Kirk, 1968). A summary of the ANOVA results, the statistical significance of the influence of the independent variables and their interactions on the dependent variables, will be presented.

6.6 Results

The primary results of the experiments are given by the dependent variables, the standard deviation of the error $\Delta\phi_n$ of the estimated step magnitude and the mean reaction time RT. These dependent variables will be presented as a function of the independent experimental variables. These independent variables are different for the three experiments.

From the independent variables the display configuration, the exposure time, and the natural frequency of the second-order system are the most important, whereas the subjects and the replications are secondary. The influence of the primary independent variables of the three experiments on the dependent variables will be shown. From the secondary independent variables the subjects normally turn out to perform statistically different. In the ANOVA the subjects are considered a random variable whereas the other independent variables are

deterministic or "fixed" variables. When the training of the subjects has been successfully completed, they should perform at a constant performance level with a small variance. Hence, if a significant difference between the replications is found by the ANOVA then the cause of the difference has to be determined.

In addition, some data on the estimation error $\Delta\phi$ and the reaction time as a function of stimulus magnitude will be presented. All results of the experiments are summarized in Appendix 2.

Experiment I

The standard deviation of the estimation error, $\sigma_{\Delta\phi}$, and the mean reaction time RT as a function of exposure time and display configuration are summarized in Appendix 2 and presented in Figs 6.9 and 6.10.

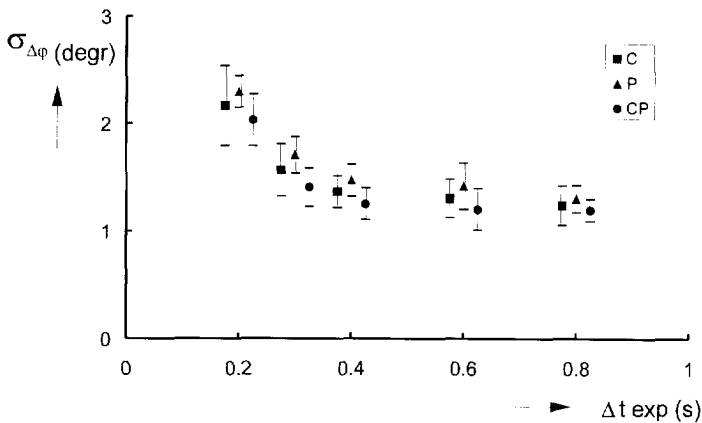


Figure 6.9 The standard deviation of the estimation error $\sigma_{\Delta\phi}$ as a function of the exposure time Δt_{exp} and the display configuration.

As can clearly be seen in Fig. 6.9, the estimation error $\Delta\phi$, as expressed by the $\sigma_{\Delta\phi}$, decreases with increasing exposure time Δt_{exp} . This could be expected based on the results of the experiments described in Ch. 5. However, the step response stimulus is much more complicated to perceive than the discrete rate stimuli as used in Ch. 5. This becomes clear from Fig. 6.9 because for the three display configurations an approximately equal exposure time is required ($\Delta t_{exp} \geq 0.6$ s) to obtain the final estimation accuracy. The exposure time necessary to reach the best perception accuracy is much longer than the exposure times required to perceive pure roll rate in Ch. 5 ($\Delta t_{exp} = 0.2$ s for the peripheral displays and 0.3 s for the central display).

In Table 9, a summary of the results of the ANOVA is presented. The main effects Display Configuration and Exposure Time have a significant influence on the performance parameter. In addition, a significant interaction between the display configurations, exposure time and subjects is found.

In Fig. 6.10, the reaction time as a function of exposure time and display configuration is presented. The increase of the reaction time with exposure time has also been found for rate

Table 9 Summary of the results of the ANOVA of Experiment I.

| | $\sigma_{\Delta\varphi}$ | RT | |
|---------------------------------------|--------------------------|----|--------------------|
| <u>Main effects</u> | | | |
| Display Configurations | ** | - | |
| Exposure time Δt_{exp} | ** | ** | |
| Subjects | * | ** | |
| Replications | - | - | |
| <u>Interactions</u> | | | |
| DC, S | - | - | |
| Δt_{exp} , S | - | - | |
| DC, Δt_{exp} | - | * | $\alpha < 0.05$ * |
| DC, Δt_{exp} , S | ** | | $\alpha < 0.01$ ** |

perception in Ch. 5. The main reason seems to be that the subject's reaction time is influenced by the longer exposure duration. For $\Delta t_{\text{exp}} \geq 0.6$ s the differences among the three display configurations correspond with the results for roll rate perception in Ch. 5.

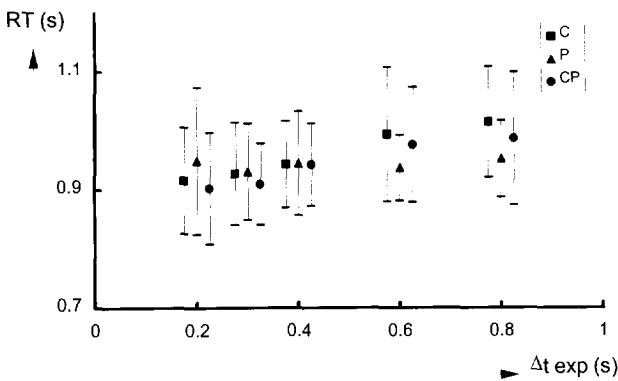


Figure 6.10 The mean reaction time RT as a function of the exposure time Δt_{exp} and the display configuration.

The reaction time for the peripheral displays RT_p is approximately 0.060 s shorter than the reaction time for the central display RT_c , which fits nicely with the results for roll rate perception.

According to the ANOVA, the influence of the exposure time on the reaction time is significant, while there is a possible significant influence of the interaction between the display configuration and the exposure time. This interaction is caused by the increase of the reaction time with the exposure time for the configurations C and CP and the approximately constant reaction time for the peripheral displays, P.

Experiment II

The results of the error root mean square and the reaction time as a function of display configuration are shown in Figs. 6.11 and 6.12.

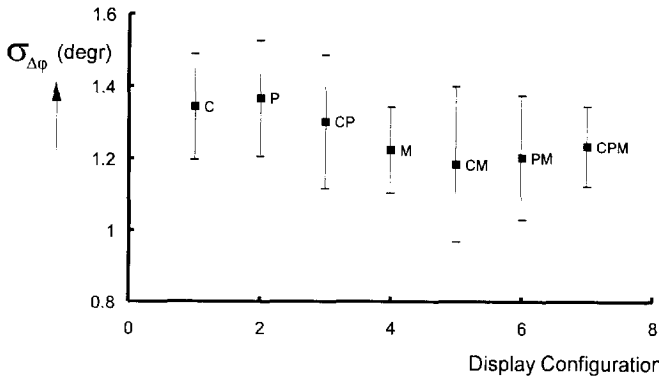


Figure 6.11 Error standard deviation as a function the display configuration.

The differences in the error standard deviation, $\sigma_{\Delta\phi}$, are small and, due to the large spread, not significant. Although the configurations with motion cues seem to be more accurate, this means that the step magnitude can be estimated with approximately equal accuracy independent of the display configuration. The results of the ANOVA are summarized in Table 10.

The differences in the reaction times due to display configurations and subjects are significant. Notable is the difference between the contribution of the visual displays and simulator motion. The reaction time with the central display only, RT_C , is the longest. Peripheral displays and simulator motion both cause shorter reaction times RT_P and RT_M . The reaction times for the display configurations CP, CM and CPM are in between those for C and P, C and M and C and PM, respectively. For the combination PM, however, the effect is enhanced and the reaction time is shorter than for P and M separately.

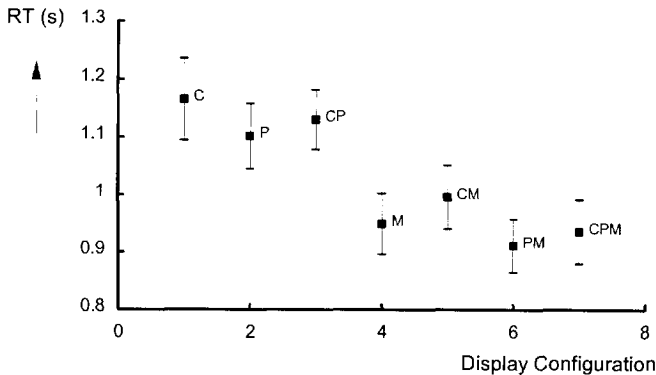


Figure 6.12 The mean reaction time as a function of the display configuration.

Table 10. Summary of the results of the ANOVA of Experiment II.

| Main effects | $\sigma_{\Delta\phi}$ | RT | |
|------------------------|-----------------------|----|--------------------|
| Display Configurations | - | ** | |
| Subjects | - | ** | |
| Replications | - | - | |
| Interactions | | | $\alpha < 0.05$ * |
| DC, S | - | - | $\alpha < 0.01$ ** |

Experiment III

The results of Experiment III can be divided into two parts. First, the mean perception accuracy and the reaction time for the experimental conditions will be discussed. Secondly, the influence of the stimulus magnitude on the estimation accuracy and reaction time will be considered. The estimation error standard deviation, $\sigma_{\Delta\phi}$, and the mean reaction time RT are presented in Fig. 6.13 and 6.14.

The mean values of the $\sigma_{\Delta\phi}$ are presented in Fig. 6.13. With increasing natural frequency of the second-order system, $\sigma_{\Delta\phi}$ decreases significantly. The display configurations have a significant influence on the estimation error. Central display with simulator motion (CM) gives the smallest estimation error, peripheral displays (P) give the largest error. At $\omega_0 = 0.65$ rad/sec the central display gives a good perception performance, whereas at $\omega_0 = 2.0$ rad/sec simulator motion gives the best performance, suggesting that at the low natural frequency the central display provides more accurate information for the estimation task than motion. At the high natural frequency, motion stimulation gives better information. This corresponds with the remark in section 6.3 that the small step magnitudes at the lowest natural frequency are in the order of the vestibular perception threshold. The interaction of display configurations and natural frequency on estimation error is significant. A summary of the results of the ANOVA is presented in Table 11.

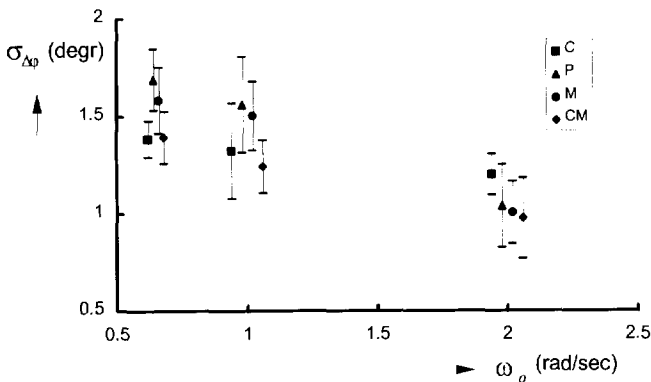


Fig. 6.13 The error standard deviation as a function of the display configuration and the natural frequency of the second-order system.

Table 11. Summary of the results of the ANOVA for Experiment III.

| Main effects | $\sigma_{\Delta\phi}$ | RT |
|------------------------------|-----------------------|----|
| Display Configuration | ** | ** |
| Natural frequency ω_0 | ** | ** |
| Subjects | ** | * |
| Replications | - | - |
| Interactions | | |
| DC, ω_0 | ** | ** |
| DC, S | - | - |
| ω_0 , S | - | * |
| DC, ω_0 , S | - | - |

$\alpha < 0.05$ *
 $\alpha < 0.01$ **

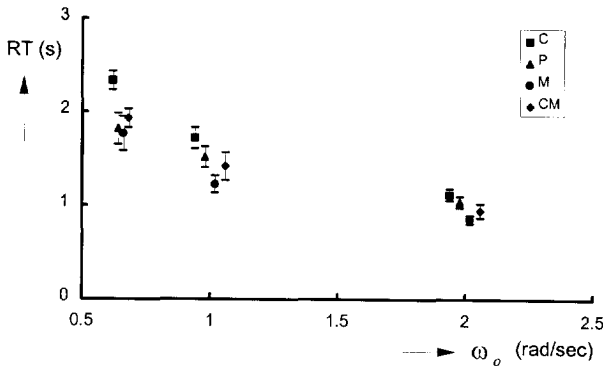


Figure 6.14 Mean reaction time as a function of display configuration and natural frequency of the second-order system.

The reaction time RT decreases with the increase in natural frequency ω_0 of the second-order system. From the four display configurations simulator motion (M) gives the shortest reaction times. The central display (C) gives the longest reaction times, whereas the reaction times for the configuration with the central display and motion (CM) are in between those for C and M. The results correspond with those of Experiment II. The influence of the display configuration and the natural frequency on the reaction time is significant.

In Table 12, the time advance Δt , as defined in Sect. 6.2, is presented as a function of the natural frequency and is compared with the results of the Experiments I and II and the roll rate perception experiment, Experiment 2, of Ch. 5. The results of the three experiments for the natural frequency $\omega_0 = 2$ rad/sec are slightly different and may be the result of the larger number stimuli magnitudes involved in Experiment III.

The model for visual motion perception, Eq. 4.4, predicts $RT_C - RT_P$ to be independent of the time course of the stimulus, and consequently, independent of the natural frequency ω_0 . This is clearly not the case.

As predicted in section 6.2, the trend of the time advance caused by the characteristics of the semi-circular canals, is confirmed by the experimental results, Fig. 6.15. The difference between the time advance for the display configurations CM and M is quite large (± 150

Table 12. The time advance Δt as a function of the natural frequency of the stimulus-generating second-order system.

| | Exp. III | | | Exp. I | Exp. II | Roll rate Ch. 5. Exp. 2 |
|-----------------------------|------------------------------|-----------------------------|--------------------------|--------|---------|-------------------------------|
| Time advance Δt (s) | $\omega_0 = 0.65$ rad/sec | $\omega_0 = 1.0$ rad/sec | $\omega_0 = 2.0$ rad/sec | | | |
| $RT_C - RT_P$ | 0.512 | 0.203 | 0.076 | 0.063 | 0.063 | 0.072 |
| $RT_C - RT_M$ | 0.563 | 0.493 | 0.262 | | 0.216 | |
| $RT_C - RT_{CM}$ | 0.401 | 0.301 | 0.171 | | 0.169 | |

msec). Hence, the interaction between the visual perception and vestibular perception in this task is quit large.

In Sect. 6.2 the question was raised whether, for a low stimulus magnitude and the lowest natural frequency, the roll acceleration of the stimulus would exceed the threshold for motion perception. In the Figs 6.16 and 6.17 the mean estimation error have caused a longer reaction time. Part of the differences between Experiments I and II, on one hand, and Experiment III, on the other hand, may be the result from the change of subjects, Sect. 6.5.

The most important results of the experiments are the changes of the dependent variables, the estimation error standard deviation $\sigma_{\Delta p}$, and the reaction time RT , as a function of the independent variables, exposure time Δt_{exp} , display configuration and natural frequency ω_0 of the second-order system generating the stimulus. The differences in the dependent variables for equal experimental conditions, Table 13, over the experiments are considered to be acceptable.

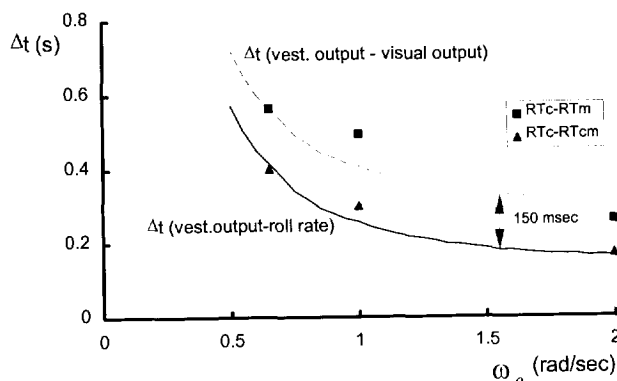


Figure. 6.15 The time advance as a function of the natural frequency of the stimulus generated by the second-order system.

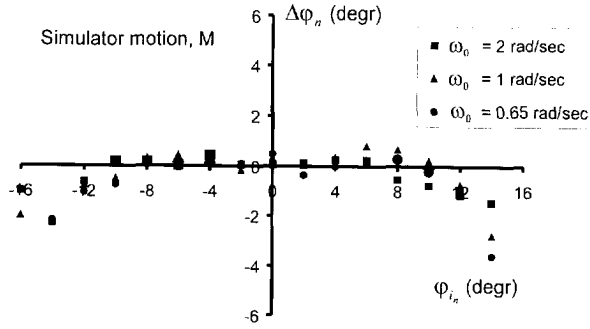


Figure 6.16a The mean estimation error $\Delta\phi_n$ for simulator motion stimulation as a function of the stimulus magnitude and the natural frequency ω_0 .

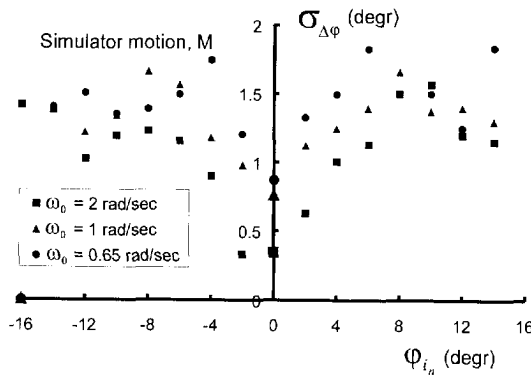


Figure 6.16b The standard deviation $\sigma_{\Delta\phi}$ for simulator motion stimulation as a function of the stimulus magnitude and the natural frequency ω_0 .

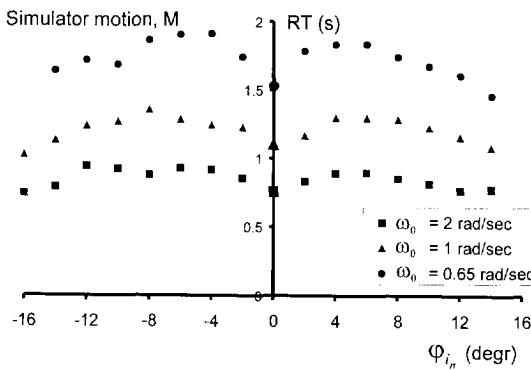


Figure 6.17 The mean reaction time RT_M for simulator motion stimulation as a function of the stimulus magnitude and the natural frequency

$\Delta\phi_n$, the $\sigma_{\Delta\phi}$, and the reaction time RT for the display configuration with only motion, M , are presented. These figures show that the estimation accuracy is hardly influenced by the natural frequency of the stimulus-generating second-order system. The reaction time, however, is strongly influenced by the natural frequency, as was expected. The $\sigma_{\Delta\phi}$ starts to increase with the increase in stimulus magnitude. However, for the larger stimulus magnitudes $\sigma_{\Delta\phi}$ decreases with increasing magnitude, Fig. 6.16b.

The reaction time RT , Fig. 6.17, is dependent on the stimulus magnitude. This is especially the case for $\omega_0 = 0.65$ rad/sec. At the small magnitudes the subjects react relatively quickly and accurately, which means that the subjects are aware of the stimulus. Hence, the stimulus was not below the threshold for motion perception.

6.7 Discussion and conclusions

The results of the three experiments described in this chapter provide information on the perception of motion based on visual and vestibular stimulation of the subject. In Sect. 6.2 the response of the visual and vestibular system to the second order step response stimulus was evaluated. In this section, the results of the present experiments will be compared with each other, with the predictions and with the results of the preceding chapter. Further, the meaning of the experimental results will be discussed and the conclusions drawn.

From the results of the three experiments an impression of the reliability of the results can be obtained by comparing corresponding experimental conditions. The results of these conditions are summarized in Table 13.

The results of Experiment I are slightly better than those of Experiment II. The shorter reaction times of Experiment I may be explained by the limited exposure time. Fig. 6.10 shows that the reaction time increases with the increase of the exposure time. In Experiment III the distribution of the stimulus magnitude was slightly changed which resulted in a larger number of stimulus magnitudes used. This may be. When increasing the exposure time in Experiment I, the estimation accuracy improves to a final value which is reached at $\Delta t_{exp} = 0.6$ seconds. This is much longer than the exposure time required for the perception of roll rate as described in Ch. 5. In the roll rate perception experiment, a discrete stimulus of constant roll rate was used, whereas, in the experiments described in this chapter, a continually changing stimulus was applied. To obtain an accurate estimate of the final step magnitude the subject has to observe the time course of the stimulus for at least 0.6 second in the case of a natural frequency of 2.0 rad/sec. For the roll rate experiment the minimum exposure time for the central display was 0.3 second. In the roll rate experiment the decrease in perception error as a function of exposure time was dependent on the display configuration used, Figs 5.8 and 5.9. In the present step response experiment the decrease in estimation error, Fig. 6.9, is independent of the display configuration used. This corresponds with the fact that there is no significant interaction between display configuration and exposure time, Table 9. Therefore, the longer exposure time for the step response experiments does not result from the characteristics of the bilocal motion detectors. To extrapolate the time course of the stimulus and to estimate the final step magnitude, the subject has to observe the stimulus for a certain time interval, the minimum exposure time.

Table 13. Summary of the results of corresponding experimental conditions of the three experiments.

| Exp. Condition | Experiment I | | Experiment II | | Experiment III | |
|----------------|---|-----------|---------------------------------|-----------|----------------------------------|-----------|
| | $\sigma_{\Delta\phi}$ (degr) | RT (s) | $\sigma_{\Delta\phi}$ (degr) | RT (s) | $\sigma_{\Delta\phi}$ (degr) | RT (s) |
| | $\Delta t_{\text{exp}} = 0.8 \text{ s}$ | | | | $\omega_0 = 2.0 \text{ rad/sec}$ | |
| C | 1.245 | 1.015 | 1.344 | 1.165 | 1.203 | 1.116 |
| P | 1.308 | 0.952 | 1.367 | 1.102 | 1.041 | 1.040 |
| CP | 1.200 | 0.986 | 1.302 | 1.130 | | |
| M | | | 1.224 | 0.949 | 1.006 | 0.853 |
| CM | | | 1.184 | 0.996 | 0.978 | 0.945 |

The results of Experiment I show that the perception accuracy, as expressed in $\sigma_{\Delta\phi}$, is not essentially influenced by the display configuration. This is in agreement with the experiment on roll rate perception where, except for the shorter exposure times, no essential difference in perception accuracy was found between the display configurations.

Although the present experiment features notable differences in the time course of the roll angle, roll rate and roll acceleration - the primary input variables for the central visual field, the peripheral visual field and the semi-circular canals - it turns out that the step magnitude can be estimated equally well from the central display and the peripheral displays. According to the results of Experiments II and III, slightly better estimation performance is obtained when motion is incorporated in the presentation of the stimulus. Extension of the display configurations to CP, CM, etc. does not essentially influence the estimation accuracy.

In the Experiments II and III the influence of visual and motion stimuli on the subject's estimation accuracy and reaction time was investigated. Considering the dynamic characteristics of the semi-circular canals, it was predicted in Sect. 6.2 that the output of the vestibular system leads to the angular rate of the stimulus. In addition, it was shown that the visually perceived angular rate lags behind the actual angular rate due to the neural processing and neural transport delays. Furthermore, it was shown that the time advance Δt between the vestibular output and the angular rate is influenced by the time course of the motion stimuli, whereas the delay of the visually perceived motion is independent of the time course of the stimulus. These notions were confirmed by the results of the experiments. The only restriction is that the time advance $\Delta t = RT_C - RT_p$ does not correlate with the model for visual perception of angular rate. According to that model, Eq. (4.4), the difference between RT_C and RT_p should be independent of ω_0 and approximately 60 msec. However, it has been shown in Sect. 4.2 that at low stimulus velocity ($< V_c$), the reaction time increases inversely with stimulus velocity, Eq. (4.3). The stimulus velocities on the central display and the peripheral displays are smaller than in Experiment II of Ch. 5. The critical velocity for the central visual system $V_c \geq 1 \text{ degr/s}$ and, for the peripheral visual system $V_c \geq 10 \text{ degr/s}$, whereas the maximum stimulus velocity was 12 degr/s .

The results of Experiment III show that the subject's reaction time increases with decreasing natural frequency ω_0 of the second-order system for all display configurations. The difference between the reaction times RT_C and RT_M also increases with decreasing ω_0 . As shown in Fig. 6.15 this difference corresponds quite well with the model predictions of Sect. 6.2.

In normal flight conditions the pilot will perceive the aircraft motions from the combination of the artificial horizon, the central display C, and by the vestibular system from the aircraft motions M. Therefore, the difference between the reaction time for the central display, C, and the combined display configuration, central display with cockpit motion, CM, is of importance. In Fig. 6.18, the reaction time RT for the display configurations C, CM and M is presented as a function of the natural frequency ω_0 . The reaction time RT_{CM} tends to be closer to RT_M than to RT_C . Nevertheless, the visual sensory output induced by the central display has a strong delaying influence on the perception process.

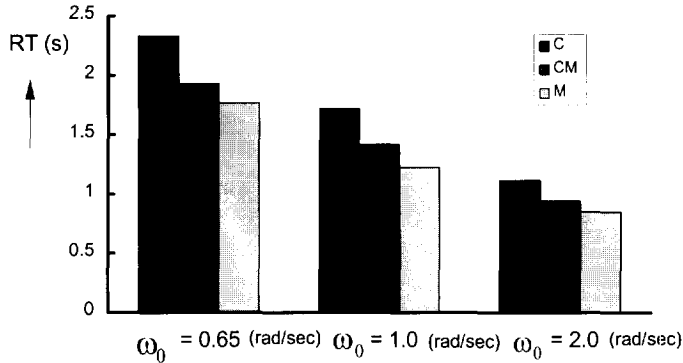


Fig. 6.18. The reaction time RT as a function of natural frequency ω_0 and the display configurations C, CM and M.

Three conclusions can be drawn from the experiments described in this chapter:

1. The estimation accuracy of the final value of a complex motion stimulus is essentially independent of the display configuration.
2. The reaction time due to the estimation of the step magnitude is significantly decreased (200 to 400 msec) by adding cockpit motion to the visual presentation of the stimulus to the subject.
3. In motion perception cockpit motion cues, as well as peripheral visual cues, speed up the perception process.

7. TRACKING EXPERIMENT

7.1 Introduction

The conclusions of Ch. 2 clearly demonstrate that the addition of peripheral visual- and/or vestibular motion cues has an influence on a pilot's tracking behavior. This influence turns out to be dependent on the type of the tracking task (disturbance- or target following task), on system dynamics (second- or higher order), and on the stimuli (central- and/or peripheral visual and vestibular) presented to the subject. However, to obtain a good understanding of how the different motion stimuli influence a pilot's tracking behavior, a reliable data base obtained from measurements in tracking tasks is needed. This data base should clearly demonstrate the effect of the different motion stimuli on tracking performance and dynamic control behavior. Considering the conclusions of Ch. 2, it was decided to design and perform a tracking experiment where the influence of motion stimuli on manual control of a second-order system would be investigated. Given the differences found between the target following task and the disturbance task, it was clear that both tasks had to be incorporated in the experiment.

For the system to be controlled by the subjects a double integrator, $K / (j\omega)^2$, was chosen. Such a system is manually difficult to control (McRuer, 1965) and has the advantage of specific dynamic characteristics; constant slope of the magnitude, -2, and constant phase angle $\varphi = -180$ degr. in the bode diagram. Hence, the subject has to generate lead in the crossover region to obtain an adequate phase margin independent of the crossover frequency.

An important aim of the experiment was to obtain tracking data that allow the separation of the influence of the different input stimuli on the subject's control behavior. To reach that goal there were two possibilities which both have their advantages and disadvantages.

- Apply the different stimuli (central- and peripheral visual and vestibular) in all possible combinations to present the required stimuli to the subject in the tracking task. This is only feasible in the disturbance task. In the target following task the central visual display is necessary to present the error signal, Fig 2.3.
- Apply two independent forcing functions, one as the forcing function in the target following task and one as the disturbance function in the disturbance task, Fig. 2.8. Stapleford et al. (1969) showed that in such an experimental configuration two transfer functions, describing the visual- and the vestibular contribution to human operator behavior, could be determined.

In the decision to use one of both alternatives two arguments have to be mentioned.

In control of a vehicle the human operator has to perceive the motion of the vehicle. In this perception process there are interactions at different levels between the visual- and the vestibular system. As discussed in Ch. 3, the information processing by the human operator has to be considered as a multi input single channel process. Based on the visual-vestibular

interaction as described by Howard (1982, 1986), the motion perception process provides the operator with one percept of the motion state of the vehicle, the system to be controlled. Thus after the perception stage the information is processed in a single channel.

In the multi-input tracking task, as used by Stapleford, two describing functions of the human operator's control behavior, $H_{p,vis}(\omega)$ and $H_{p,motion}(\omega)$ as defined in Fig. 2.8, have been defined. These describing functions, however, are valid only in the specific experimental set-up used by Stapleford. As will be shown in this and the next chapter, a pilot's control behavior in the target following task and the disturbance task is quite different. It is therefore questionable if the subject's describing functions obtained in the target following task with visual input and in the disturbance task with motion input can be used to explain changes in a subject's control behavior due to motion feedback.

In the period when the experiment was designed, the software available to process measurements from tracking experiments was limited to single input tracking tasks. It was expected that by choosing the right display configurations, adequate insight into the influence of motion cues could be obtained based on the subject's frequency responses.

The disturbance task can be performed with feedback of the system output $y(t)$ by using central visual-, peripheral visual- or motion cues. In this way, the influence of these stimuli on human operator's control behavior can be obtained independently. In addition to these experimental conditions, the influence of the combined stimuli on control behavior may be established in the disturbance as well as in the target following task.

The research flight simulator of the Faculty of Aerospace Engineering was available for the experiment. As in the experiments described in Chs 5 and 6 central- and peripheral visual cues and motion cues could be presented to the subject.

In this chapter the tracking experiment is described and the results are presented. The chapter ends with a discussion and conclusions.

7.2 Instrumentation and data reduction.

7.2.1 Instrumentation

All measurements were performed in the laboratory of the Disciplinary Group for Stability and Control. Because the training of the subjects took a long time and part of the training and the experiment could be performed without the simulator motion system, the experiment was divided into two parts to limit the required simulator time. The first part with only visual input to the subjects was performed in a low noise room. The second part was carried out in the research flight simulator of the Faculty. Due to the differences in the positions of the left peripheral display relative to the subject in the two parts of the experiment, additional experimental conditions were added to verify that in both parts of the experiment approximately equal performance standards were reached.

To present the roll angle ϕ in the disturbance task and the roll angle error e_ϕ in the target following task, the central (foveal) CRT display was installed in the instrument panel in front of the subject, Fig. 5.1. As in the experiments described in the Chs 5 and 6, two black and white TV monitors were used to present the peripheral stimuli to the subjects, Fig. 5.2. In Fig. 7.1, an overview of the experimental station in the simulator is presented. Technical details of the displays and their position relative to the subject are described in Appendix 1.



Figure 7.1 Overview of the experimental station on the right-hand side of the simulator cockpit.

The three degrees of freedom (pitch, roll and heave) motion system of the flight simulator, Fig. 7.2, had high fidelity motion characteristics. The use of electro-hydraulic servo actuators with hydrostatic bearings in the motion system resulted in very smooth and almost rumble free simulator motions (den Hollander et al. 1977). Under normal operating conditions motion noise was well below the thresholds of motion perception (Hosman et al. 1978). This made the simulator a suitable tool to generate the motion stimuli for the tracking task experiment.

The static and dynamic characteristics of the motion system are described in Appendix 1. The actuator position signals controlling the roll attitude of the simulator were compensated for the motion system dynamics. After this compensation, the transfer function of the motion system position as a function of control input could be described by a gain of 1 ± 0.004 and a mean time delay of 0.006 sec over the frequency range of the forcing function ($\omega = 0.153$ to 13.8 rad/sec).

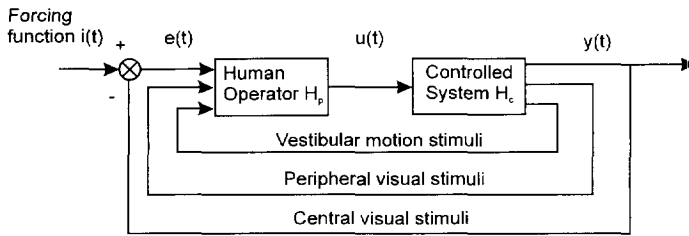
No motion filters were used, which meant that subjects were able to perceive a lateral force component due to simulator tilt. The roll excursions of the simulator during the tracking tasks, however, remained small as will be clear from the results. Nevertheless, small lateral specific force cues due to roll tilt and roll acceleration were present.

A spring centered side stick controller was used to generate the control inputs to the system. Details of the side stick are described by Mooij (1972). The calibration of the relation between the input stick displacement and the output signal and the spring and damper characteristics are described in Appendix 1.

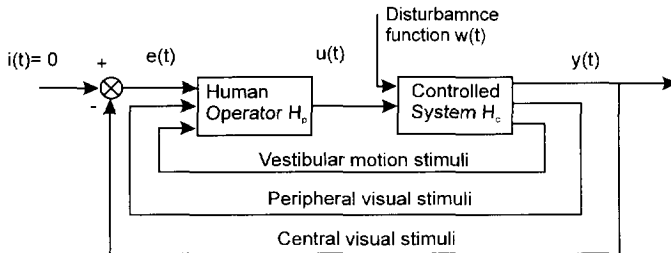
The dynamics of the controlled system, $K/(j\omega)^2$, were simulated on an EAI Pacer 100 hybrid computer. This computer system also generated the quasi-random forcing function, as well as the signals controlling the displays and the simulator motion system.



Figure 7.2 Outside view of the simulator cockpit with the TV monitors serving as peripheral displays.



a. Target following task



b. Disturbance task

Figure 7.3 Configuration of the experimental tracking tasks with visual and vestibular feedback.

The forcing function was generated by the digital part of the hybrid computer system whereas all parts of the control loop were simulated with the analog part of the system. The computer

Table 14 Frequency, magnitude and phase angle of the 10 sinusoids of the quasi random forcing function.

| Frequency rad/sec | Number of cycles | Magnitude | Phase degrees |
|----------------------|---------------------|-----------|------------------|
| 0.153 | 2 | 1.106 | 4 |
| 0.230 | 3 | 1.100 | 151 |
| 0.383 | 5 | 1.083 | 43 |
| 0.537 | 7 | 1.058 | 122 |
| 0.997 | 13 | 0.957 | 324 |
| 1.457 | 19 | 0.842 | 184 |
| 2.378 | 31 | 0.646 | 281 |
| 4.065 | 53 | 0.428 | 194 |
| 7.440 | 97 | 0.248 | 162 |
| 13.576 | 177 | 0.138 | 43 |

algorithms driving the visual displays and the motion system were implemented on the analog computer so that the time differences in the visual and vestibular stimuli generated by these systems were within 0.01 second.

Target following task and disturbance task were configured as shown in Fig. 7.3. One realization of the forcing/disturbance function was used throughout the experiment. It consisted of the sum of 10 sinusoids with a first order break in amplitude at a frequency of 1.7 rad/sec. The frequency, magnitudes and phase angles of the 10 sinusoids are presented in Table 14.

A test run lasted 104 seconds in total. The first 22 seconds gave the subjects the opportunity to stabilize their control. During the remaining 82 seconds measurements were taken at a rate of 25 cycles per second. In case of the disturbance tasks the roll angle ϕ , the roll rate $\dot{\phi}$ and the side stick deflection s_a were recorded. In the target following task the roll angle error e_ϕ , was recorded together with ϕ , $\dot{\phi}$ and s_a .

7.2.2 Data reduction

A few minutes after the completion of the test run, data analysis was performed by the digital computer program, yielding the standard deviation of the recorded variables and the score parameter. Simultaneously the subject's frequency response was obtained using a Fast Fourier Transform (F.F.T) routine.

The original frequency response data of the individual experimental runs were averaged to obtain the mean values as published by Hosman and van der Vaart (1980, 1981a, 1981b). The averaging of the original data had to be corrected as described by van der Vaart (1992). Two corrections have been considered.

- Given the frequency response $H_p(\omega)$ of the 15 individual measurement runs for each configuration, the average of each forcing function input frequency ω_i has to be taken. This has to be done by averaging the real and complex parts of $H_p(\omega)$ at each frequency ω_i .
- The phase angles of the frequency responses were computed on-line with a routine that yielded only angles between -90 and +90 degrees. Therefore a correction of the phase

angles was performed keeping the results of other tracking experiments in mind (McRuer 1965).

The first correction was performed by van der Vaart (1992) for 8 of the 13 experimental configurations. Because obvious "outsiders" were still present in the experimental data the second correction was applied if necessary. These corrections were especially necessary for some data points at low input frequency in the target following tasks.

Some additional remarks have to be made about the reliability of the frequency response magnitude and phase angles.

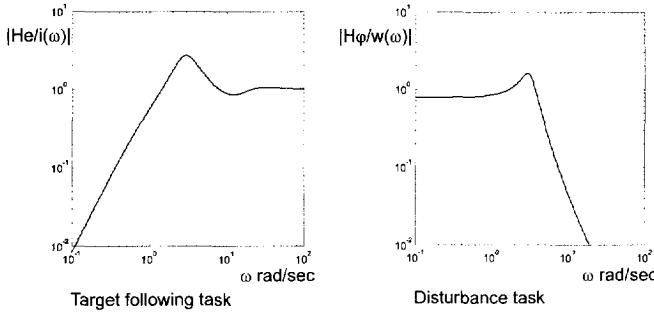


Figure 7.4 The moduli of the estimated transfer functions $H_{e_\phi, i}(\omega)$ for the target following task and $H_{\phi, w}(\omega)$ for the disturbance task.

From the data presented in this chapter it is clear that at low input frequencies the uncertainty, as expressed by the standard deviation of the modulus of the average frequency response, is high for the target following task. The same holds for the high input frequencies in case of the disturbance task. This is confirmed by the magnitudes of the describing functions relating the error, e_ϕ in the target following task and ϕ in the disturbance task, with the input forcing function i or w .

$$H_{e_\phi, i}(\omega) = \frac{1}{(1 + H_p(j\omega)H_c(j\omega))}, \quad (7.1)$$

for the target following task and

$$H_{\phi, w}(\omega) = \frac{H_c(j\omega)}{(1 + H_p(j\omega)H_c(j\omega))}, \quad (7.2)$$

in the case of the disturbance task.

An estimate of the describing functions of Eqs 7.1 and 7.2 can be obtained by replacing the describing functions $H_p(\omega)$ by the transfer functions of the simplified

precision model for the target following task and the disturbance task. In Fig. 7.4 the moduli of these transfer functions are presented. It is clear that the presented error signal e_ϕ for the target following task is small at low frequencies. In the case of the disturbance task the roll angle ϕ is small at high frequencies. This adversely influences the accuracy of the frequency

responses. Thus small values of the error signal correspond with a high uncertainty of the frequency response.

The model used to fit to the data is the Simplified Precision Model from McRuer (1965). For the control of a double integrator this model has the following form:

$$H_p(\omega) = K_p(T_L j\omega + 1)e^{-j\omega\tau_c} \quad (7.3)$$

7.3 Subjects and experimental set-up

Three subjects, qualified jet transport pilots, volunteered for the experiment. As mentioned before, the measurements during the non-motion runs were performed outside the simulator in a separate experimental set-up. The actual experiment was divided into two parts. Within each part of the experiment, Table 15, control tasks and configurations were presented in random order.

The subjects were asked to direct their gaze into the central display in all experimental configurations. The checker board pattern did not provide a clear cue of the attitude of the horizon so that the peripheral displays stimulated only the peripheral visual field with a velocity input. Consequently, the subjects could perceive only the roll rate from the peripheral displays.

The configurations CP, CPR and CPS in the disturbance task, Table 15, were used to check the influence of the differences of the relative position of the left peripheral display and differences in performance in both parts of the experiment. In the display configuration CPR only the right peripheral display is used to present the peripheral visual stimulus. In the flight simulator, configuration CPS, the left display had to be placed at a larger distance from the subject. The positions of the peripheral displays in the configurations CP, CPR and CPS are described in Appendix 1.

Mixture of the training for the target following task and the disturbance task and the different configurations made it impossible to establish clear learning curves. Extensive training was performed until stable performance, as expressed by the standard deviation of the tracking error, σ_{e_c} and σ_{e_o} , was reached. In total 350 test runs were completed among the three subjects

before starting the first part of the main test program. An additional 110 test runs were performed for the second part. Each series of measurement runs, presented to the subjects (6 or 7 runs), lasted approximately 20 to 25 minutes.

To obtain adequate statistical power, five replications were performed, resulting in a total of $4 \cdot 3 \cdot 5 = 60$ runs for the target tracking task and $9 \cdot 3 \cdot 5 = 135$ test runs for the disturbance task.

In the sense of Experimental Design, the two parts of the experiment were set up as a Randomized Factorial Design. The experimental configurations were considered to be fixed independent variables when applying the ANOVA on the output variables. The subjects, however, represent a random sample from a population of subjects. Therefore, the influence of the subjects had to be considered as a random variable in the ANOVA. Hence, the ANOVA has to be based on the mixed effects model (Hays, 1963 and Kirk, 1968).

It is assumed that significant differences in the output variables due to configurations and subjects are found if the probability of the risk to make a type one error is $\alpha < 0.01$. Possible significant differences are found if $\alpha < 0.05$.

Table 15. Overview of the experimental conditions, C = Central display, P = Peripheral display, M = Cabin motion, R = only one peripheral display on the right-hand side, S = both peripheral displays in the simulator.

| Configuration number | Target following task | Disturbance task |
|-------------------------|-----------------------|------------------|
| <u>Low noise room</u> | | |
| 1 | C | C |
| 2 | | P |
| 3 | CP | CP |
| 3a | | CPR |
| <u>Flight Simulator</u> | | |
| 3b | | CPS |
| 4 | CM | CM |
| 5 | | PM |
| 6 | | M |
| 7 | CPM | CPM |

7.4 Results

From the variables recorded during each test run of the experiment, a number of results can be extracted. They will be presented in this paragraph. The performance is expressed with the score parameter S_c , Eq. (2.4). Additionally, the standard deviations of the subject's input and output will be presented.

The subject's control behavior is expressed by the frequency response $H_p(\omega)$. The crossover frequency and phase margin of the open loop will also be presented. The performance will be discussed first in Sect. 7.4.1, followed by the control behavior in Sect. 7.4.2.

7.4.1 Performance

The subject's performance in the control tasks is expressed by a score parameter based on the measured subject's control error, the roll angle error e_ϕ for the target following task and the roll angle ϕ for the disturbance task. The score parameter S_c is presented in Table 16 and the RMS of the error are shown in Fig. 7.5.

Target following task

Base line performance for the target following task is considered the performance for the central display alone, C, Fig. 7.5. Adding the peripheral displays to the central display, CP, is seen to have a beneficial effect on the performance. The influence of the addition of simulator motion to the central display, CM, however, is stronger. A further small decrease of the score parameter S_c is seen resulting from the addition of the peripheral displays and simulator motion together, CPM.

As shown in Sect. 2.2 and in Fig. 7.3, in the following task peripheral-visual and vestibular-motion stimuli present system output to the subject, which do not directly correspond with the

Table16. The score parameters for the target following and disturbance task as a function of the display configurations.

| Display configuration | Score parameter S_c | |
|-------------------------|-----------------------|------------------|
| | Target following task | Disturbance task |
| <u>Low noise room</u> | | |
| 1 C | 1.417 | 1.074 |
| 2 P | | 2.025 |
| 3 CP | 0.754 | 0.762 |
| 3a CPR | | 0.978 |
| <u>Flight Simulator</u> | | |
| 3b CPS | | 0.902 |
| 4 CM | 0.497 | 0.172 |
| 5 PM | | 0.283 |
| 6 M | | 0.278 |
| 7 CPM | 0.448 | 0.140 |

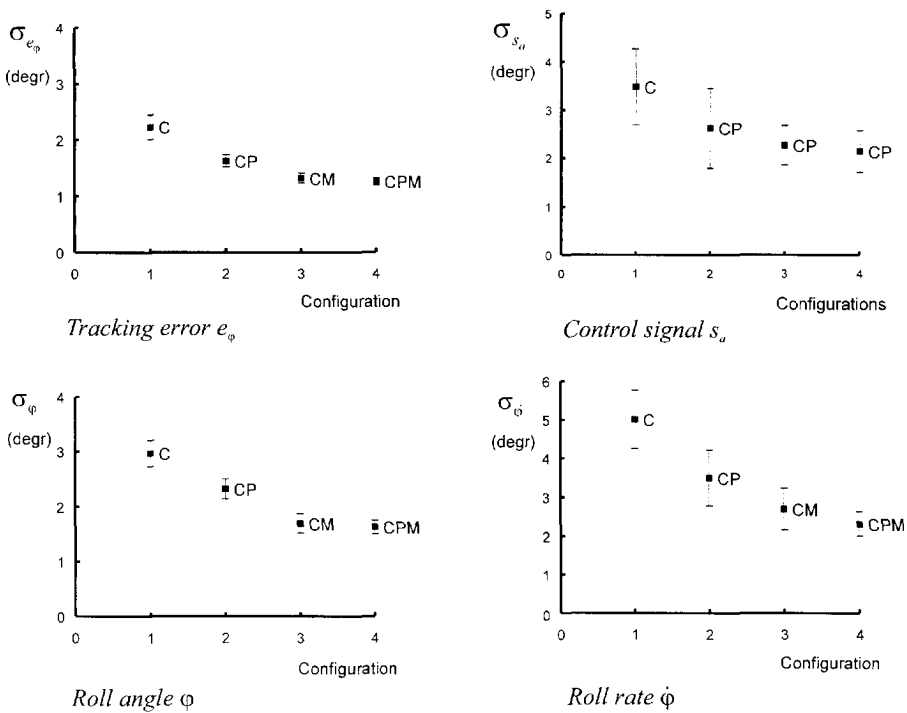


Figure 7.5 Standard deviation of the error e_φ , roll angle φ , roll rate $\dot{\varphi}$ and control signal s_a , during the target following tasks and the standard deviations over 15 measurement runs.

centrally displayed error signal e_ϕ . The peripheral displays present roll rate $\dot{\phi}$ and the simulator motion system presents roll acceleration $\ddot{\phi}$ to the subjects. However, the same trend of decreasing standard deviations is found for both ϕ and $\dot{\phi}$, Fig. 7.5, although these variables are not the directly controlled ones. The standard deviation of the subject's control input s_ϕ follows a similar trend.

Disturbance task

For the disturbance task, the performance for the configuration with the central display alone, C, is considered to be base line performance, Fig. 7.6. In the disturbance task, a decrease in the score parameter S_c is found due to the addition of peripheral displays, simulator motion or both, Table 16.

Quite remarkable is the performance for the configuration with only simulator motion, M. Here the lateral specific force A_y , Eq. 6.2, provides the subjects with the required attitude cues. Considering next the configuration with the central display and motion, CM, a significant improvement is found. This improvement results from the more accurate roll attitude perception from the central display.

Once vestibular motion stimuli are present, little appears to be gained by adding peripheral displays. (Configurations CM and M compared to CPM and PM).

The added configurations CPR and CPS, where the (most important) peripheral visual information is coming from the right side peripheral display, both show a performance just between the performances of the C and CP configurations. The almost equal performance in these two configurations (CPR and CPS) demonstrate that the general performance level of the subjects in the two parts of the experiment (low noise room and flight simulator) do not differ significantly.

Finally, the configuration with the peripheral displays only, P, demonstrate the worst performance. This results from the absence of adequate roll attitude information.

The standard deviations of the roll rate $\dot{\phi}$ and the control output s_ϕ , Fig. 7.6, demonstrate the significant influence of the addition of motion stimuli on these variables. The peripheral visual stimuli have no significant influence on these standard deviations.

From the data presented so far, it appears that the influence of the peripheral displays is relatively stronger for the following task than for the disturbance task. The influence of motion seems to be slightly weaker.

In summary, it can be observed that for both the target following task and the disturbance task, addition of peripheral visual stimuli improves the performance of the subjects just as vestibular motion stimuli do. The influence of vestibular motion stimuli, however, is much stronger. Virtually no further improvement is obtained by adding the peripheral visual stimuli once vestibular motion stimuli are present.

The mean effect of adding peripheral displays, motion or both peripheral displays and motion to the central display can be summarized by the following relative decreases in standard deviations of the tracking errors σ_{e_ϕ} , and σ_ϕ , Table 17.

An ANOVA on the output variables of the measurement runs, the standard deviation of the measured variables, was performed. The results of the analyses provide data on the statistical significance of the changes in the output variables due to the independent variables; the display configurations, the subjects and the replications.

The results of the ANOVA on the standard deviations of the measured variables of the 60 runs in the following task and of the 135 runs in the disturbance task are summarized in Table 18.

Table 17. Decrease in RMS tracking error due to the addition of peripheral displays and motion to the central display.

| Task | Peripheral displays | Motion | Peripheral displays and motion |
|-----------------------|---------------------|--------|--------------------------------|
| Target following task | 27 % | 41 % | 44 % |
| Disturbance task | 15 % | 60 % | 64 % |

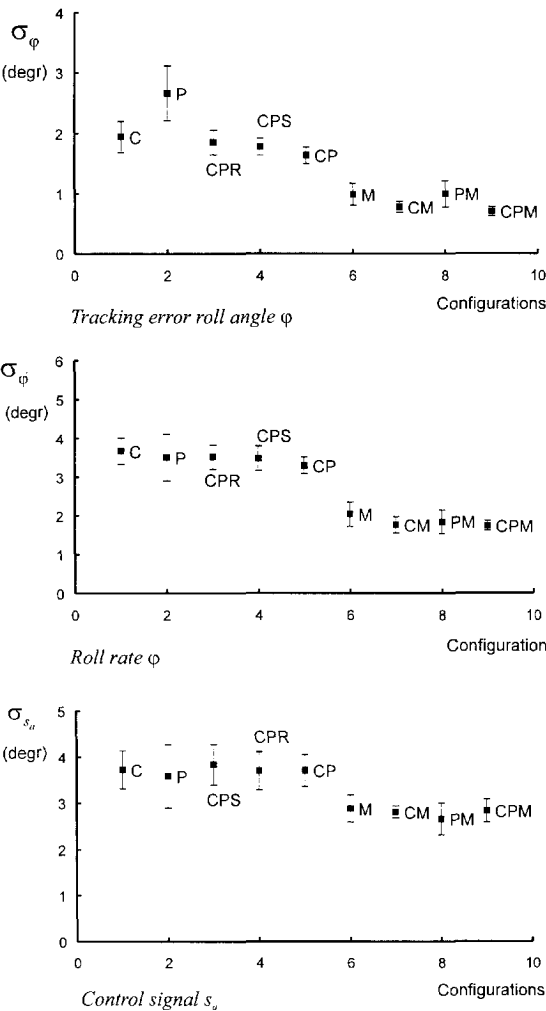


Figure 7.6 Standard deviation of the roll angle φ , roll rate $\dot{\varphi}$ and control signal s_a during the disturbance tasks.

Table 18. Summary of the ANOVA on the standard deviation of the measured variables.

| Target following task | σ_{e_φ} | σ_φ | $\sigma_{\dot{\varphi}}$ | σ_{s_a} |
|------------------------------|----------------------|--------------------------|--------------------------|----------------|
| Configurations | ** | ** | ** | * |
| Subjects | - | ** | ** | ** |
| Interactions, Subjects-Conf. | - | - | * | ** |
| Replications | - | - | - | * |
| Disturbance task | σ_φ | $\sigma_{\dot{\varphi}}$ | σ_{s_a} | |
| Configurations | ** | ** | ** | |
| Subjects | - | ** | ** | |
| Interactions, subjects-conf. | - | ** | ** | |
| Replications | - | - | - | |

** = significant influence, $\alpha < 0.01$

* = significant influence, $0.01 < \alpha < 0.05$

They show that the changes in performance, as expressed by σ_{e_φ} and σ_φ , due to the configurations, are significant for both tasks.

This holds for both the standard deviation of φ , $\dot{\varphi}$, and s_a in the target following task and $\dot{\varphi}$ and s_a in the disturbance task. In addition, a significant influence of the subjects and interaction between subjects and configurations is demonstrated for these variables. This indicates that subjects, while obtaining approximately equal performance, used different control strategies and reacted differently to the changes due to the configurations.

7.4.2 Control behavior

From the measurements, the subject's frequency responses $H_p(\omega_i)$, describing the relation between the subject's input e_φ or φ to the subject's output s_a , were calculated for each experimental run as mentioned in Sect. 7.2. The mean frequency responses for the three subjects and five replications were determined as described by van der Vaart (1992). The results are presented in Fig. 7.7. Tables with the mean frequency response and the standard deviations are given in Appendix 2. The differences in these frequency responses due to the differences in control tasks and configurations will be discussed below.

Target following task

In Fig. 7.7 the subject's frequency responses, as obtained in the target following task, are presented. The positive slope of the modulus of the frequency response $|H_p(\omega_i)|$ corresponds with the positive phase angle at low frequencies. The frequency response of the basic configuration, C, corresponds well with the results of McRuer et al. (1965, 1967) for the controlled element $H_c(\omega) = K_c / (j\omega)^2$. The changes in the subject's frequency response $H_p(\omega_i)$ when adding cockpit motion correspond with the results of the literature review in Sect. 2.2. The modulus decreases and the phase angle increases (more positive) at low frequencies. At the high-input frequencies, the phase angle decreases (more negative). The bode plots of the frequency response for each display configuration with the standard deviation of the modulus and phase angle are presented in Fig. 7.9.

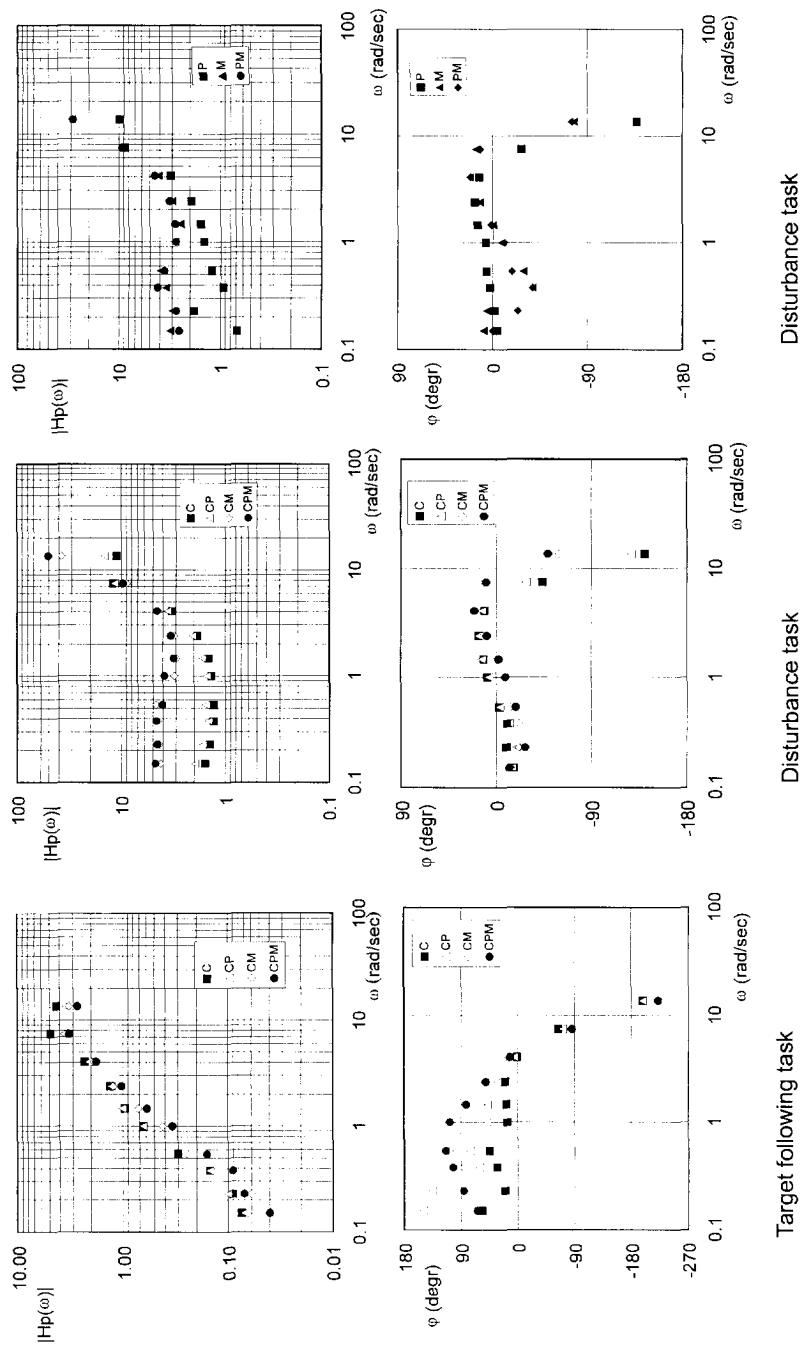


Figure 7.7 The mean pilot's frequency response in the target following task and the disturbance task.

Crossover frequency ω_c and phase margin φ_m were determined by fitting the crossover model to the open-loop describing function $H_p(\omega_i)H_c(\omega_i)$ in the crossover region. They are presented in Fig. 7.8. The crossover frequency for the basic configuration, C, $\omega_c = 2.18$ rad/sec, is low compared to the 3.25 rad/sec found by McRuer, whereas the phase margin, $\varphi_m = 19$ degrees, quite well matches with McRuer's data. This lower crossover frequency originates from the different forcing function. The crossover frequency decreases from 2.18 to 1.49 rad/sec whereas the phase margin increases from 19 to 85 degrees when peripheral visual and motion cues are added.

Disturbance task

The bode plots of the mean frequency response $H_p(\omega_i)$ in the disturbance task for all display configurations are presented in Figs 7.7. The modulus $|H_p(\omega_i)|$ for the basic configuration, C, at low frequency ($\omega < 1$ rad/sec) is almost constant, which corresponds to the small phase angle. At frequencies above 1 rad/sec a positive slope (differentiating behavior) of the magnitude is found combined with a positive phase angle, decreasing with increasing frequency. This effect is expressed by the time delay τ in the quasi linear pilot model, Eq. 7.5. Due to the addition of peripheral-visual and motion cues to the central display the modulus $|H_p(\omega_i)|$ increases over almost the whole frequency range tested, while the phase angle increases (more positive or less negative) for $\omega > 3$ rad/sec. It turns out that the subjects were quite capable of performing the control task without the central display.

The bode plots of the frequency response for each display configuration with the standard deviations of the modulus and phase angle are presented in Fig. 7.10.

In Fig. 7.8 the crossover frequency ω_c and phase margin φ_m for all configurations are plotted. The crossover frequency ω_c increases only slightly as a result of the peripheral displays (from 3.2 to 3.3 rad/sec), but strongly as a result of cockpit motion (from 3.2 to 5.0 rad/sec). The phase margin φ_m is hardly affected by the addition of the peripheral displays and motion.

Summarizing the results concerning the performance and control behavior in both tasks, it can be concluded that performance improvement resulting from the addition of peripheral visual and simulator motion cues, coincides with changes in the subject's control behavior as expressed by the frequency response.

In the case of the target following task, the performance improvement is accompanied by a strong increase in the phase angle of the frequency response at the low frequencies and a decrease in the modulus, especially at the low frequencies. These changes of the subject's control behavior result in a slight decrease in the crossover frequency and a strong increase in the phase margin.

For the disturbance task, the performance improvement can easily be explained by the changes in the subject's frequency response, increase of the modulus especially at low frequencies and an increase of the phase angle at high frequencies. This results in an increase in crossover frequency at an almost constant phase margin.

7.5 Influence of the task and the display configuration on pilot model parameters.

Despite the clear differences in the frequency response due to changes in the task and the display configuration, it is necessary to quantify these differences by the parameters of the quasi linear pilot model. This has been performed for a limited number of the experimental

configurations (van der Vaart, 1992). Due to some additional corrections of the describing functions necessary as discussed in paragraph 7.2, this exercise has been repeated to obtain the corresponding model parameters.

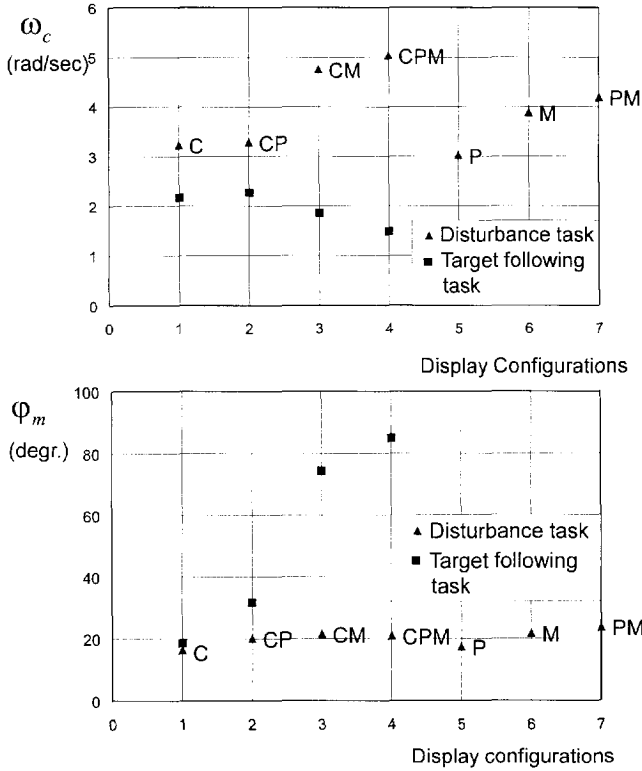


Figure 7.8 Crossover frequency and phase margin for all display configurations in the target following task and the disturbance task.

The model used is the Simplified Precision Model from McRuer (1965). For the control of a double integrator this model has the following form:

$$H_p(\omega) = K_p(T_L j\omega + 1)e^{-j\omega\tau_e}, \quad (7.3)$$

and has been used to fit both the target following task and the disturbance task frequency responses. It becomes clear from the standard deviations of the modulus $|H_p(\omega_i)|$ and the phase angle $\phi(\omega_i)$, Figs 7.9 and 7.10, that the frequency response data have a limited reliability. The model of Eq. (7.3) fits the frequency response $H_p(\omega_i)$ only at the forcing-function input frequencies ω_i where the standard deviation $\sigma|H_p(\omega_i)| < |H_p(\omega_i)|$. The results are presented in the Tables 19 and 20. The number n denotes the number of input frequencies at which the frequency response data have been used to fit the model.

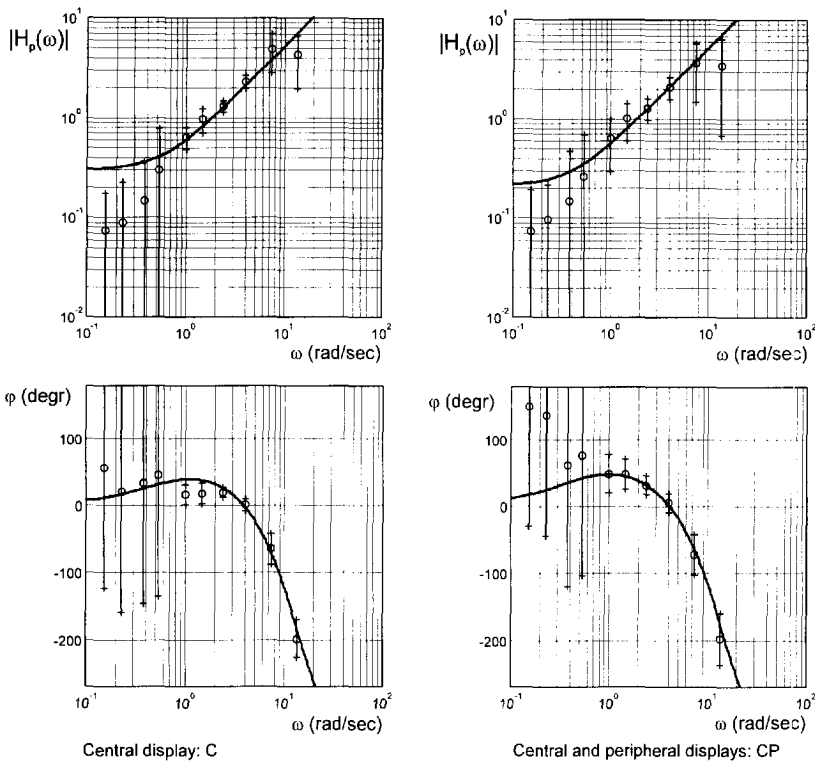


Figure 7.9a The measured frequency response combined with the fitted models. Target following task, Configurations C and CP.

Target following task

The frequency response, the standard deviations, and the fitted models are presented in Fig. 7.9 a and b for the four configurations of the target following task. The model parameters in Table 19 show that the time delay $\tau \cong 0.37$ s. and is independent of the display configuration. The lead time constant T_L , however, increases when motion cues, peripheral visual or vestibular, of the system output are fed back. The lead time constant magnitude, in case of motion cues feed back, is so large that a change of the lead term $(T_L j\omega + 1)$ in the numerator to a pure differentiator $j\omega$ could be considered. Rate feedback dominates the subject's control behavior. The bandwidth of the forcing function is too small to extend the model with a reliable neuromuscular term.

Disturbance task

The frequency response, the standard deviations of the modulus and the phase angle, and the fitted models are presented in Fig. 7.10 a, b and c. From the model parameters in Table 20 it is clear that the feedback of motion cues has a clear and distinct influence on the model parameters. Due to the peripheral visual and/or vestibular motion feedback, the pilot's gain K_p is increased from 1.3 to 2.9, the lead time constant T_L is decreased from 0.50 to 0.30 s and the time delay τ is decreased from 0.23 to 0.13 s.

Table 19. Model parameters of the simplified precision model for the target following task.

| Display Configuration | n | K_p | T_L (sec) | τ (sec) |
|-----------------------|---|--------|-------------|--------------|
| C | 6 | 0.301 | 1.74 | 0.37 |
| CP | 6 | 0.214 | 2.46 | 0.36 |
| CM | 7 | 0.0039 | 93.7 | 0.37 |
| CPM | 9 | 0.0013 | 250. | 0.37 |

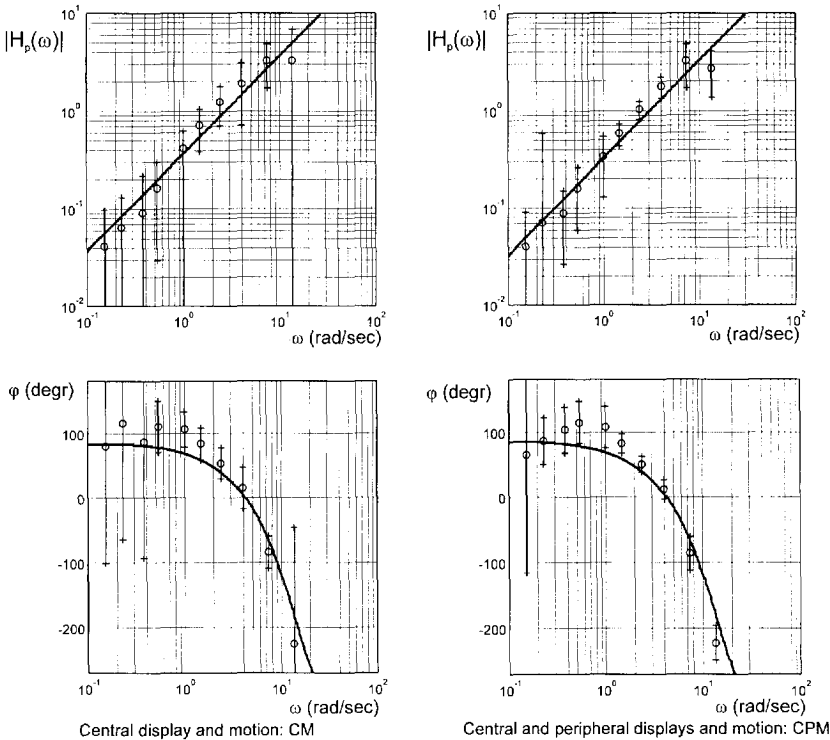


Figure 7.9b The measured frequency response combined with the fitted model. Target following task, Configurations CM and CPM.

The difference between the time delays for the central display configuration, C, in the target following task ($\tau = 0.37$ s) and the disturbance task ($\tau = 0.23$ s) is remarkable, Fig. 7.11. The pilot's task is to minimize the displayed control error. He has limited possibilities to adjust his control behavior, and to optimize his performance. A smaller time delay obviously gives the pilot the ability to improve his performance in the disturbance task.

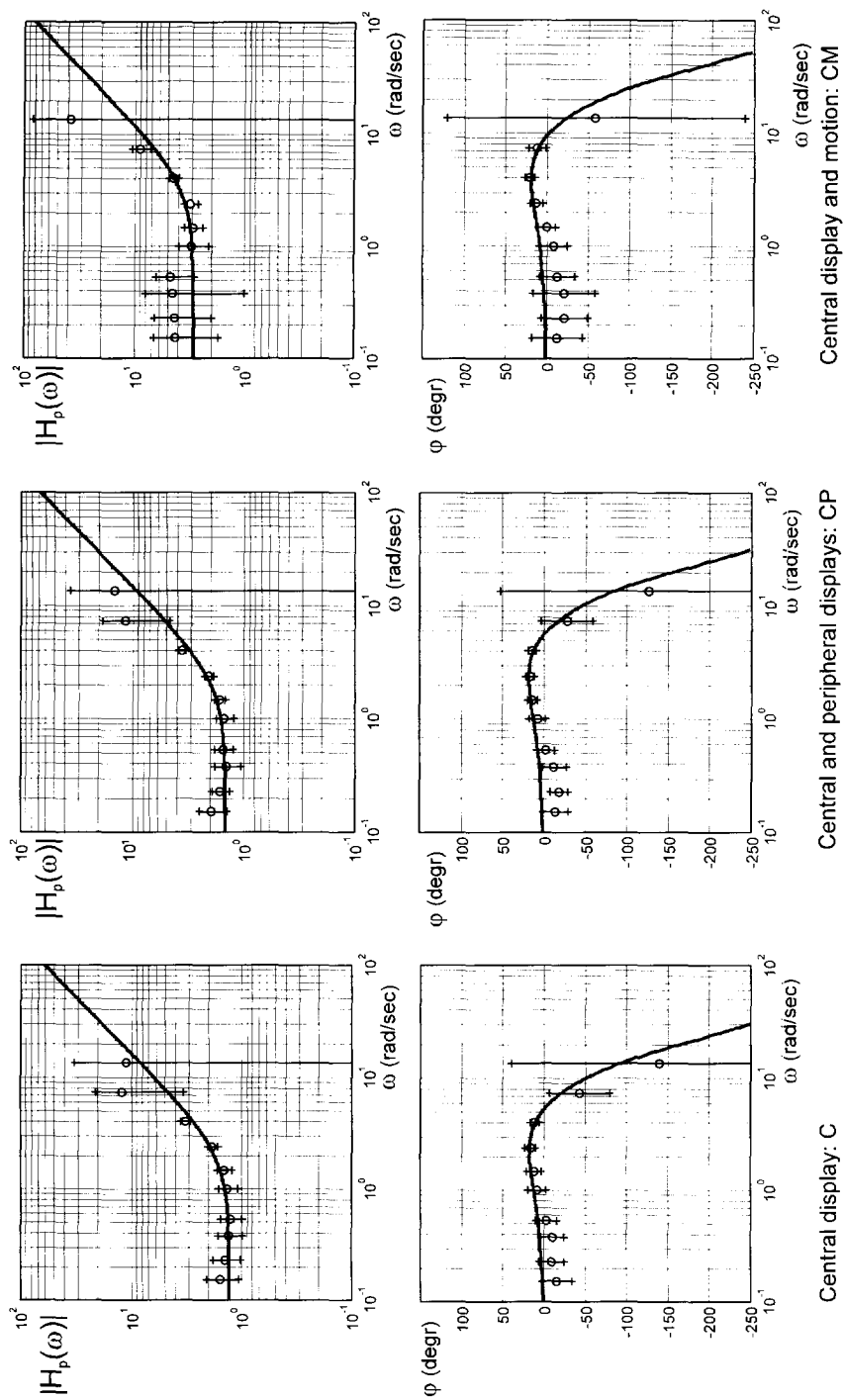


Fig. 7.10a. The measured frequency response combined with the fitted model. Disturbance task, configurations C, CP and CM.

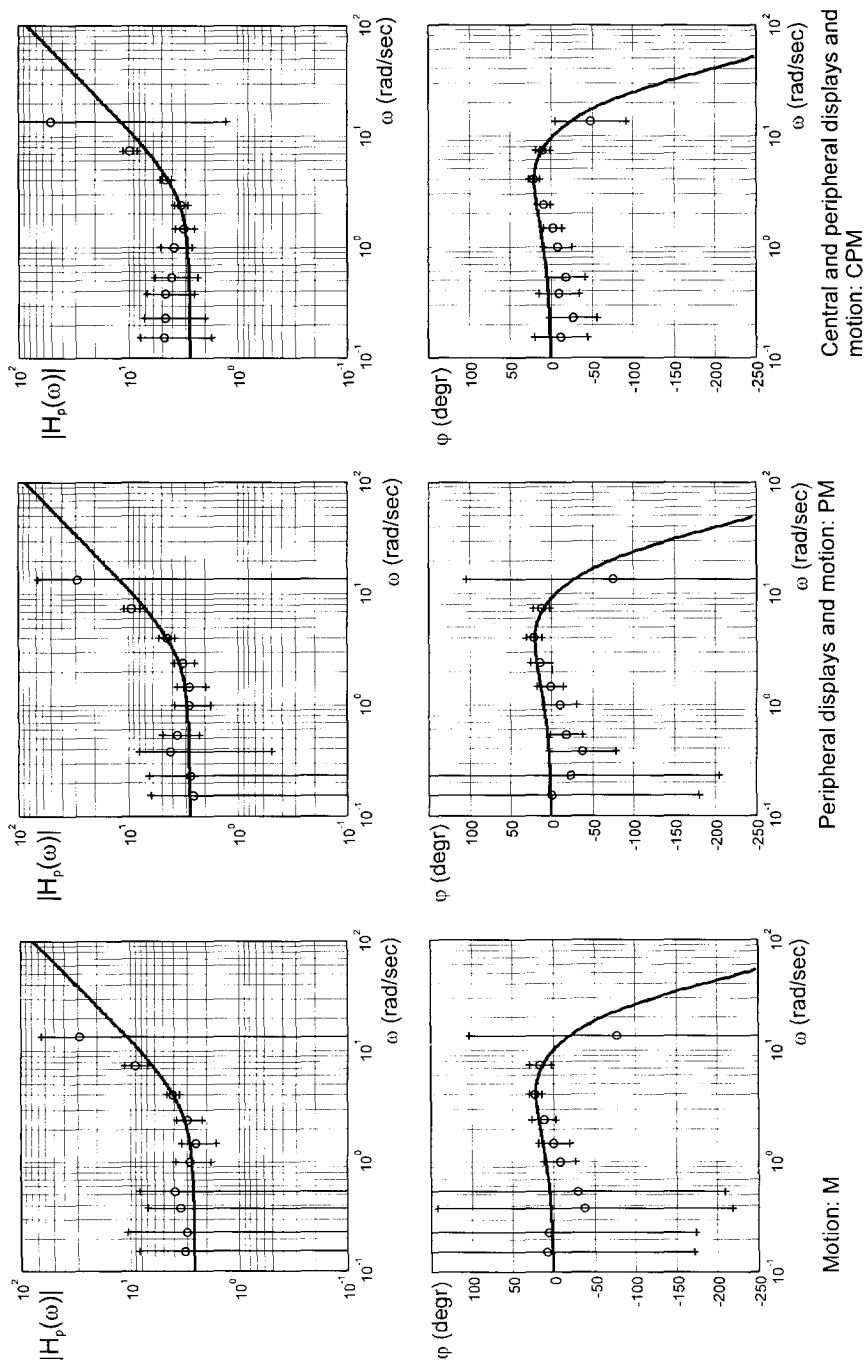


Fig. 7.10b. The measured frequency response combined with the fitted model. Disturbance task, configurations M, PM and CPM.

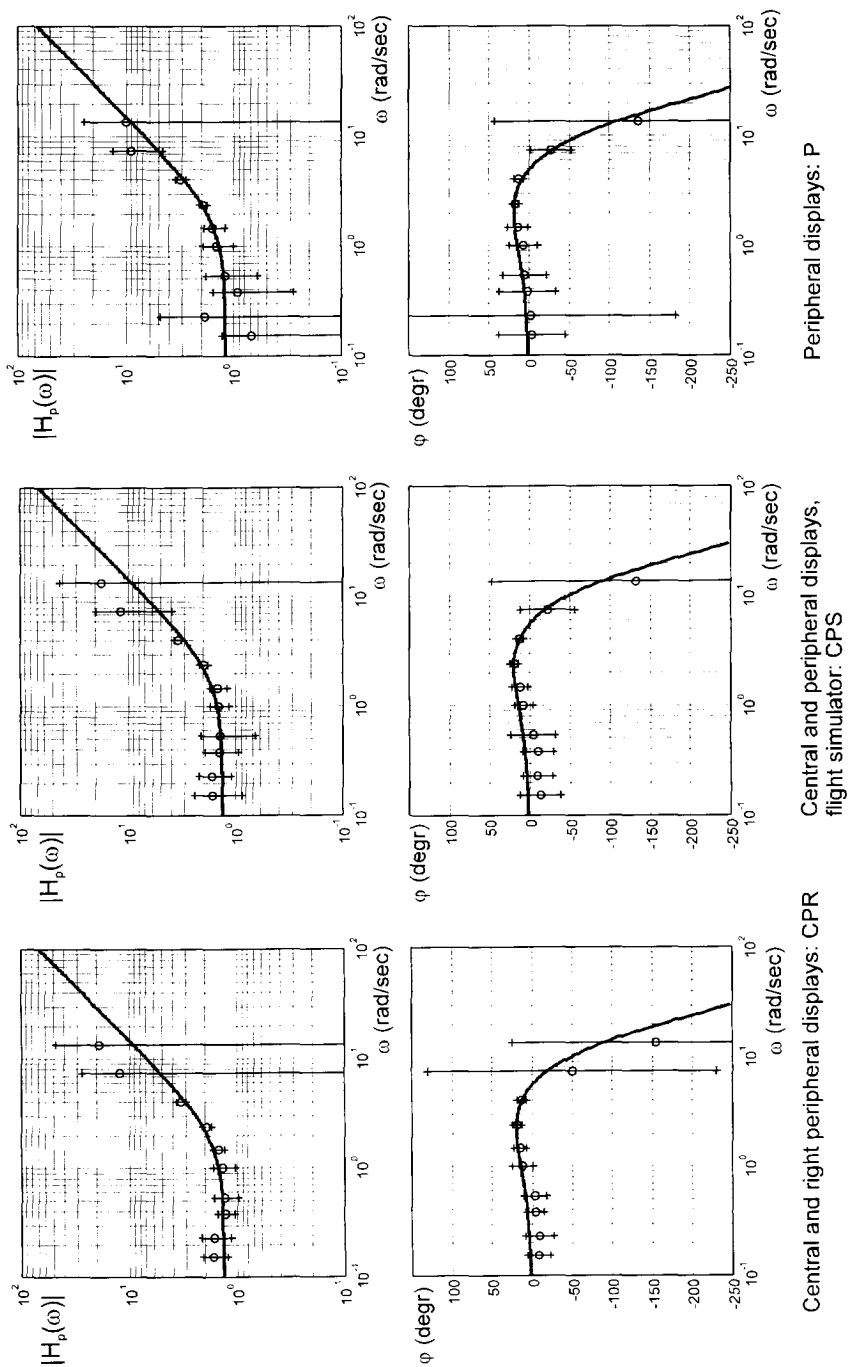


Fig. 7.10c. The measured frequency response combined with the fitted model. Disturbance task, configurations CPR, CPS and P.

Table 20. Model parameters of the simplified precision model for the disturbance task.

| Display Configuration | n | K_p | T_L (sec) | τ (sec) |
|-----------------------|----|-------|-------------|--------------|
| C | 9 | 1.28 | 0.50 | 0.23 |
| CPR | 8 | 1.34 | 0.50 | 0.22 |
| CPS | 9 | 1.34 | 0.50 | 0.22 |
| CP | 9 | 1.47 | 0.46 | 0.22 |
| CM | 9 | 2.91 | 0.28 | 0.13 |
| CPM | 10 | 2.78 | 0.30 | 0.13 |
| P | 8 | 1.20 | 0.55 | 0.25 |
| M | 5 | 2.61 | 0.29 | 0.12 |
| PM | 7 | 2.79 | 0.31 | 0.14 |

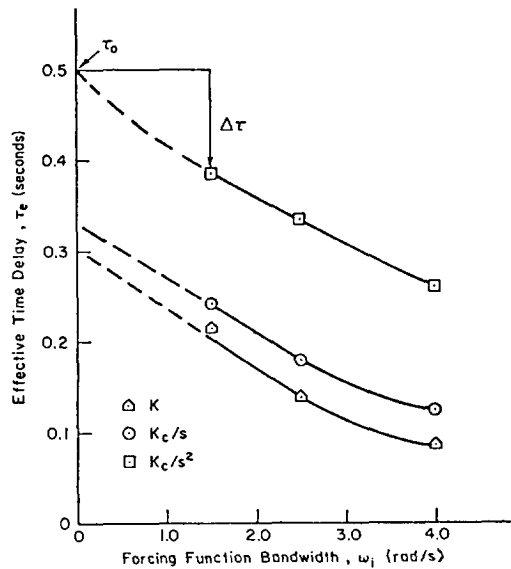


Figure 7.11 Variation of effective time delay on type of controlled element and input bandwidth, from McRuer (1967).

7.6 Discussion and conclusions

Compared to the experiments reviewed in Sect. 2.3, the results of the present experiment demonstrate an equal but clear and strong influence of the addition of peripheral visual and cockpit motion stimuli on the subject's tracking performance and control behavior. The results of this experiment in general highlight the final conclusions of Sect. 2.3 that.

1. In the case of first-order system dynamics, an influence of vestibular-motion cues may be found on the subject's tracking performance and dynamic behavior in both the target following task and disturbance task. If the system dynamics are of the second or higher order, peripheral-visual and vestibular-motion cues have an influence in both the target following task and disturbance task.
2. The changes in the subject's dynamic behavior for the target following task and disturbance task are different. In the case of the target following task, the subject increases his low frequency lead, which increases the phase margin at an approximately constant crossover frequency. In the case of the disturbance task, the subject increases his high frequency lead. This enables the subject to increase his gain and the crossover frequency at an approximately constant phase margin.
3. In the case of the disturbance task, the time delay τ of the fitted pilot model (Eq. 2.8) is decreased by 0.1 to 0.15 sec due to the addition of motion cues.

Considering the results of the present experiment, the conclusions can be modified:

1. Peripheral visual and vestibular motion cues influence the subject's tracking performance and dynamic behavior in both the target following tasks and disturbance tasks if the system dynamics are second or higher order.
2. The changes in the subject's dynamic behavior in the cases of the target following and disturbance task are different. In the case of the target following task, the subject increases his low frequency phase advance and decreases his low frequency gain. As a consequence the phase margin increases at an approximately constant or slightly decreasing crossover frequency. In the case of the disturbance task, the subject increases (more positive) his high frequency phase which enables the subject to increase his gain and the crossover frequency at an almost constant phase margin.
3. Resulting from the addition of cockpit motion stimuli, a decrease in the time delay τ has been reported by some authors. In the present experiment a decrease of approximately 0.1 to 0.15 s. has only been found in the disturbance task.

The much stronger effects of the addition of peripheral displays and/or cockpit motion in the present experiment may result from one or more of the following factors:

- The chosen system dynamics of $K/(j\omega)^2$.
- The wide bandwidth of the flight simulator motion system, which made it possible to compensate for the motion system dynamic characteristics. This made a one to one simulation of the controlled system dynamics in all configurations possible.
- The extensive training of the subjects.

The extend to which the above factors may have influenced the present results can only be established by further research which is beyond the scope of this thesis. However, some remarks can be made. The combined dynamics of the controlled element and the simulator motion system, $H_c(\omega)$, as used in the experiments described in sect. 2.3, differ considerably from the corresponding controlled element dynamics used in the present experiment, Fig. 7.12. Most systems have approximately second order dynamics in the mid frequency range ($1 < \omega < 10$ rad/sec) but deviate from the double integrator dynamics at the lower and higher frequencies. Especially the phase angle of these systems may differ from that of the double integrator. To maintain good closed-loop response characteristics in that case, the subjects had to compensate for the phase angles or they had to change their gain resulting in a change of the crossover frequency. Comparing the subject's control behavior in the experiments

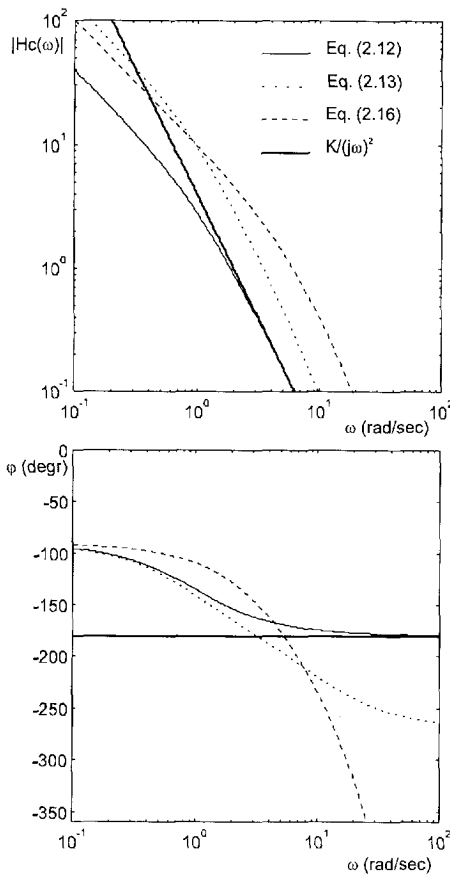


Fig. 7.12 Bode plots of systems used as controlled elements in the tracking tasks, Chs 2 and 7, to investigate the influence of motion feedback on subject's control behavior.

approximately constant or slightly decreased crossover frequency.

In the disturbance task, the subject decreases his time delay τ which results in an increase (more positive) of the phase angle in the high frequency range. This enables the subject to increase his gain and the crossover frequency at an almost constant phase margin.

Figs 7.9 and 7.10 show that with the simplified precision model (Eq. 7.3) a good fit to the frequency response data can be obtained. Due to the task differences between the target following task and the disturbance task and between the display configurations there are significant differences between the model parameters. In the case of the display configuration with the central display only, C, there is a distinct difference in the time delay τ (0.37 s) for the target following task and (0.23 s) for the disturbance task. It is the pilot's task to minimize his control error. To reach that goal he has limited possibilities. He can change his overall gain which changes the crossover frequency and phase margin. Given the small phase margin

mentioned in Sect. 2.3 with that in the present experiment, it is clear that the subjects were not able to reach the high crossover frequencies of the present experiment and had to decrease their control gain to compensate for the phase lag.

During the training of the subjects for a tracking experiment not only the tracking performance improves with training but, in addition, the crossover frequency is increased and the variation in the performance and control behavior is decreased. Thus extensive training is required for reliable experimental results.

Based on the results of the present experiment the second conclusion of Sect. 2.3 can be improved:

The changes in the subject's dynamic behavior due to peripheral visual and vestibular motion feedback in the target following and the disturbance task are different.

In the target following task, the subject increases his lead (T_L) and decreases his low frequency response magnitude. This increases the phase angle advance at low frequency and the phase margin at an

of 16 degrees, Fig. 7.8, the gain looks almost optimal. In the present task the pilot can generate more lead by increasing the weighing of the error rate. Finally the pilot can decrease his time delay. The effect of changing the lead time constant and/or the time delay can be evaluated by computing the error standard deviation σ_ϕ with the transfer function $H_{\phi,w}(\omega)$, Eq. (7.2), relating the error ϕ and the disturbance signal w in the disturbance task given the disturbance signal w , Table 14, and by neglecting the pilot's remnant.

$$H_{\phi,w}(\omega) = \frac{H_c(j\omega)}{1 + H_p(j\omega)H_c(j\omega)}, \quad (7.2)$$

The transfer function $H_p(\omega)$, Eq. (7.3) substituted in Eq. (7.2) has been based on the simplified precision model as fitted to the measured frequency response for the display configuration C. The results are presented in Table 21 below.

As can be seen in Table 21a, an increase in the lead time constant allows the pilot to increase his time delay at the cost of an increase in error standard deviation. A decrease in the time lead results in a decrease in error standard deviation at the cost of an additional decrease in the time delay. Table 21b shows that an increase in the time delay decreases the crossover frequency at the maximum phase margin and an increase in error standard deviation. A decrease in the time delay results in an improvement of the error. The time delay of 0.225 s seems to be the minimum value the pilot can achieve considering the phase margin. It is optimal to the tracking performance in the disturbance task.

According to Ch. 3, the information processing by the human operator due to a specific task can be divided in a number of stages performed in series. In the two tracking tasks the only changes affecting the information processing are the changes in the display configurations. The only difference between the display configurations is the stimulation of the selected sensors with visual and vestibular cues. Therefore, one would expect that the changes in the subject's dynamic behavior result from the changes in the perception process forced by the changes of the display configuration.

In the disturbance task both the single input configurations C, P and M and the combined input configurations CP, CM, PM and CPM have been studied. The frequency response of combined input configurations can not be derived by simply adding the frequency responses of the corresponding single input configurations. The frequency response is the result of the contributions of the individual stages of the information processing. The frequency response of a combined input configuration may, however, be obtained by the weighted sum of the frequency responses of the corresponding single input configurations. For the configuration with the central display and motion, CM, the describing function should be equal to:

$$H_{p(CM)}(\omega) = a(\omega) \cdot H_{p(C)}(\omega) + b(\omega) \cdot H_{p(M)}(\omega), \quad (7.4)$$

where $a(\omega)$ and $b(\omega)$ are frequency dependent. An example at a particular input frequency is given in Fig 7.13. The weighting coefficients $a(\omega)$ and $b(\omega)$ may be derived from the measured frequency response at the input frequencies ω_i . Fig. 7.14 presents the results of $a(\omega)$ and $b(\omega)$ for all possible configuration combinations in the disturbance task. The scatter in the weighting factors $a(\omega)$ and $b(\omega)$ is rather high due to the uncertainty in the measured frequency response $H_p(\omega_i)$, Fig. 7.10. Small or even negative values of $a(\omega)$ and $b(\omega)$ (≤ 0.01) are not presented.

Table 21a The influence of the lead time constant T_L on the error standard deviation at constant crossover frequency and phase margin in the disturbance task. The shaded row presents the nominal precision model for the measured condition.

| K_p | T_L (s) | τ (s) | ω_c (rad/sec) | Φ_m (degr.) | σ_φ (degr.) |
|-------|-----------|------------|-------------------------|---------------------|-----------------------------|
| 1.725 | 0.3 | 0.148 | 3.00 | 16 | 1.23 |
| 1.30 | 0.5 | 0.225 | 3.00 | 16 | 1.57 |
| 0.73 | 1.0 | 0.316 | 3.00 | 16 | 2.42 |
| .50 | 1.5 | 0.349 | 3.00 | 16 | 3.18 |

Table 21b The influence of the time delay on the error standard deviation at constant phase margin in the disturbance task. The shaded row presents the nominal precision model for the measured condition.

| K_p | T_L (s) | τ (s) | ω_c (rad/sec) | Φ_m (degr.) | σ_φ (degr.) |
|-------|-----------|------------|-------------------------|---------------------|-----------------------------|
| 2.53 | 0.5 | 0.175 | 5.14 | 16 | 0.74 |
| 1.90 | 0.5 | 0.200 | 4.03 | 16 | 1.03 |
| 1.3 | 0.5 | 0.225 | 3.00 | 16 | 1.57 |
| 0.74 | 0.5 | 0.250 | 2.02 | 15 | 3.05 |
| 0.62 | 0.5 | 0.275 | 1.80 | 12 | 3.90 |

Fig. 7.14 shows that in the case of the display configurations CM, PM and CPM, the visual stimuli are weighted with a gain decreasing with increasing frequency, and the motion stimuli are weighted with an almost constant gain. The combination of central and peripheral displays, CP, shows that the central display has the highest weight at low frequencies whereas the peripheral displays have a weighting factor larger than 1 at the highest input frequencies.

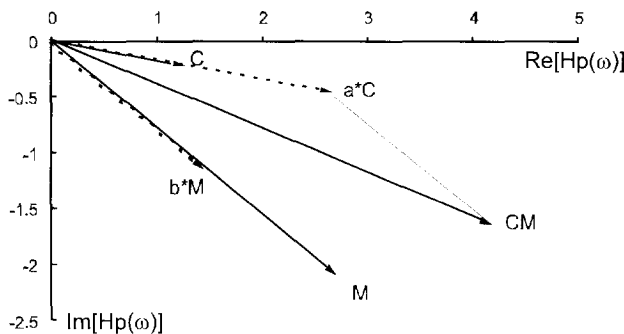


Fig.7.13. The weighting factors a and b for the construction of $H_{p(CM)}(\omega)$ based on $H_{p(C)}(\omega)$ and $H_{p(M)}(\omega)$ for the input frequency $\omega_i = 0.383$ rad/sec.

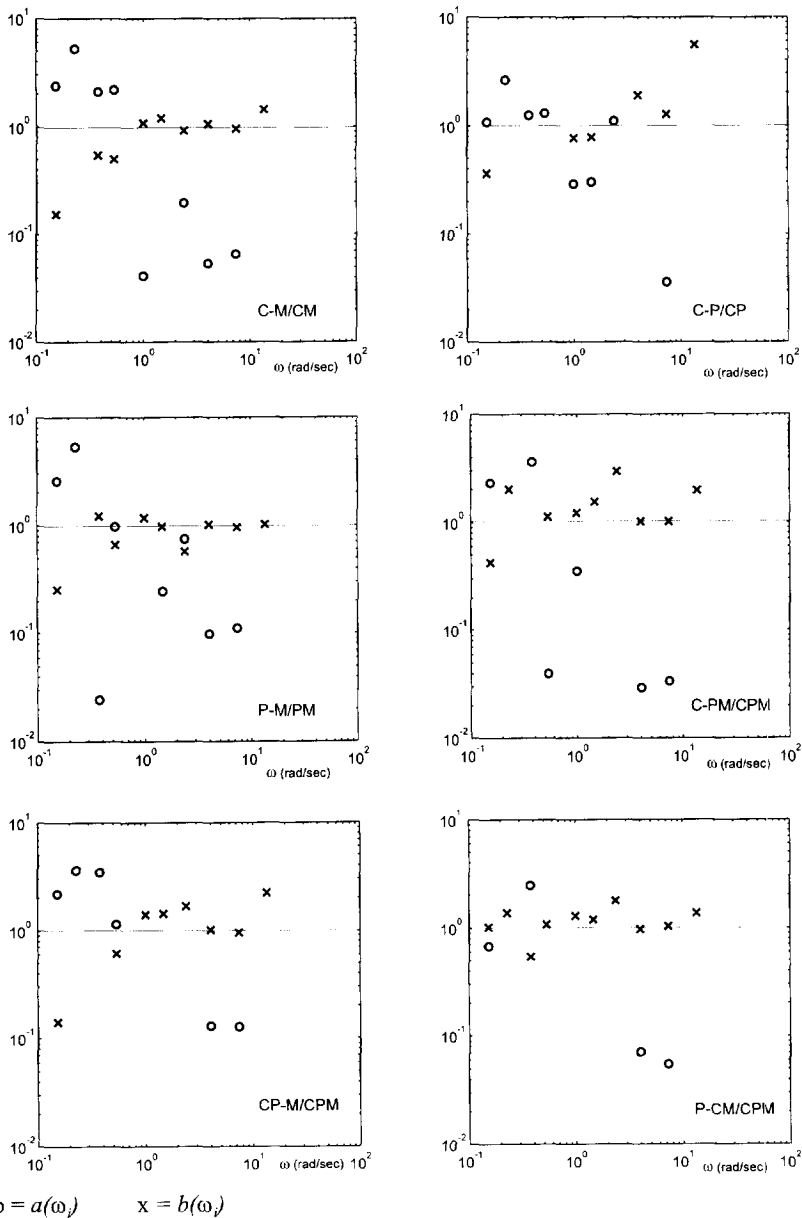


Figure 7.14 The weighting factors $a(\omega)$ and $b(\omega)$ for the six possible combinations of display configurations.

Addition of the peripheral displays P to the combined configuration CM shows that the peripheral displays are taken into account only at the lowest input frequencies. A fair conclusion is that for the well-trained subject the rate sensors, the peripheral visual system and the semi-circular canals dominate the perception process at the higher input frequencies in the disturbance task.

Two remarks have to be made here. In Ch. 3 it was discussed that the information processing by the human operator has to be considered a single channel process with multiple sensor input. Based on Sternberg's (1969) Additive Factors Paradigm and the results of the experiments in Chs 5 and 6, the addition of an supplementary sensor influences only the perception process in the stimulus response task.

The results of the disturbance task, however, show that the subject's control behavior changes due to alterations in the display configuration. When motion is added to the display configuration the crossover frequency increases at an approximately constant phase margin. This means that when adding motion cues in the closed-loop control task not only the perception process is influenced but also the decision and control response stages are affected. It is assumed that in these stages the pilot adjusts his overall control gain to optimize the control loop closure and his performance.

Therefore the meaning of the weighting factors is that the perception and decision processes of a well-trained operator balance the influence of the sensor outputs on the perceived state of the system and the subject's control output. On the other end, the meaning of the values of the weighting factors, as presented in Fig. 7.14, is limited. When the subject's frequency response is considered to be the description of the information processing in the frequency domain, then the weighting factors weigh the information processing between the stimulus input and the control output. It should, however, be more correct, if only the frequency response of the sensors and their influence on the perception stage should be weighted as they are influenced by the display configurations. In that case, the contribution of stages not influenced by the display configuration should remain constant.

Conclusions

The results of the tracking experiment described in this chapter highlight the three conclusions of Ch.2. In addition to these conclusions the results show that:

4. For tracking tasks with the presentation of the error signal on a central display the pilot's effective time delay in the disturbance task is approximately 0.15 seconds shorter than in the target following task.
5. In the dynamic environment of the closed-loop control task the addition of motion cues not only changes the perception stage of information processing but also influences the overall control gain.

8. EVALUATION, DISCUSSION AND CONCLUSIONS

8.1 Introduction

In the Chs 5, 6 and 7, three groups of experiments were described to investigate the perception of vehicle motion and its impact on subject's control behavior and performance in control tasks. In this final chapter, the results of the individual experiments will be reviewed and placed into one framework. The framework used is the model of the information processing discussed in Ch. 3, Fig. 8.1.

In Ch. 3, it was argued that more than one sensor may be involved in the perception of a certain stimulus. In the case of motion perception, the visual system, the vestibular system, and the proprioceptive system are all sensitive to motion inputs. In Ch.4, it was shown that the visual and the vestibular system dominate the motion perception process and that the proprioceptive system may be ignored. As described in Ch.3 the input stimuli are processed in parallel by the sensors and transformed to sensory output. The sensory outputs are the input to the perception process in the central nervous system. The sensory outputs do not have a specific meaning in the conscious perception process unless they are placed in a context, the context of the task and its environment. If the human operator does not have the specific knowledge on how he and the vehicle are expected to move, he will not be able to correlate the sensory output with his movements. In that case no reliable perception of motion is possible.

Considering the results obtained experimentally, the model subsystems will be incorporated as far as possible. This exercise is not only meant to propose a new pilot model. But it is also intended to demonstrate that with the data on pilot's control behavior already available in the literature, and the objective data obtained from the experiments, a well-founded understanding of the influence of motion cues on pilot's control behavior can be established.

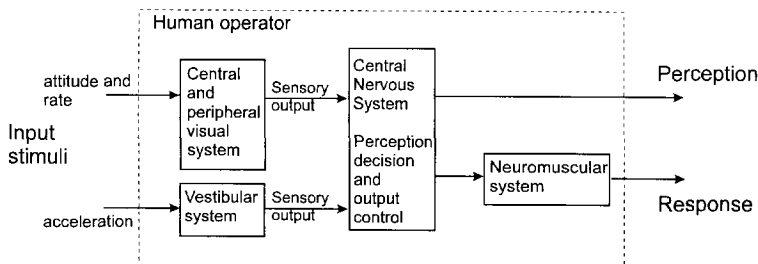


Figure 8.1 The visual- and vestibular pathway of information processing in the control task.

The subsystems of the model of Fig. 8.1 to be specified are primarily the visual and vestibular system and the interaction of both systems in the perception and decision process in the central nervous system.

In Sect. 2.3, it was hypothesized that subject's performance improvements and changes in dynamic control behavior due to motion feedback could have been obtained in two ways. Improved perception accuracy could occur, resulting from peripheral visual and vestibular motion feedback, on the one hand, and reduced perception latency could occur due to the dynamic characteristics of the peripheral visual- and vestibular system, on the other. The latter was considered to be more likely. The results of the stimulus response experiments in Chs 5 and 6 prove the second hypothesis. Therefore the differences in perception time will dominate the discussion below.

8.2 Evaluation of the experimental results

In Ch. 5, the stimulus-response experiments to determine the speed and accuracy of visual perception of roll attitude and roll rate were described. For the perception of roll attitude an artificial horizon, simulated on a CRT display, was used and observed by the subjects with the central or foveal visual system. Roll rate could be perceived by the motion-detection circuits of the central-visual and peripheral-visual system. To stimulate the peripheral-visual field two TV monitors presenting moving checkerboard patterns were used.

The relevant conclusions based on the results of the roll attitude and rate perception experiments as formulated in Ch. 5 are:

1. The reaction time for roll rate perception with the central visual field is longer (100 to 150msec) than for roll attitude perception.
2. The reaction time for roll rate perception from the peripheral visual field is shorter (about 60 msec) than that from the central visual field.
3. The perception of roll rate from the peripheral visual field and that from the central visual field are different processes.

Based on the results of Ch. 5, the relations between the inputs to the visual system and the visual sensor output can now be described. In section 4.2.2, a model for visual-motion perception was proposed:

$$H_{velocity}(\omega) = Ke^{-j\omega(\tau_1 + \tau_2)}, \quad (4.4)$$

where $K \cong 1$ and $(\tau_1 + \tau_2)$ were not exactly known. The relations between stimulus input and sensor output for visual perceived roll attitude and rate (which are described by time delays) can be fixed relative to each other. Thus, if it is assumed that the total time delay is the sum of one fixed minimum time delay τ^* for attitude perception and an additional time delay for the velocity detectors, i.e. τ_c and τ_p respectively, then for perceiving attitude in the central visual field:

$$H_{C,att}(\omega) = Ke^{-j\omega\tau^*}, \quad (8.1)$$

for perceiving rate in the central visual field:

$$H_{C,rate}(\omega) = Ke^{-j\omega(\tau^* + \tau_c)}, \quad (8.2)$$

and for perceiving rate in the peripheral visual field:

$$H_{P,rate}(\omega) = Ke^{-j\omega(\tau^* + \tau_p)}. \quad (8.3)$$

First the delays τ_c and τ_p will be defined. Thereafter, the delay τ^* is determined. Considering the data presented in Sect. 6.2, the following values of the time delays $\tau_c = 100$ msec and $\tau_p = 40$ msec will be assumed in these describing functions. Thus the output of the foveal- and peripheral-visual system due to attitude and rate stimuli in Fig. 8.1 can be described as shown in Fig. 8.2.

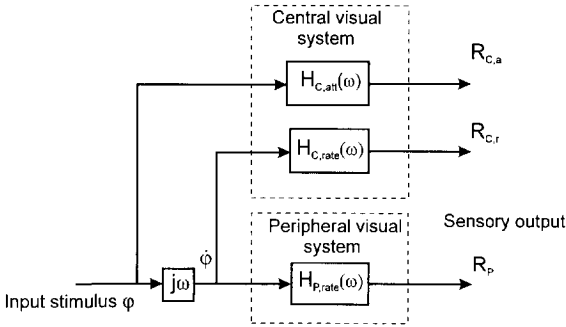


Figure 8.2 Central and peripheral subsystems of the visual system.

In Ch. 6, three stimulus-response experiments were described to investigate the interaction between visually and vestibularly perceived motion cues. A second-order system step response was used as the stimulus. To determine the influence of the display configuration, the second-order system natural frequency, and the exposure time Δt_{exp} , on the reaction time RT and the perception accuracy, three experiments were performed. The conclusions, based on the results of the three step-response experiments, were:

1. The accuracy of the estimation of the final value of a complex motion stimulus is practically independent of the display configuration.
2. The reaction time to the step-magnitude estimation is significantly decreased (200 to 400 msec) by adding cockpit motion to the visual presentation of the stimulus to the subject.
3. In motion perception, cockpit-motion cues, as well as peripheral-visual cues, speed up the perception process.

As shown in Ch. 6, faster vestibular perception of motion relative to the visual perception is the result of the dynamic characteristics of the vestibular system, on the one hand, and of the longer neural processing time of the visual system, on the other. Considering the results of Ch. 6, the scheme of Fig. 8.2 can be extended with the vestibular system. By combining the data obtained in Experiments II and III of Ch. 6, a fair estimate of the yet unknown minimum time delay τ^* for attitude perception is: $\tau^* \cong 50$ msec.

The dynamic characteristics of the semi-circular canals and the otoliths are described by transfer functions discussed in Ch. 4, Eqs (4.8) and (4.11). The lateral specific force at the position of the subject's head depends on the component of the gravitational force along the

lateral axis and the angular acceleration, Sect. 6.2. For a rotation around the roll axis the specific force A_y is:

$$A_y(t) = \ddot{\varphi}(t) \cdot l - g \cdot \sin \varphi(t) = f\{\varphi(t)\}. \quad (6.2)$$

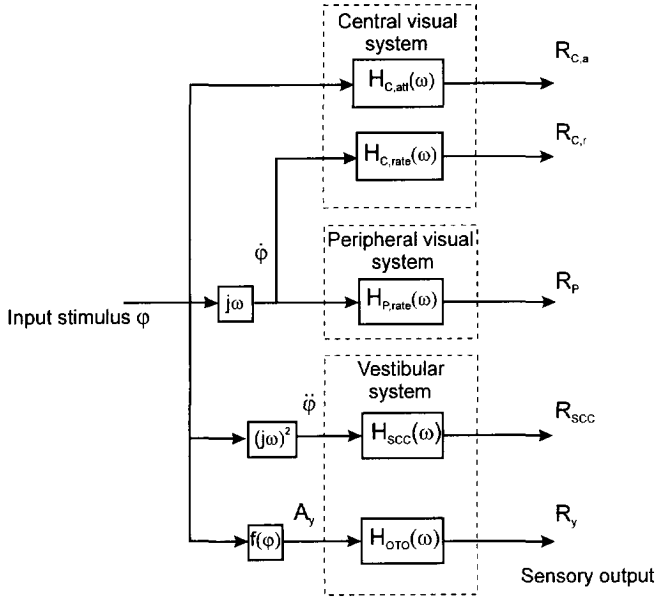


Figure 8.3 Visual and vestibular components of the sensor system.

If the roll angle φ remains small, then $\sin \varphi$ may be approximated by φ . In that case the relation between input roll angle φ and the otoliths output, due to the specific force along the lateral axis R_y , can be described by the transfer function:

$$\frac{R_y(\omega)}{\varphi(\omega)} = K \cdot [(j\omega)^2 \cdot l - g] \cdot H_{oto}(\omega), \quad (8.4)$$

where $H_{oto}(\omega)$ is the transfer function of the otoliths system, Eq. (4.11).

To maintain the mean roll angle in the disturbance task around zero, the subjects used either the roll attitude φ , as presented on the central display, C, or the lateral specific force A_y , when only motion feedback was available, M. Therefore, the otoliths were included in the model. However, the perception accuracy of the roll attitude based on the otoliths output (Hosman and van der Vaart, 1978) is less accurate than the visual perception of the attitude from the central display, Ch.5. This is confirmed by the improvement of tracking performance when the central display is added to the simulator motion in the disturbance task, Fig. 7.6. It is therefore assumed that the otoliths add information to the perception process only if no central visual attitude information is available.

In Fig. 8.4, the transfer functions, describing the relation between the roll attitude input with sensory output, are presented. Fig. 8.4a presents the Bode plots for attitude output of the central-visual system (Eq. 8.1) and the otoliths (Eq. 8.4). The otoliths output leads to the central or foveal visual system output. For high frequency inputs the position of the head above the axis of rotation, distance l , has a strong influence on the otoliths output. Fig. 8.4b shows the Bode plots for the rate sensitive sensors, the foveal- and peripheral- visual system and the semi-circular canals. The transfer function of the semi-circular canals, Eq. (4.8), relates input angular acceleration with the neural sensory output in impulses per second. To make the transfer function of the semi-circular canals comparable to that of the visual system, the input has to be changed to roll attitude and the gain has to be adjusted so that the same modulus is obtained for visual rate perception at $\omega = 1$ rad/sec. The semi-circular canals output leads to the visual system output as has been demonstrated in Ch. 6.

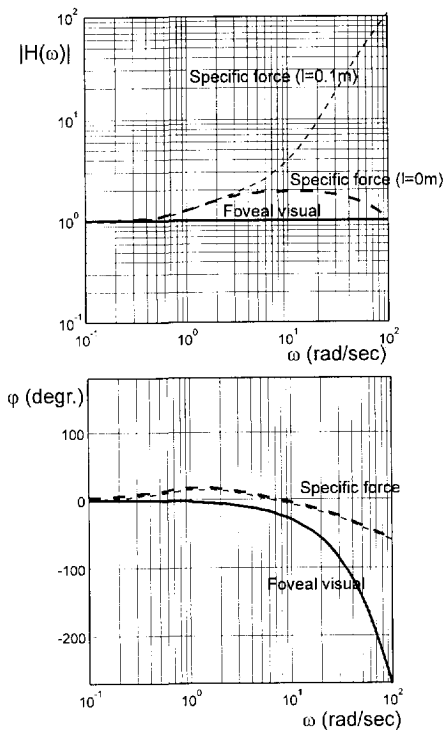


Figure 8.4a The transfer function of the attitude sensitive sensors, the central visual system and the otoliths. The transfer function of the otoliths is presented for two values of l : 0 m and 0.1 m (Eq. 7.2).

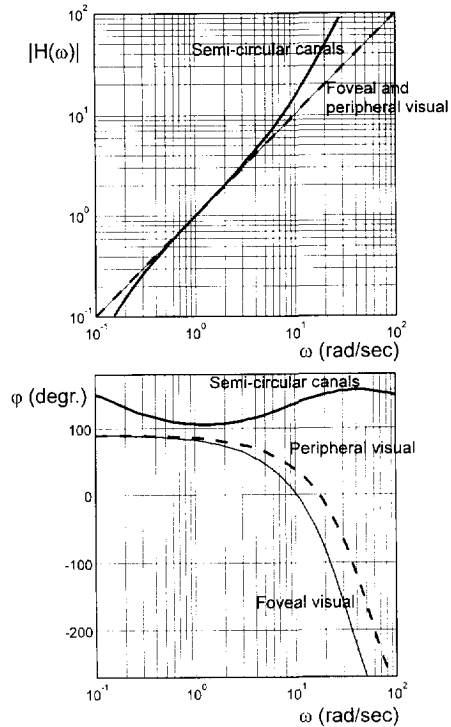


Figure 8.4b The transfer function of the rate sensitive sensors, the foveal and peripheral visual system and the semi-circular canals.

As mentioned in the introduction to this chapter, the sensory output does not have a meaning in conscious perception if it is not related to the environment and the task at hand. The question now arises how the sensory output is transferred to the perceived state and the control

output. This question can not be answered yet. What can be done is to look at the relation between the subject's dynamic behavior for specific display configurations in the disturbance task. Since the only difference between the tracking tasks with the different display configurations is the stimulation of the selected sensors, the changes in the subject's dynamic behavior are primarily due to the forced changes in the perception process.

As shown in Sect. 7.6, the subject's describing function for a configuration with two or three display inputs can be obtained by the weighted sum of the describing functions for the individual configurations. For the configuration with the central display and motion, CM, the describing function should be equal to:

$$H_{p(CM)}(\omega) = a(\omega) \cdot H_{p(C)}(\omega) + b(\omega) \cdot H_{p(M)}(\omega), \quad (7.6)$$

where $a(\omega)$ and $b(\omega)$ are dependent on the frequency ω . As discussed in Sect. 7.6 the meaning of the weighting factors $a(\omega)$ and $b(\omega)$ is limited. Considering the single channel information processor where information is processed in subsequent stages, it is more likely that the sensory outputs are weighted individually in the perception process. For practical reasons it has been assumed that the sensory outputs are weighted with frequency independent weighting factors K . Considering this assumption, the descriptive model of the information processing may be further detailed in Fig. 8.5.

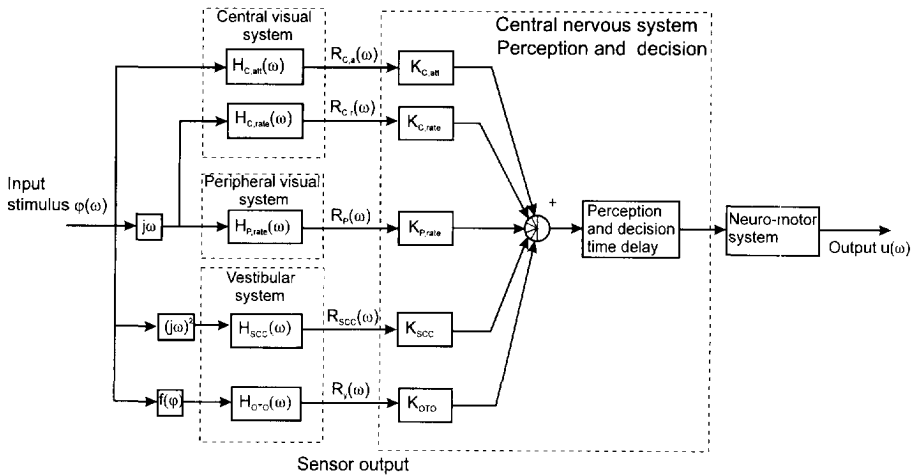


Figure 8.5 Block diagram of the descriptive model for the information processing by the human operator in a disturbance task.

It is assumed that the processing in the perception and decision stages by the Central Nervous System can be described by a gain K and a lumped time delay τ . This time delay is considered to be dependent on the task to be performed but independent of the display configuration. For the stimulus response task, for instance, the reaction time is, according to the Hick-Heyman law, Ch.3, dependent on the information content of the stimulus. In the case of tracking tasks the time delay τ may also be dependent on the specific tracking task, disturbance task or target following task.

The information processing is completed by the neuro-muscular system to generate the control output. McRuer and Krendel (1974), Magdaleno and McRuer (1971) and Van Paassen (1994, 1995) described the neuro-muscular-manipulator dynamics. The neuro-muscular-manipulator system of the well-trained human operator can be approximated over a wide frequency range by a third order transfer function. For the subject under investigation, the influence of motion perception on the pilot's control behavior, the bandwidth of the neuro-muscular dynamics is high and relatively unimportant. From the frequency responses, Figs 7.9 and 7.10, the high-frequency contribution of the neuro-muscular system can hardly be distinguished. Therefore, a pure time delay, τ_{NM} , can be used as a low-frequency approximation, up to ± 10 rad/sec, of the contribution of the neuro-muscular system to the subject's control behavior.

For further application of the descriptive model, the time delays, resulting from the information processing in the perception and decision stages and the neuro-muscular system, are combined and described by one time delay for the information processing:

$$H_I(\omega) = K_I e^{-j\omega\tau_I}, \quad (8.6)$$

with $K_I = 1$.

Based on the above considerations, the descriptive model for the target following task and the disturbance task will be evaluated in the next section using three display configurations; central display, C, central and peripheral displays, CP and central display with motion, CM.

8.3 The evaluation of the descriptive model

Target following task

To evaluate the descriptive model, firstly it will be applied to the target following task of Ch. 7. In Fig.8.6, the descriptive model is incorporated in the block diagram of the target following task. As mentioned in the previous section, the otoliths subsystem is not incorporated in the model because the central visual system has to be activated in the target following task to present the tracking error. In addition, it dominates the attitude perception with its higher accuracy. In the evaluation only the linear part of the pilot's control behavior is considered and the description of the non-linear part of the pilot's behavior, the remnant, can be ignored.

First, the display configuration with the central display is considered. For this configuration only the gains $K_{C,att}$ and $K_{C,rate}$ for attitude and rate perception with the central visual system are non-zero. In addition to these gain factors, the information processing time delay τ_I has to be determined.

McRuer (1965, 1969) performed a series of experiments in the target following task for a number of controlled system dynamics and determined the parameters of the Simplified Precision Model. In Fig. 7.11, the effective time delay τ_e , according to McRuer, is plotted as a function of system dynamics and forcing function bandwidth. This effective time delay τ_e is the sum of all sensor, information processing-, transport- and neuro-motor delays between the operator's input and output. According to the Adjustment Rules (McRuer, 1967), the human operator adjusts his dynamic behavior to the dynamic characteristics of the system. In the case of a single integrator, $H_c(\omega) = K/j\omega$, the overall dynamic behavior of the operator can be described by:

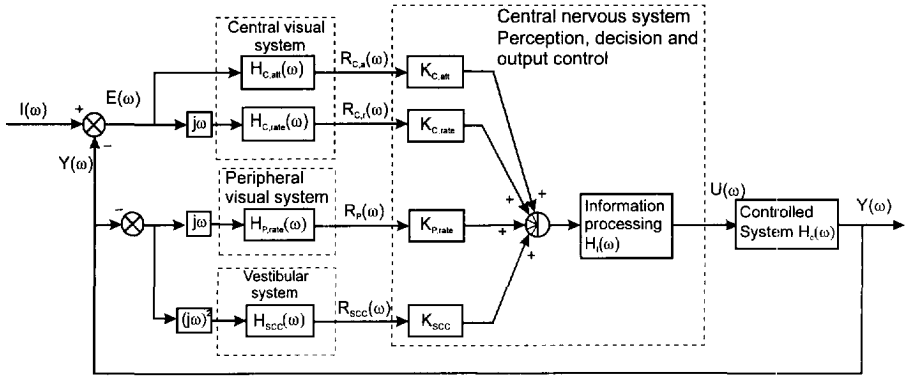


Figure 8.6 The descriptive model in the target following task.

$$H_p(\omega) = K_p \cdot e^{-j\omega\tau_e} \quad (8.7)$$

In this special case, the operator has to perceive only the magnitude of the error signal $e(t)$ to generate his output. In that case, and with a forcing function bandwidth of 1.5 rad/sec, the effective time delay $\tau_e \cong 0.25$ s, Fig. 7.11. For control of the double integrator, $H_c(\omega) = K/(j\omega)^2$, the effective time delay of the corresponding pilot model, Eq. 7.5,

$$H_p(\omega) = K_p \cdot (T_L j\omega + 1) \cdot e^{-j\omega\tau_e}, \quad (7.5)$$

is $\tau_e \cong 0.38$ s. In this case, the pilot has to perceive roll attitude and rate. As discussed in Sect. 5.5, the difference between the two time delays corresponds quite well with the increase in the reaction times for the perception of the roll attitude and roll rate in the stimulus response experiments of Ch.5. Thus, the increase in the effective time delay τ_e due to the change of the system dynamics from single to double integrator corresponds with the increase in the perception time. This means that the increase in the effective time delay can be attributed to the changes in the perception stage and that the time delay of the subsequent information processing stages are independent of the dynamics of the controlled system.

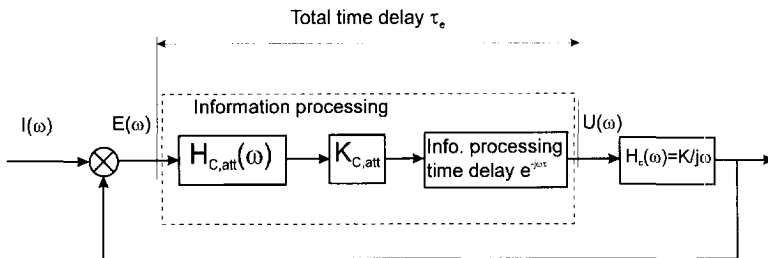


Figure 8.7 The descriptive pilot model for the control of a single integrator $K/j\omega$ in the target following task.

In Fig. 8.7 the model subsystems for the control of a single integrator in the target following task are shown. As discussed in the previous section, the time delay τ^* of the transfer function $H_{C,att}(\omega)$ is $\tau^* = 50$ msec. Considering these data, the remaining time delay has to be attributed to the information processing.

For the target following task this time delay is estimated at:

$$\tau_l = \tau_e - \tau^* = 0.2 \text{ s} \quad (8.8)$$

As mentioned before, this time delay τ_l should be independent of the dynamic characteristics of the system, $H_c(\omega)$, and may be used as the characteristic time delay for the information processing in the target following task. For control of the double integrator $K/(j\omega)^2$, the error signal $e(t)$ and its first derivative $\dot{e}(t)$ have to be perceived. The transfer function of the descriptive model for the target following task with the central display only, $H_{C,roll}(\omega)$, is:

$$H_{C,roll}(\omega) = [K_{C,att} \cdot H_{C,att}(\omega) + K_{C,rate} \cdot H_{C,rate}(\omega) \cdot j\omega] \cdot K_l e^{-j\omega\tau_l} \quad (8.9)$$

The next step is extending the model with the feedback of the system output $y(t)$ by using the peripheral displays and/or the motion system. Van der Vaart and Hosman (1987) analyzed the influence of the vestibular feedback in the target following task. They used a simple block diagram for the target following task with motion feedback, Fig. 8.8. Due to the motion feedback which is obtained by the peripheral visual system and/or by the semi-circular canals, the control behavior of the operator changes.

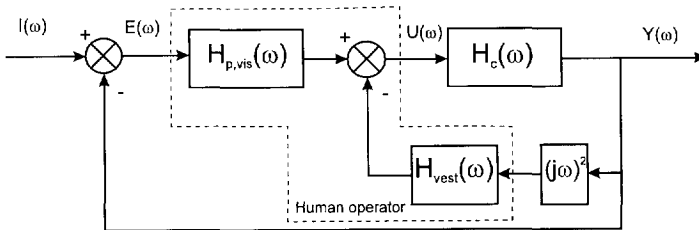


Figure 8.8 Simplified block diagram of motion feedback in the target following task (van der Vaart and Hosman, 1987).

If, for instance, the vestibular system output is fed back, the human operator describing function can be derived by:

$$H_p(\omega) = \frac{U(\omega)}{E(\omega)} = \frac{H_{p,vis}(\omega)}{1 + H_{vest}(\omega)(j\omega)^2 \cdot H_c(\omega)} \quad (8.10)$$

As shown before, the transfer functions of the peripheral visual system and the semi-circular canals may be approximated by a differentiator, Fig. 8.4. Thus, the feedback is a velocity feedback. The change in the control behavior $H_p(\omega)$ of the human operator due to this velocity feedback is described by the denominator in the transfer function of Eq. (8.10).

Table 21. The gain factors of the descriptive model configured for the target following task for three display configurations, Central display, Central and Peripheral displays and Central display and Motion.

| Transfer function | $K_{C,att}$ | $K_{C,rate}$ | $K_{P,rate}$ | K_{SCC} | τ_I (s) |
|-------------------------|-------------|--------------|--------------|-----------|--------------|
| $H_{C_{roll}}(\omega)$ | 0.31 | 0.47 | - | - | 0.2 |
| $H_{CP_{roll}}(\omega)$ | 0.31 | 0.47 | 0.10 | - | 0.2 |
| $H_{CM_{roll}}(\omega)$ | 0.28 | 0.43 | - | 0.27 | 0.2 |

Therefore the Eq. (8.10) can be approximated by:

$$H_p(\omega) = \frac{U(\omega)}{E(\omega)} \cong \frac{H_{p,vis}(\omega)}{1 + j\omega \cdot H_c(\omega)}. \quad (8.11)$$

The denominator, $1/(1 + j\omega \cdot H_c(\omega))$, which is the change in the human operator model transfer function due to velocity feedback, turns out to be a first-order high pass filter when the double integrator dynamics $H_c(\omega) = K/(j\omega)^2$ is substituted. The high pass filter characteristics cause a decrease in modulus and an increase in phase in the low frequency range. This corresponds with the changes in the subject's control behavior in the target following task when peripheral visual cues and/or motion cues were presented to the subject, Sect. 7.4.2. Based on the above considerations, the transfer functions of the descriptive model (Fig. 8.6), with peripheral visual- or vestibular feedback in the target following task can be derived. For peripheral-visual feedback the descriptive model in the case of the target following task is described by:

$$H_{CP_{roll}}(\omega) = \frac{[K_{C,att} \cdot H_{C,att}(\omega) + K_{C,rate} \cdot H_{C,rate}(\omega) \cdot j\omega]}{[1 + K_{P,rate} H_{P,rate}(\omega) \cdot j\omega \cdot H_c(\omega)]} \cdot K_I e^{-j\omega\tau_I}, \quad (8.12)$$

and for vestibular feedback by:

$$H_{CM_{roll}}(\omega) = \frac{[K_{C,att} \cdot H_{C,att}(\omega) + K_{C,rate} \cdot H_{C,rate}(\omega) \cdot j\omega]}{[1 + K_{SCC} \cdot H_{SCC}(\omega) \cdot (j\omega)^2 \cdot H_c(\omega)]} \cdot K_I e^{-j\omega\tau_I}. \quad (8.13)$$

In the transfer functions of Eqs (8.9), (8.12) and (8.13), only the gain factors have to be chosen. The time delays have been determined based on the experimental results of Chs 5 and 6. In Fig. 8.9 the bode plots of these transfer functions are presented together with the measured frequency response and the fitted simplified precision models of Ch. 7. The gains were adjusted manually and are presented in Table 21. As mentioned above, it is supposed that the information processing gain $K_I = 1$.

Considering the four display configurations used in the target following task of Ch. 7, the descriptive human operator model can be fitted to the measured describing function with two to four gains, depending on the display configuration at hand.

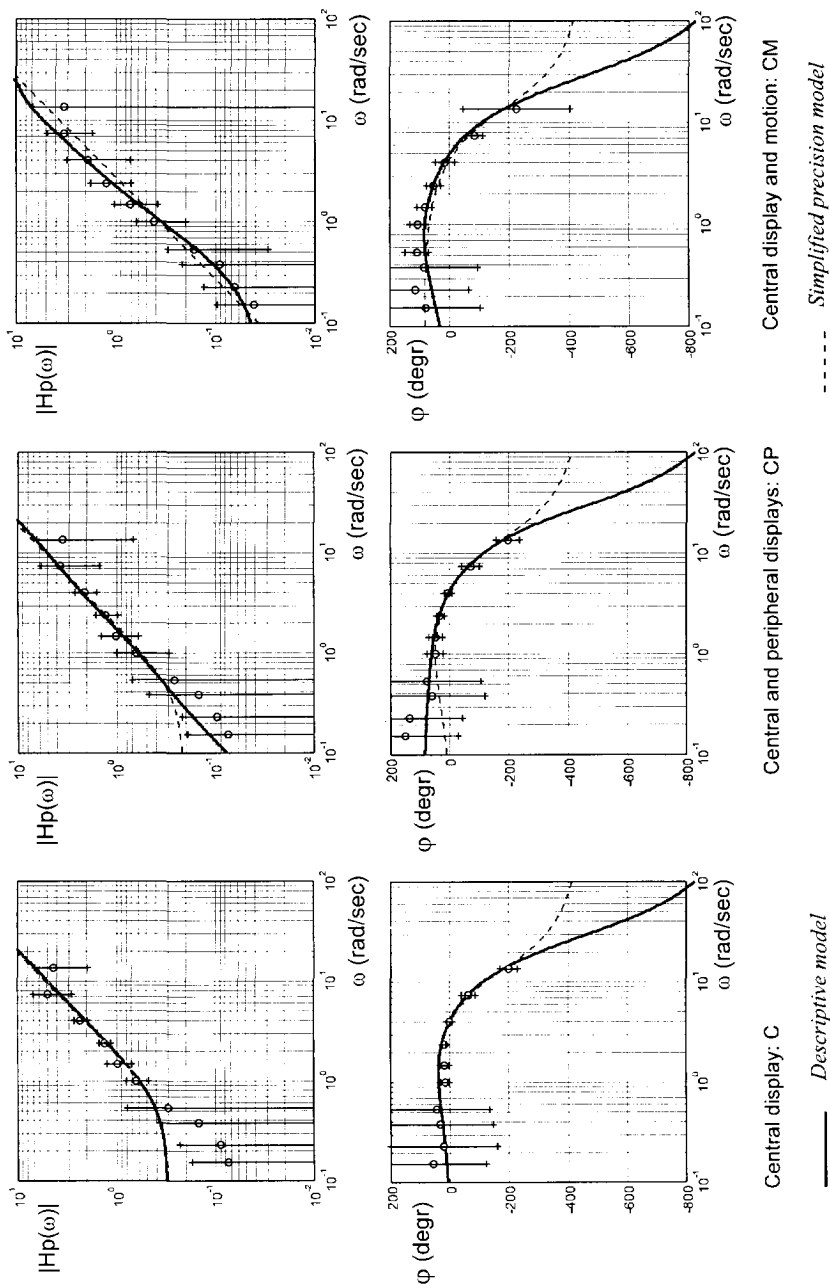


Figure 8.9 Bode plots of the descriptive model transfer function in the target following task. The simplified precision model and the frequency response of Ch. 7 are added. Display configurations C, CP, and CM.

The disturbance task

In the case of the disturbance task, all sensors are stimulated with the same stimulus $e(t) = -\varphi(t)$. Considering the block diagram of the descriptive model in Fig. 8.10, the transfer function of the model can be derived for the display configurations, as used in Ch. 7. Here the same display configurations as for the target following task will be evaluated, the central display, C, central and peripheral displays, CP, and central display and motion, CM.

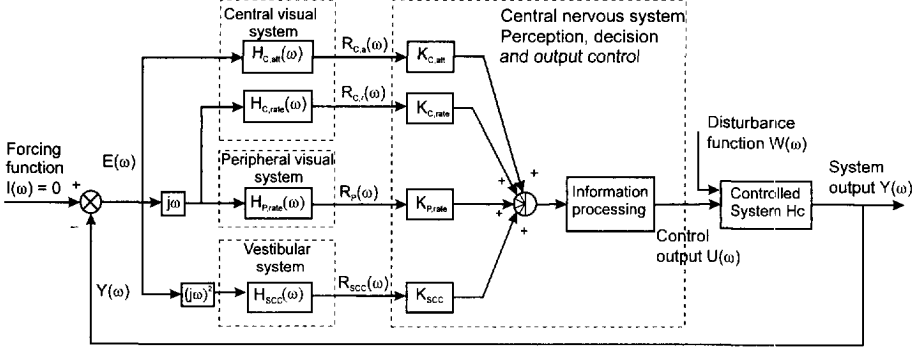


Figure 8.10 The descriptive model in the disturbance task.

The model transfer functions for these display configurations are for the central display:

$$H_{C_{Dist}}(\omega) = [K_{C,att} \cdot H_{C,att}(\omega) + K_{C,rate} \cdot H_{C,rate}(\omega) \cdot j\omega] \cdot K_I \cdot e^{-j\omega\tau_I}; \quad (8.14)$$

for the central and peripheral displays:

$$H_{CP_{Dist}}(\omega) = \frac{[K_{C,att} \cdot H_{C,att}(\omega) + K_{C,rate} \cdot H_{C,rate}(\omega) \cdot j\omega + K_{P,rate} \cdot H_{P,rate}(\omega) \cdot j\omega] \cdot K_I \cdot e^{-j\omega\tau_I}}{K_{P,rate} \cdot H_{P,rate}(\omega) \cdot j\omega}; \quad (8.15)$$

and for the central display and motion:

$$H_{CM_{Dist}}(\omega) = \frac{[K_{C,att} \cdot H_{C,att}(\omega) + K_{C,rate} \cdot H_{C,rate}(\omega) \cdot j\omega + K_{SCC} \cdot H_{SCC}(\omega) \cdot (j\omega)^2] \cdot K_I \cdot e^{-j\omega\tau_I}}{K_{SCC} \cdot H_{SCC}(\omega) \cdot (j\omega)^2}. \quad (8.16)$$

The model transfer function $H_{C_{Dist}}(\omega)$, Eq. (8.14), is equal to the transfer function $H_{C_{Full}}(\omega)$ for the target following task, Eq. (8.9). The gains and the information processing time delay, however, are different, Table 22. In Fig. 8.11 the bode plot of the transfer function is presented.

To adjust the transfer function $H_{C_{Dist}}(\omega)$ of the model to the measured frequency response in the disturbance task, the information processing time delay has to be chosen at 100 msec. This is half of the 200 msec for the target following task and it is in correspondence with the

Table 22. The gain factors of the descriptive model configured for the disturbance task for three display configurations, Central display, Central and Peripheral displays and Central display and Motion.

| Transfer function | $K_{C,att}$ | $K_{C,rate}$ | $K_{P,rate}$ | K_{SCC} | τ_I (s) |
|-------------------------|-------------|--------------|--------------|-----------|--------------|
| $H_{C_{Dist}}(\omega)$ | 1.28 | 0.51 | - | - | 0.1 |
| $H_{CP_{Dist}}(\omega)$ | 1.46 | 0.20 | 0.38 | - | 0.1 |
| $H_{CM_{Dist}}(\omega)$ | 2.90 | 0.25 | - | 0.97 | 0.2 |

difference in effective time delay of the simplified precision model in the target following task and the disturbance task, Sect. 7.5.

The model transfer function $H_{CP_{Dist}}(\omega)$ is extended with the contribution of the peripheral visual system according to Eq. (8.15). The information processing time delay is again 100 msec.

For the configuration with the central display and motion, the semi-circular canal dynamics are incorporated in the model transfer function, Eq. (8.16). To adjust the model to the measured describing function, the information processing time delay has to be chosen at 200 msec.

To fit the descriptive model to the measured frequency response, an information processing time delay of 100 msec has to be chosen for the display configurations C and CP instead of 200 msec. Especially for $H_{C_{Dist}}(\omega)$ this is remarkable because the display configuration and the controlled-system dynamics in the disturbance task are exactly the same as in the following task. Therefore, one would not expect a change in the information processing stage. The difference between both tasks is the point in the control loop where the forcing function signal is inserted, see Figs 8.6 and 8.10. This results in an increase in the modulus of the subject's frequency response at low frequencies and a decrease in the information processing time delay in the descriptive model fitted to the measured describing functions.

The question here arises: What causes the difference in the information processing time delay between the disturbance- and the target following task? In Sect. 7.2.2 the transfer functions, relating the error signal with the forcing function, $H_{e,i}(\omega)$ for the target following task, Eq. (7.1), and $H_{\varphi,w}(\omega)$ for the disturbance task, Eq. (7.2), are presented. In Sect. 7.4 it was shown that the addition of cockpit motion to the display configuration improves the tracking performance both in the target following task as well as in the disturbance task. In the target following task the subject is able to increase the phase margin, which suppresses the amplification of $H_{e,i}(\omega)$ around the crossover frequency. In the disturbance task the subject increases his gain, which results in a smaller modulus of $H_{\varphi,w}(\omega)$ for $\omega < \omega_c$. Using the transfer functions relating the error signals with the forcing functions, the contribution of the forcing function to the error signal, roll attitude φ or roll attitude error e_φ , and the first derivatives, roll rate $\dot{\varphi}$ or error rate \dot{e}_φ , as a function of the input frequency, can be derived. In this calculation the contribution of the operator remnant to the error signal is ignored. The results are presented in Fig. 8.12.

There is a clear difference in error and error rate magnitude resulting from the addition of motion for both the disturbance task and the target following task. However, in the case of the disturbance task the error magnitudes are much more decreased. This corresponds with the strong decrease in tracking error standard deviation in the disturbance task due to the addition

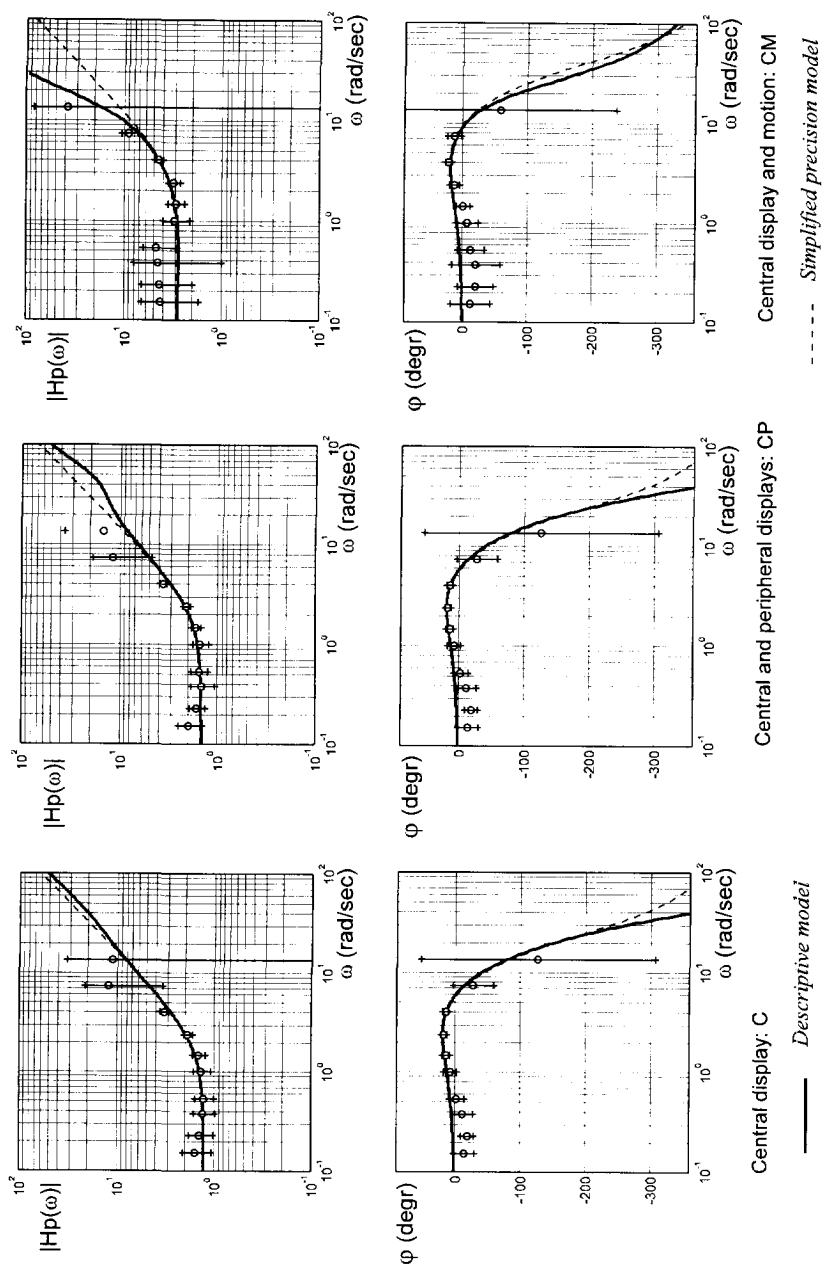


Figure 8.11 Bode plots of the descriptive model transfer function in the disturbance task. The simplified precision model and the frequency response of Ch. 7 are added. Display configurations C, CP, and CM.

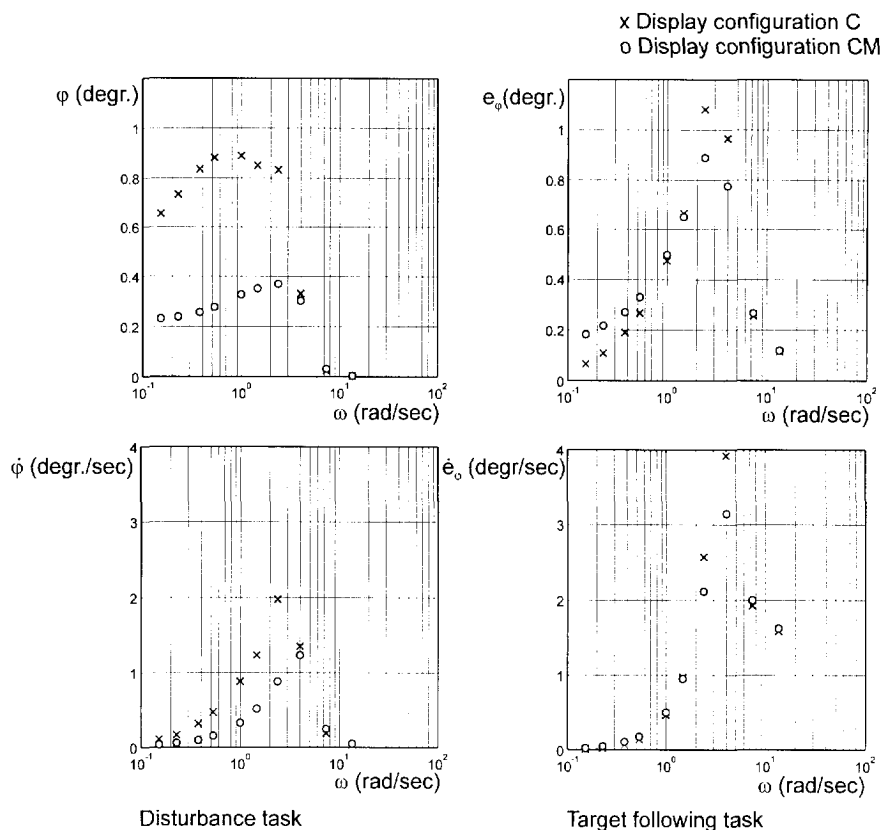


Fig. 8.12 Calculated amplitude of the tracking error and error rate at the forcing function input frequencies for the disturbance and target following task for the display configurations C and CM.

of motion, Fig. 7.4. As shown in Sect. 7.6, an increase in the information processing time delay, and consequently in the effective time delay, leads to a further increase in the tracking error. Therefore, the differences between the disturbance task and the target following task are the most likely cause for the changes in information processing time delay between the disturbance task and the target following task.

8.4 Discussion and conclusions

In this thesis, the influence of the perceived aircraft motion on a pilot's tracking behavior in aircraft control has been investigated. The study is based on a number of well-known and accepted considerations documented in the literature and on the results of a series of stimulus-response and tracking experiments described in this thesis. In this section, a short review of

the preceding chapters will be given, the results will be discussed and the conclusions will be drawn.

In Ch. 2, a review of the literature most pertinent to the influence of motion feedback on tracking performance and control behavior showed that there is a distinct improvement of tracking performance due to the addition of motion feedback. In addition, it can be seen that there is a difference between the influence of motion feedback on the changes in control behavior in the target following task and the disturbance task. The question arose as to how the feedback of the aircraft motions by the peripheral visual system and the vestibular system influenced a pilot's perception and control behavior.

In Ch. 3, it was shown that for the task conditions under investigation, the information processing by the pilot can be described by a single channel information processor with a multi-sensor input. The characteristics of the components of the information processing channel can be investigated by using stimulus response experiments based on the Additive Factors Paradigm proposed by Sternberg (1969). The sensors considered in the motion perception process were the central and peripheral visual system and the vestibular system. The dynamic characteristics of these sensors were reviewed in Ch.4.

In Ch.5, two experiments, investigating the speed and accuracy of aircraft roll attitude and roll rate perception with the central and peripheral visual system, were described. The results showed that roll attitude perception is more accurate and faster than roll rate perception. Roll rate perception with the peripheral visual system was faster than with the central visual system. The results for rate perception corresponded with the model discussed in Ch. 4. In addition, it was shown that the perception of angular rate by the central visual system and the peripheral visual system have to be considered as different processes. Hence, the central visual system and the peripheral visual system have to be considered as angular rate sensors with different characteristics.

In Ch. 6, three experiments, investigating the speed and accuracy of the perception of the final magnitude of a dynamic movement, a second-order step response, with three sensors, the central visual system, the peripheral visual system, and the vestibular system, were described. Each of these three sensors was applied in single form and in combination. The results corresponded quite well with the simulations generated with the models for the visual and the vestibular system. The results showed the strong influence of the vestibular sensory output on the perception process. The vestibular system responded much faster to the motion stimulus than the visual system.

In Ch. 7, a roll tracking experiment was described. This experiment was performed to establish the influence of the visually and vestibularly perceived motion on a subject's tracking performance and control behavior. The controlled element had uncomplicated second-order system dynamics, a double integrator. Both the target following task and the disturbance task were incorporated in the experiment. In both tracking tasks all possible display configurations, stimulating one or more sensors, were applied. The results enhanced the findings from the literature review in Ch. 2 on the influence of motion feedback in tracking tasks. In addition, the results constitute a data base to evaluate the multi-sensor input single-channel information processor model described in Ch. 3.

In Ch. 8, the experimental results obtained in the Chs 5, 6 and 7 were evaluated by using the multi-sensor input single-channel information processor model as a descriptive model. The descriptive model parameters were primarily based on the well-known characteristics of the visual and the vestibular system, Ch.4, and supplemented with the experimental results of Chs 5 and 6. The results of the evaluation show that the descriptive model nicely matches with the frequency responses obtained in the target following tasks and the disturbance tasks. However, some aspects remain to be discussed.

The results of the experiments described in Chs 5 and 6 have one important aspect in common. The reaction time for the display configurations (CP, CM, PM and CPM) with more than one sensor is in between the reaction times for the display configurations (C, P and M) with one sensor. This means that for the combined display configurations, the two or three stimulated sensors each contribute to the perception process. The same holds for the results of the tracking experiment in Ch. 7. In Sect. 7.6 it was shown that the subject's frequency response in the disturbance task for a combined display configuration equals the weighted sum of the frequency responses for the display configurations with the individual sensors. As shown in Fig. 7.14, the vestibular motion feedback has the highest weight at the higher frequencies, whereas the visual perceived roll attitude error has the highest weight at the lower frequencies.

As became clear in Ch. 6 and Sect. 8.2, the vestibular sensory output and, to a lesser extent, the peripheral visual sensory output, leads the central visual system sensory output. Due to dynamic characteristics of the peripheral visual system and vestibular system, motion is perceived faster. In the case of the target following task, the feedback of the controlled-system output rate changes a subject's dynamic behavior roughly by a high pass filter, Eq. (8.11). The characteristics of this filter depend on the sensor dynamics, the peripheral visual- or vestibular system, involved in the motion feedback, Eqs (8.12) and (8.13). With the change in dynamic control behavior the subject obtains better tracking performance at a slightly lower crossover frequency and a larger phase margin.

For the disturbance task peripheral visual and/or vestibular motion feedback means that the subject's total time delay decreases and the phase angle of the subject's frequency response increases (more positive or less negative). This is formulated by the descriptive model, Eqs (8.14), (8.15), and (8.16). Consequently, the subject increases his gain and crossover frequency at an approximately equal phase margin. The higher bandwidth of the subject's control improves the tracking performance in the disturbance task.

The evaluation of the experimental results, using the descriptive model in the previous section, shows good results. This implies that the results obtained from the stimulus response experiments of Chs 5 and 6 can readily be applied in describing closed-loop control. In the case of the target following task, the descriptive model could be easily adjusted to the frequency response by choosing the gain factors for the stimulated sensors. This means that the assumption that the human operator may be considered as a single channel information processor with multiple sensor input was not rejected. For the disturbance task the model can be adjusted to the measured frequency responses. However, for the display configurations with central and peripheral displays, the information processing time delay, τ_i , had to be decreased from 0.2 to 0.1 second. This corresponds with the difference in the time delay of the fitted Simplified Precision Model, Tables 19 and 20, for the central display configuration between the target following task and the disturbance task. In Sect. 7.6 it was shown that the human operator has to decrease his total time delay in the disturbance task to obtain a reasonable tracking performance. The only way for the human operator to obtain a smaller time delay is to decrease the information time delay. The cost for this smaller time delay is a faster processing of less information, according to the Hick-Heyman law, Sect. 3.2. This means that the processed information may be less accurate.

The results of the present study contribute to an improved understanding of a pilot's motion perception and its influence on a pilot's control behavior. The experimental results turn out to be directly applicable to the proposed descriptive model. The multi-sensor single-channel information processor model was easily fitted to the measured frequency response in the target following tasks and the disturbance tasks. As already mentioned in the introduction to this thesis, an important field of application of the obtained understanding is vehicle

simulation in general and flight simulation in particular. As is stated in the introduction, the characteristic differences between real and simulated flight are a delay of the presented motion cues and a mismatch between the visual cues and the motion cues.

These characteristic differences between real and simulated flight determine the changes in perceived aircraft motions in flight simulation. The proposed descriptive model provides the opportunity to study the effects of the above mentioned differences due to the simulation process, on pilot's motion perception and control behavior. For each individual sensor the effect of the simulation process on pilot's control behavior and performance can be studied. Inversely, the descriptive model can be used to optimize the "washout filters" which transform the aircraft motions to simulator motions. However, in that case, some optimization criterion has to be formulated. The optimum in flight simulation is reached if there is no difference in a pilot's perceived motion between real and simulated flight. Whether that optimum can be reached is questionable and depends on three subjects.

The first subject is related to the above-mentioned characteristics of flight simulation. The simulation time delays mentioned above have to be decreased. The further development of digital computers and computer graphics will provide the opportunity to increase the computing rate and to decrease the delays due to the flight simulation program and the CGI displays.

The second subject implies an improvement of the simulation of the motion cues by proper control of the simulator motion system. The traditional 'washout filters' are optimized by minimizing the differences between the pilot's vestibular output during real and simulated flight. The present descriptive model provides the tool to optimize the control of the motion system, given the visual-vestibular contribution to the pilot's motion perception process. In the optimization of the motion system control laws, both the remaining time delays and the visual-vestibular interaction have to be taken into account. The optimization should minimize the differences between the pilot's motion perception and control behavior during simulated flight and actual flight. It is extremely important to prevent mismatches between the visual and vestibular sensory output noticed by the human operator.

The third subject concerns the match between the physical limitations of the motion system and the simulated flight envelope. It is, for instance, impossible that aerobatic maneuvers, spins or spiral dives can be realistically simulated with a flight simulator equipped with a standard six-degree-of-freedom motion system. The physical and dynamic characteristics of the motion system have to match the required motion platform excursions to obtain the correct motion perception and control behavior by the pilot. The descriptive model can be used as a tool to determine the motion system specifications for a certain simulation task.

Conclusions

- The results of the present study contribute to an improved understanding of a pilot's motion perception and its influence on a pilot's tracking behavior. Based on the experimental results and the multi-sensor single-channel information processor, a descriptive pilot model could be proposed which is capable of explaining pilot's control behavior for control tasks with different display configurations.
- The application of the results lies primarily in the field of flight simulation. The descriptive model has the capacity to evaluate the influence of the simulation time delays and washout filters on pilot's control behavior. Inversely, the descriptive model can be used to optimize the motion system control algorithms or washout filters and to specify the motion system capabilities.

9. REFERENCES

- Ball, K., and R. Sekuler (1980). Models of stimulus uncertainty in motion perception. *Psychological Review*, Vol 87, pp 435-469.
- Berg, A.V.van den, and W.A. van de Grind (1989). Reaction times to motion onset and motion detection thresholds reflect the properties of bilocal motion detectors. *Vision Research*, Vol. 29, N0. 9, pp 1261-1266.
- Bergeron, H.P. (1980). The effects of motion cues on compensatory tracking tasks. AIAA Visual and Motion Simulation Technology Conference, Cape Canaveral, Florida, March 18-18, 1980. AIAA Paper No. 70-352.
- Donders, F.C. (1868). Over de snelheid van psychische processen. Onderzoekingen gedaan in het Physiologisch Laboratorium der Utrechtsche Hoogeschool, 1868-1869, Tweede reeks, II, 92 - 120. 'On the speed of mental processes' Translation by W.G. Koster, *Acta Psychologica*, 30, Attention and Performance II, 412-431.
- Egmond, A.A.J. van, J.J. Groen, and L.B.W. Jongkees (1949). The mechanics of the semicircular canals. *Journal of Physiology*, Vol. 110, pp. 1-17.
- Fernandez, C., and J.M. Goldberg. (1976). Physiology of peripheral neurons innervating otolith organs of the squirrel monkey. I Response to static tilts and to long-duration centrifugal force. *Journal of Neurophysiology*, Vol.39, no. 5.
- Fernandez, C., and J.M. Goldberg. (1976). Physiology of peripheral neurons innervating otolith organs of the squirrel monkey. II Directional selectivity and force-response relations. *Journal of Neurophysiology*, Vol.39, no. 5.
- Fernandez, C., and J.M. Goldberg. (1976). Physiology of peripheral neurons innervating otolith organs of the squirrel monkey. III Response dynamics. *Journal of Neurophysiology*, Vol.39, no. 5.
- Fernandez, C., and J.M. Goldberg (1971). Physiology of peripheral neurons innervating semicircular canals of the squirrel monkey: II Response to sinusoidal stimulation and dynamics of peripheral vestibular system. *Journal of Neurophysiology*, Vol. XXXIV, no. 4.
- Fitts, P.M.(1954). The information capacity of the human motor system in controlling the amplitude of movement. *Journal of Experimental Psychology*, Vol. 42, 381-391.
- Goldberg, J.M., and C. Fernandez (1971). Physiology of peripheral neurons innervating semicircular canals of the squirrel monkey: I Resting discharge and response to constant angular accelerations. *Journal of Neurophysiology*, Vol. XXXIV, no. 4.

- Gopher, D., and E. Donchin, (1986). Worload - An Examination of the Concept. In: K.R. Boff, L. Kaufman, and J.P. Thomas (Eds.) *Handbook of Perception and Human Performance*. John Wiley and Sons, N.Y. 1986.
- Grind, W.A. van de, J.J. Koenderink, and A.J. van Doorn, (1986). The Distribution of Human Detector Properties in the Monocular Visual Field. *Vision Research*, Vol. 26, No. 5, 797-810.
- Grind, W.A. van de (1988). The possible structure and role of neuronal smart mechanisms in Vision. *Cognitive Systems*, 2-2, June 1988, 163-180.
- Hardy, M. (1934). Observations on the innervation of the macula sacculi in Man. *Anatomical Record*, 59, 403-478.
- Harter, M.R., and C.J. Aine (1984). Brain Mechanisms of Visual Selective Attention. In: R. Parasuraman and D.R. Davies. *Varieties of Attention*. Academic Press, Inc. New York.
- Hays, W.H. (1963). *Statistics for Psychologists*. Holt, Rinehart and Winston, New York.
- Heyman, R. (1953). Stimulus information as a determinant of reaction time. *Journal of Experimental Psychology*, Vol. 45, 188-196.
- Hick, W.E. (1952). On the rate of gain of information. *Quarterly Journal of Experimental Psychology*, Vol. 4, 11-26.
- Hollander, J.G. den, and M. Baarspul. (1977). Measurement of motion quality of a moving base flight simulator. Delft University of Technology, Faculty of Aerospace Engineering. Memorandum M-264.
- Hosman, R.J.A.W., and J.C. van der Vaart, 1978. Vestibular models and thresholds of motion perception. Results of tests in a flight simulator. Delft University of Technology, Department of Aerospace Engineering, Report LR-265, 1978.
- Hosman, R.J.A.W., J.C. van der Vaart, and G.A.J. van de Moesdijk, 1979. Optimisation and evaluation of linear motion filters. *Proceedings of the Fifteenth Annual Conference on Manual Control*, AFFDL-TR-79-3134.
- Hosman, R. J.A.W., and J.C. van der Vaart (1980). Thresholds of motion perception and parameters of vestibular models obtained from tests in a motion simulator. Effects of vestibular and visual motion perception on task performance. Delft University of Technology, Department of Aerospace Engineering, Memorandum M-372, 1980.
- Hosman, R.J.A.W., and J.C. van der Vaart (1981a). Effects of vestibular and visual motion perception on task performance. *Acta Psychologica*, 48 (1981) 271-287.
- Hosman, R.J.A.W., and J.C. van der Vaart (1981b). Effects of visual and vestibular motion perception on control task performance. *First European Annual Conference on Human Decision Making and Manual Control*. Delft University of Technology.
- Hosman, R.J.A.W., and J.C. van der Vaart (1982). Accuracy of visually perceived roll angle and roll rate using an artificial horizon and peripheral displays. *Proceedings of the Second European Annual Conference on Human Decision Making and Manual Control*, Forschungsinstitut für Anthropechnik, Bonn, June 2-4, 1982.
- Hosman, R.J.A.W. and J.C. van der Vaart (1988). Active and passive side stick controllers: Tracking task performance and pilot control behavior. *Proceedings of the AGARD Conference on "The Man-Machine Interface in Tactical Aircraft Design and Combat Automation*. AGARD Conference Proceedings No. 425.

- Howard, I.P. (1982). Human visual orientation. John Wiley and Sons, New York.
- Howard, I.P. (1986). The vestibular system. In: Handbook of Perception and Human Performance, Volume I. K.R. Boff, L. Kaufman and J.P. Thomas Eds. John Wiley and Sons, New York.
- Huang, J., and L.R. Young (1981). Sensation of Rotation About a Vertical Axis with a Fixed Visual Field in Different Illuminations and in the Dark. *Experimental Brain Research*, 41, 172-183, 1981.
- Hubel, D.H. (1988). Eye, Brain and Vision. Scientific American Library. W.H. Freeman and Company, New York.
- Junker, A.M., and W.H. Levison (1977). Use of the optimal control model in the design of motion cue experiments. *Proceedings of the Thirteenth Annual Conference on Manual Control*, MIT, Cambridge, Mass. June 15-17, 1977.
- Junker, A.M., and C.R. Replogle (1975). Motion effects on the human operator in a roll axis tracking task. *Aviation, Space and Environmental Medicine*, 46: 819-822.
- Junker, A.M., and D. Price (1976). Comparison between a peripheral display and motion information on human tracking about the roll axis. *Conference Proceedings of the AIAA Vision and Motion Simulation Conference*.
- Kirk, R.E. (1968). *Experimental Design: Procedures for the Behaviour Sciences*. Brooks/Cole Publishing Company. Belmont, California.
- Kleinman, D. L, S. Baron, and W.H. Levison (1971a). A Control Theoretic Approach to Manned-Vehicle System Analysis. *IEEE Transactions on Automatic Control*, Vol.AC-16, No.6, 1971.
- Kleinman, D, L., and S. Baron (1971b). *Manned Vehicle Analysis by Means of Modern Control Theory*. NASA CR-1753.
- Kok, J.J., and H.G. Stassen (1980). Human Operator Control of Slowly Responding Systems: Supervisory Control. *Journal of Cybernetics and Information Science*. Special Issue on Man-Machine Systems. American Society for Cybernetics, Vol. 3, Number 1-4, 1980.
- Kok, J.J. and R.A. van Wijk (1978). Evaluation of models describing human operator control of slowly responding complex systems. Delft University of Technology, Delft University Press.
- H.H. Kornhuber (Ed.) (1971). *Handbook of Sensory Physiology*, Vol. VI, Vestibular System, Part I: Basic Mechanisms. Springer Verlag, Berlin.
- Kwakernaak, H., and R. Sivan, (1972). *Linear Optimal Control Systems*. Wiley-Interscience, New York, 1972.
- Levison, W.H. (1976). Use of motion cues in steady state tracking. *Conference Proceedings of the Twelfth Annual Conference on Manual Control*, NASA TM-X73, 1976.
- Levison, W.H. (1978). A model for the pilot's use of roll axis motion cues in steady-state tracking tasks. Bolt Beranek and Newman Inc. Report No. 3808, Cambridge, Ma.
- Levison, W.H., and A.M.Junker (1977). A model for pilot's use of motion cues in roll-axis tracking tasks. Bolt Beranek and Newman Inc. Report No. 3528, Cambridge, Ma.

Levison, W.H., and A.M. Junker (1978). A model for the Pilot's Use of Motion Cues in Steady-State Roll-Axis Tracking Tasks. AIAA Flight Simulation Technology Conference. Arlington, Texas

Levison, W.H., and G.L. Zacharias (1978). Motion Cue Models for Pilot Vehicle Analysis. AMRL-TR-78-2, Wright Patterson AFB, OHIO.

Levison, W.H., and G.L. Zacharias (1980). An Optimal-Control Model for the Joint Use of Visual and Motion Cues in Continuous Tracking Tasks: Theory and Experiments. Journal of Cybernetics and Information Science, Special Issue on Man-Machine Systems. Vol. 3, Number 1-4, 1980.

Magdaleno, R.E., and D.T. McRuer (1971). Experimental Validation and Analytical Elaboration for Models of the Pilot's Neuromuscular Subsystem in Tracking Tasks. NASA CR-1757.

Malcolm, R., and G. Melvill Jones (1970). A Quantitative Study of Vestibular Adaptation in Humans. Acta Otolaryngologica, Vol. 70, 126-153, 1970.

McRuer, D.T., D. Graham, E.S. Krendel, and W. Reisener (1965). Human Pilot Dynamics in Compensatory Systems. Theory, Models, and Experiments with Controlled Element and Forcing Function Variations. AFFDL-TR-65-15, Wright Patterson AFB, OHIO.

McRuer, D.T., and H.R. Jex (1967). A Review of Quasi-Linear Pilot Models. IEEE Transactions on Human Factors in Electronics. Vol. HFE-8, no 3, September 1967.

McRuer, D.T. and E.S. Krendel (1974). Mathematical Models of Human Pilot Behavior. AGARDograph No. 188.

Meiry, J.L., (1965). The vestibular system and human dynamic space orientation. Massachusetts Institute of Technology, Man-Vehicle Lab. Rept. T65-1, Sc.D. Thesis./ NASA CR-628, 1966.

Miller, G.A. (1956). The magical number seven, plus or minus two. Psychological Review, 63, 87-97.

Mooij, H.A. (1972). Airborne equipment used during in-flight measurement of human pilot describing functions. National Aerospace Laboratory, NLR. Amsterdam, Memorandum VS-72-001.

Moriarty, T.E., A.M. Junker, and D.R. Price (1976). Roll axis tracking improvement resulting from Peripheral vision motion cues. Conference Proceedings of the Twelfth Annual Conference on Manual Control, NASA TM-X73, 170.

Neil, T.P. and R.E. Smith (1970). An In-Flight Investigation to Develop Control System Design Criteria for Fighter Airplanes. Wright Patterson AFB, OHIO, AFFDL-TR-70-74, 1970.

Newell, F.D. (1968). Human Transfer Characteristics in Flight and Ground Simulation for the tracking Task. Wright Patterson AFB, Ohio, AFFDL-TR-67-30.

Newell, F.D. (1969). In-Flight and Ground Simulation of Pilot Transfer Characteristics in Compensatory Roll Tracking tasks. Proceedings of the Third Annual NASA-University Conference on Manual Control. Univ. of Southern California, Los Angeles. NASA SP-144, 1969.

Newell, F.D., and H.J. Smith (1969). Human Transfer Characteristics in Flight and Ground Simulation for a Roll Tracking task. NASA TN-D-5007, 1969.

Paasen, M.M. van (1995). A Model of the Arm's Neuromuscular System for Manual Control. Preprints of the 6th IFAC/IFIP/IFORS/IEA Symposium on Analyses, Design and Evaluation of Man-Machine Systems. Massachusetts Institute of Technology, Cambridge, Ma, June 27-29, 1995.

Paasen, M.M. van (1994). Biophysics in Aircraft Control - A Model of the Neuromuscular system of the Pilot's Arm. PhD thesis. Delft University of Technology, Faculty of Aerospace Engineering.

Peters, R.A. (1969). Dynamics of the vestibular system and their relation to motion perception, spatial disorientation and illusions. NASA Contractory Report, CR-1309.

Repperger, D.W., and A.M. Junker (1977). Using Model Order Tests to Determine Sensory Inputs in a Motion Study. Proceedings of the Thirteenth Annual Conference on Manual Control, MIT, Cambridge, Ma. June 15-17, 1977.

Ringland, R.F., and R.L. Stapleford (1972). Motion Cue Effects on Pilot Tracking. Seventh Annual Conference on Manual Control. NASA SP-281.

Rolfe, J.M., and K.J. Staples (1986). Flight Simulation. Cambridge University Press. Cambridge, U.K.

Seckel, E., I.A.M. Hall, D.T. McRuer, and D.H. Weir (1958). Human Pilot Dynamic Response in Flight and Simulator. Wright Patterson AFB, Ohio. WADC Technical Report 57-520.

Shannon, C., and W. Weaver, (1949). The mathematical theory of communication. Urbana, Ill. University of Illinois Press, 1949.

Shirley, R.S., and L.R. Young (1968). Motion cues in Man-Vehicle control. Effects of roll-motion on human operator's behavior in compensatory systems with disturbance inputs. IEEE Transactions on Man-Machine Systems, Vol MMS9, No. 4.

Sperling, G. A. (1963). Model for Visual Memory Tasks. Human Factors. Febr. 1963.

Stapleford, R.L., R.A. Peters, and F.R. Alex, (1969). Experiments and a model for pilot dynamics with visual and motion inputs. NASA CR-1325.

Steinhausen, W. (1931). Über den Nachweis der Bewegung der Cupula in der intakten Bogengangsampulle des Labyrinthes bei der natürlichen rotatorischen und kalorischen Reizung. Pflügers Arch. Ges. Physiol., 228, 322-328.

Sternberg, S. (1969). The Discovery of Processing Stages: Extension of Donders' Method. Acta Psychologica, 30, Attention and Performance II, 276-315.

Tynan, P.D., and R. Sekuler (1982). Motion processing in peripheral vision: Reaction time and perceived velocity. Vision Research, Vol. 22, pp. 61-68.

Tomaske, W. (1982). Driving simulation including kinesthetic information. Proceedings of the Second European Conference on Human Decision Making and Manual Control, Bonn, 1982.

Vaart, J.C. van der, and R.J.A.W. Hosman (1987). Compensatory tracking in disturbance tasks and target following tasks. The influence of cockpit motion on performance and control behavior. Delft University of Technology, Faculty of Aerospace Engineering, Report LR-511, November 1987.

Vaart, J.C. van der (1992). Modeling of perception and action in compensatory manual control tasks. Ph.D. Thesis. Delft University of Technology. Delft University Press.

Vickers, D., and J. Packer (1982). Effects of alternating set for speed or accuracy on response time, accuracy and confidence in a unidimensional discrimination task. *Acta Psychologica* 50 , 179-197.

Welford, A.T.(1952). The 'psychological refractory periode' and the timing of highspeed performance: A review and a theory. *British Journal of Psychology*, 43, 2-19.

Welford, A.T.(1967). A single channel operation in the brain. *Acta Psychologica*, Vol. 25, 5-22.

Wersäll, J and D. Bagger-Sjöbäck (1971). Morphology of the vestibular sense organs. In: H.H. Kornhuber (Ed.). *Handbook of Sensory Physiology*, Vol. VI, Vestibular System, Part I: Basic Mechanisms. Springer Verlag, Berlin.

Wertheim, A.H., W.A. Wagenaar, and H.W. Leibowitz (1981). Proceedings of the Symposium of Motion Perception, Recent Development and Applications. Veldhoven, aug.1980. *Acta Psychologica*, 1981, 48, 1-341.

Wertheim, A.H., W.A. Wagenaar, and H.W. Leibowitz (1982). *Tutorials on Motion Perception*. Plenum Press, New York.

Wickens, C.D. and J. Flach (1988). Information Processing. In: E.L. Wiener and D.C. Nagel (Eds.). *Human Factors in Aviation*. Academic Press, N.Y.

White, T. (1983). Human Supervisory Control Behavior: Verification of a Cybernetic Model. Ph.D. Thesis. Delft University of Technology, Delft, the Netherlands, Sept. 8, 1983.

Young, L.R. (1967). Some effects of motion cues on manual tracking. *Journal of Spacecraft* 4, No. 10.

Young, L.R. and J.L. Meiry (1965). Manual control of an unstable system with visual and motion cues. *IEEE International Convention Record*, Vol.13, Part 6, pp. 123-127.

Zacharias, G.L. (1977). Motion Sensation Dependence on Visual and Vestibular Cues. Ph. D. Dissertation Massachusetts Institute of Technology, Cambridge, Ma.

Zacharias, G.L. and L.R. Young (1977). Manual Control of Yaw Motion with Combined Visual and Motion Cues. Proceedings of the Thirteenth Annual Conference on Manual Control, Massachusetts Institute of Technology, Cambridge, Mass. June 15-17.

Zacharias, G.L. and L.R. Young (1981). Influence of combined visual and vestibular cues on human perception and control of horizontal rotation. *Experimental Brain Research*, 41, 149-171.

APPENDIX I, INSTRUMENTATION

In this appendix the instrumentation used to perform the experiments, as discussed in Chs 5, 6 and 7, is described. The details presented give an insight into the characteristics of the instrumentation used.

I.1 The artificial horizon

As the central display, a CRT (Textronix 604 Monitor, 10.5 x 13.2 cm) was mounted in the instrument panel in front of the subject. An artificial horizon image, Fig. I.1, was generated by the EAI 680 analog computer. The refresh rate was 250 Hz.

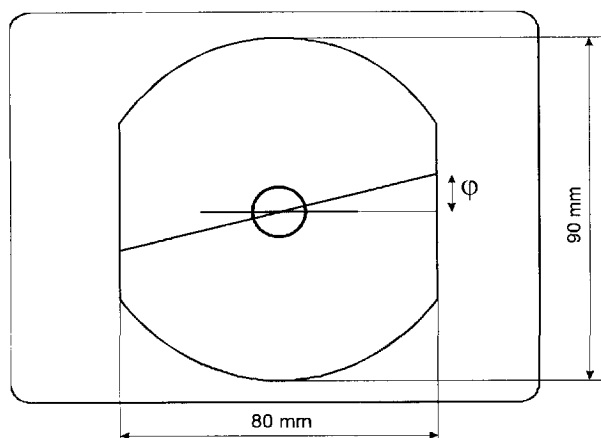


Figure I.1 The artificial horizon image on the central display

During the stimulus-response experiments of Chs 5 and 6, the duration of presentation of the stimulus, the exposition time Δt_{exp} , was controlled by the Z modulation (intensity modulation) of the CRT display. The exposition time, Δt_{exp} , was controlled by the digital computer of the EAI Pacer hybrid computer system with an accuracy of 0.001 s.

During the tracking experiments of Ch.7, the artificial horizon was used to present the roll error. The controlled system, a double integrator, was simulated by the analog computer. The forcing functions were generated by the digital computer with a sample frequency of 50 Hz.

I.2 The peripheral displays

Two black and white TV monitors, Bosch Fernseh Monitor TG1BCgA - 58 cm, were used to present the moving checkerboard patterns to the subjects in the peripheral visual field. The monitors were adjusted to the North American TV standard, an image of 525 interlaced lines with an update and refresh rate of 30 frames per second. The checkerboard pattern, Fig. I.2, consisted of 7.5×9.5 blocs of 5×5 cm and was generated by a moving pattern generator developed at the Delft University of Technology.

The roll motion of the environment was presented to the subject by opposite vertical movement of the checkerboard patterns on the monitors, placed to the left and right of the subject. The vertical velocity of the patterns was controlled by the roll rate of the stimulus in the experiments of Chs 5 and 6 and by the roll rate of the controlled system in the tracking task. To control the exposition time, Δt_{exp} , the Z-modulation of the monitors was used to switch on and of the stimulus pattern.

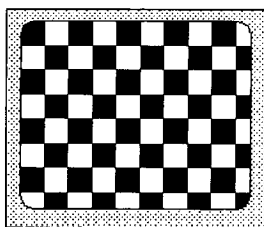


Figure I.2 . Checkerboard pattern on the TV monitor.

I.3 The motion system

The three degree of freedom motion system of the research flight simulator had three hydraulic servo actuators. These actuators, having hydrostatic bearings, produce a nearly rumble free motion of the simulator. The maximum attainable single degree of freedom performance is presented in Table I.1.

The frequency response of the motion system was determined before each of the experiments of Chs. 6 and 7. A second-order model was fitted to the frequency responses and was then used to compensate for the position control of the motion system for the dynamic characteristics. In this way, a one-to-one position control of the simulator motion system was obtained within the bandwidth of the experimental tasks. In Fig. I.3, an example of the frequency response of the motion-system roll-attitude control is presented with and without compensation. The second-order model fitted to this frequency response was approximately:

$$H_{motion}(\omega) = \frac{0.985 \cdot \omega_o^2}{(j\omega)^2 + 2\zeta\omega_o j\omega + \omega_o^2}, \quad (I.1)$$

with: $\omega_o = 25$ rad/sec
 $\zeta = 1.05$

Table I.1 Single degree of freedom performance of the three degree of freedom motion system of the flight simulator.

| | Travel | Velocity | Acceleration |
|-------|---------|----------|--|
| Heave | ± 30 cm | ± 1 m/s | + 15 m/s ² - 28 m/s ² |
| Roll | ± 16 ° | ± 73°/s | ± 1090°/s ² |
| Pitch | ± 15.5° | ± 50°/s | + 315°/s ² - 460°/s ² |

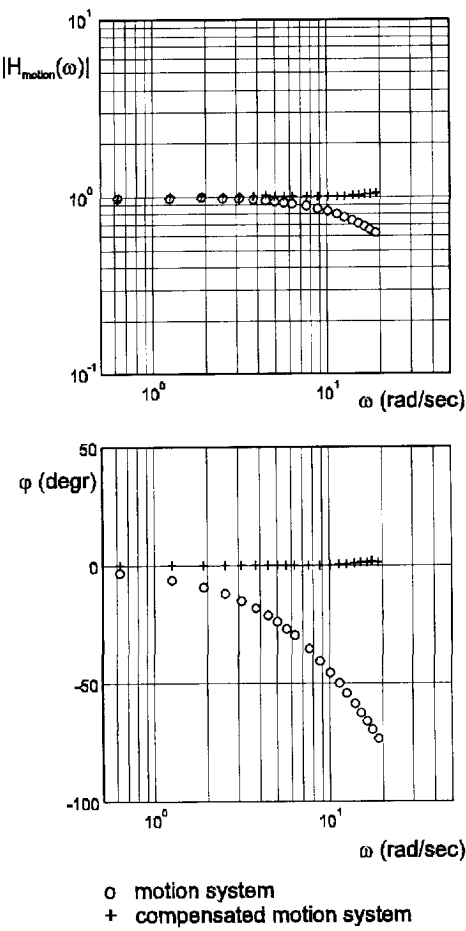


Figure I.3 The bode plot of the motion system frequency response before and after compensation.

I.4 The keyboard

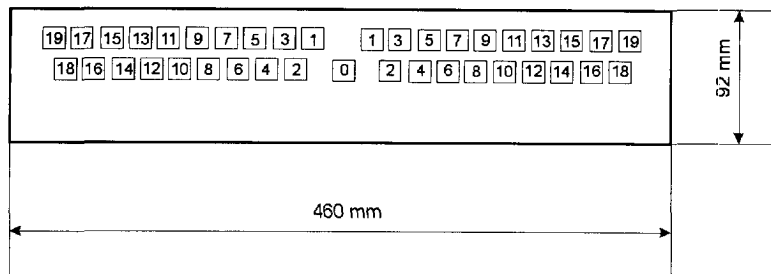


Figure I.4 The digital keyboard and its dimensions.

The digital keyboard, Fig. I.4, was developed at the Faculty of Aerospace Engineering for the present research. It has two outputs: an analog output depending on the key pressed, and a discrete impulse output at the moment any key is touched to trigger the moment of the subject's response.

I.5 The side stick

A spring centered side stick controller was used to generate the control inputs to the system. Details of the side stick are described by Mooij (1972). The distance between the point of action of the control force F_a on the stick and the roll axis is approximately 9 centimeter. The static relation between the stick force F_a and side stick displacement s_a is presented in Fig. I.5.

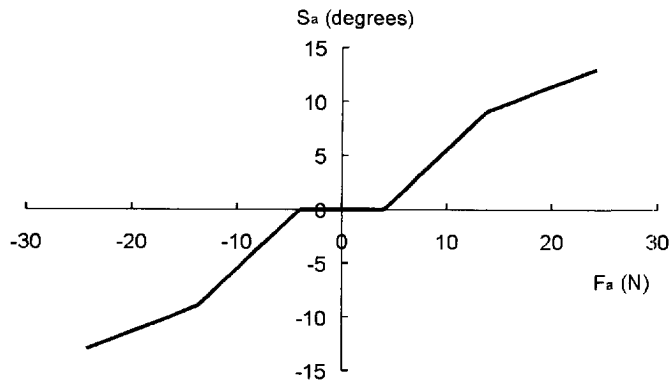


Figure I.5 Side stick displacement s_a as a function of the subject's control force F_a .

The dynamic characteristics of the side stick were determined between ± 9 degrees stick displacement. A second-order system model was fitted to the step-response from ± 9 degrees to mid the position. The characteristic parameters are: $\omega_o = 20.8$ rad/sec and $\zeta = 0.95$. The side-stick displacement was measured with a potentiometer providing the analog input to the controlled system H_c simulated in the analog computer.

I.6 The experimental set-up

The position of the subject's eye reference point, ERP, relative to the central and peripheral displays, is presented in Figs. I.6 and I.7. The set-up in the low noise room for the experiments of Ch.5, Experiment I of Ch.6, and part of the tracking experiment of Ch.7 is given in Fig. I.6. The set-up for the experiments in the flight simulator is given in Fig. I.7.

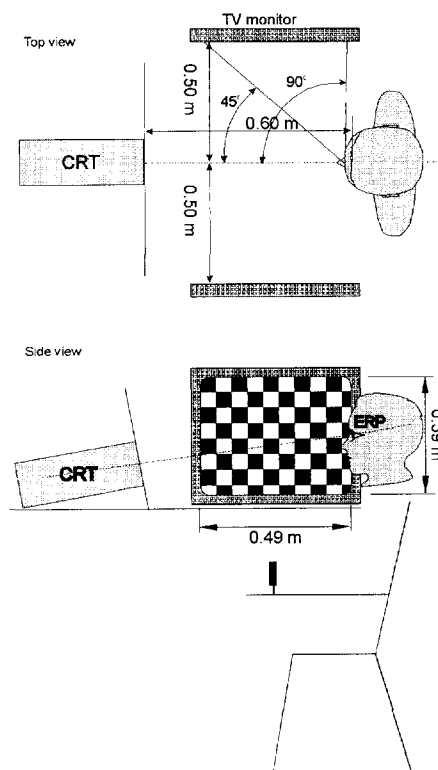


Figure I.6 The position of the subject's ERP relative to the central and peripheral displays in the low noise room.

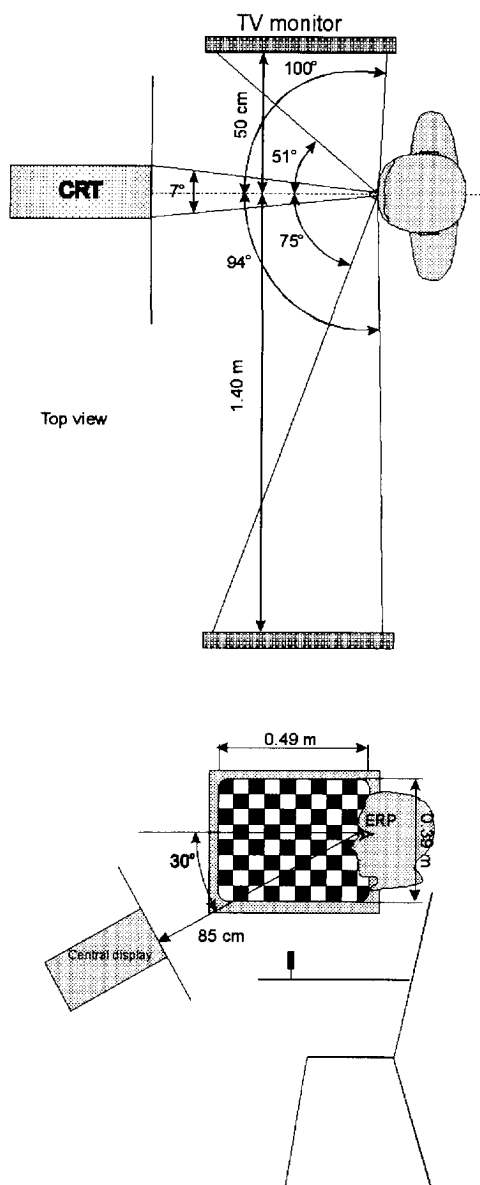


Figure I.7 The position of the subject's ERP relative to the central and peripheral displays in the flight simulator.

APPENDIX II, OVERVIEW OF EXPERIMENTAL RESULTS

II.1 Perception of roll attitude and roll rate, Chapter 5

Experiment 1, Roll attitude

Table II.1. The score S_c and the reaction time RT as function of exposure time Δt_{exp} and blanking or masking after exposure.

| Exposure time | Blanking | | Masking | |
|----------------------|----------|--------|---------|--------|
| Δt_{exp} (s) | Score | RT (s) | Score | RT (s) |
| 0.04 | 0.0384 | 0.74 | 0.148 | 0.831 |
| 0.06 | 0.0321 | 0.737 | 0.0661 | 0.756 |
| 0.08 | 0.0247 | 0.735 | 0.0351 | 0.715 |
| 0.1 | 0.028 | 0.724 | 0.0334 | 0.728 |
| RT | 0.0244 | 0.738 | | |

Experiment 2, Roll rate

Table II.2. The score S_c and the reaction time RT as function of display configuration, exposure time Δt_{exp} and blanking or masking after exposure.

Blanking

| Configuration | C | | P | | CP | |
|----------------------|--------|--------|--------|--------|--------|--------|
| Δt_{exp} (s) | Score | RT (s) | Score | RT (s) | Score | RT (s) |
| 0.1 | 0.445 | 0.836 | 0.137 | 0.818 | 0.165 | 0.799 |
| 0.15 | 0.185 | 0.831 | 0.0808 | 0.78 | 0.0894 | 0.8 |
| 0.2 | 0.123 | 0.84 | 0.0724 | 0.736 | 0.0737 | 0.789 |
| 0.3 | 0.0906 | 0.815 | 0.0714 | 0.766 | 0.066 | 0.802 |
| 0.4 | 0.0814 | 0.834 | 0.0686 | 0.763 | 0.0669 | 0.818 |
| RT | 0.077 | 0.886 | 0.0643 | 0.814 | 0.0629 | 0.817 |

Masking

| Configuration | C | | P | | CP | |
|----------------------|--------|--------|--------|--------|--------|--------|
| Δt_{exp} (s) | Score | RT (s) | Score | RT (s) | Score | RT (s) |
| 0.1 | 0.493 | 0.888 | 0.257 | 0.837 | 0.475 | 0.89 |
| 0.15 | 0.255 | 0.83 | 0.16 | 0.799 | 0.209 | 0.831 |
| 0.2 | 0.145 | 0.862 | 0.126 | 0.732 | 0.1 | 0.793 |
| 0.3 | 0.0907 | 0.817 | 0.0993 | 0.728 | 0.0742 | 0.796 |
| 0.4 | 0.0813 | 0.832 | 0.0843 | 0.714 | 0.064 | 0.792 |

II.2 Perception of cockpit motion with the visual and vestibular system, Chapter 6

Experiment I, Chapter 6.

TableII.3. The mean error standard deviation $RMS_{\Delta\phi}$, the mean reaction time RT and the variation due to subjects and replications as a function of display configuration and exposure time, Experiment I.

| Central display | | | | |
|---------------------------------|---------------------------------|---|-------------|----------------------|
| Δt_{exp} (s) | $\sigma_{\Delta\phi}$ (degr) | $\sigma(\sigma_{\Delta\phi})$ (degr) | RT (s) | σ_{RT} (s) |
| 0.2 | 2.167 | 0.371 | 0.916 | 0.090 |
| 0.3 | 1.569 | 0.240 | 0.928 | 0.087 |
| 0.4 | 1.371 | 0.145 | 0.943 | 0.073 |
| 0.6 | 1.308 | 0.178 | 0.994 | 0.113 |
| 0.8 | 1.245 | 0.184 | 1.015 | 0.094 |
| Peripheral displays | | | | |
| Δt_{exp} (s) | $\sigma_{\Delta\phi}$ (degr) | $\sigma(\sigma_{\Delta\phi})$ (degr) | RT (s) | σ_{RT} (s) |
| 0.2 | 2.298 | 0.147 | 0.949 | 0.124 |
| 0.3 | 1.711 | 0.168 | 0.931 | 0.082 |
| 0.4 | 1.476 | 0.150 | 0.945 | 0.089 |
| 0.6 | 1.425 | 0.214 | 0.937 | 0.056 |
| 0.8 | 1.308 | 0.126 | 0.952 | 0.065 |
| Central and peripheral displays | | | | |
| Δt_{exp} (s) | $\sigma_{\Delta\phi}$ (degr) | $\sigma(\sigma_{\Delta\phi})$ (degr) | RT (s) | σ_{RT} (s) |
| 0.2 | 2.035 | 0.242 | 0.903 | 0.094 |
| 0.3 | 1.411 | 0.177 | 0.909 | 0.069 |
| 0.4 | 1.258 | 0.147 | 0.942 | 0.070 |
| 0.6 | 1.209 | 0.194 | 0.976 | 0.097 |
| 0.8 | 1.200 | 0.104 | 0.986 | 0.112 |

Experiment II, Chapter 6.

Table II.4. The mean error standard deviation $\sigma_{\Delta\phi}$, the mean reaction time RT and the variation due to subjects and replications as a function of display configuration, Experiment II.

| Display Configuration | $\sigma_{\Delta\phi}$ (degr) | $\sigma(\sigma_{\Delta\phi})$ (degr) | RT (s) | σ_{RT} (s) |
|-----------------------|---------------------------------|---|-------------|----------------------|
| C | 1.344 | 0.147 | 1.165 | 0.071 |
| P | 1.367 | 0.161 | 1.102 | 0.056 |
| CP | 1.302 | 0.185 | 1.130 | 0.052 |
| M | 1.224 | 0.119 | 0.949 | 0.053 |
| CM | 1.184 | 0.216 | 0.996 | 0.055 |
| PM | 1.204 | 0.173 | 0.912 | 0.047 |
| CPM | 1.235 | 0.110 | 0.936 | 0.056 |

Experiment III, Chapter 6.

Table II.5. The mean of error standard deviation $\sigma_{\Delta\phi}$, the mean reaction time RT and the variation as a function of display configuration and natural frequency, Experiment III.

| Display Configuration | ω_0 (rad/sec) | $\sigma_{\Delta\phi}$ (degr) | $\sigma(\sigma_{\Delta\phi})$ (degr) | RT (s) | σ_{RT} (s) |
|-----------------------|-------------------------|---------------------------------|---|-------------|----------------------|
| C | 0.65 | 1.385 | 0.093 | 2.331 | 0.098 |
| | 1 | 1.324 | 0.244 | 1.720 | 0.113 |
| | 2 | 1.203 | 0.104 | 1.116 | 0.063 |
| P | 0.65 | 1.690 | 0.156 | 1.820 | 0.165 |
| | 1 | 1.561 | 0.245 | 1.517 | 0.111 |
| | 2 | 1.041 | 0.214 | 1.040 | 0.061 |
| M | 0.65 | 1.585 | 0.169 | 1.768 | 0.183 |
| | 1 | 1.504 | 0.177 | 1.227 | 0.093 |
| | 2 | 1.006 | 0.162 | 0.853 | 0.045 |
| CM | 0.65 | 1.394 | 0.133 | 1.931 | 0.101 |
| | 1 | 1.244 | 0.136 | 1.419 | 0.149 |
| | 2 | 0.978 | 0.208 | 0.945 | 0.074 |

II.3 Results of the tracking experiment, Chapter 7

II.3.1 Performance

Target following task

Table II.6 Error signal, control signal, roll angle and roll rate.

| Configurations | C | CP | CM | CPM |
|---|-------|-------|-------|-------|
| σ_{e_ϕ} (degrees) | 2.232 | 1.628 | 1.322 | 1.255 |
| Standard deviation $\sigma(\sigma_{e_\phi})$ (degrees), | 0.220 | 0.107 | 0.089 | 0.064 |
| σ_{s_a} (degrees) | 3.476 | 2.623 | 2.266 | 2.138 |
| Standard deviation, $\sigma(\sigma_{s_a})$ (degrees) | 0.789 | 0.828 | 0.410 | 0.436 |
| σ_ϕ (degrees) | 2.966 | 2.324 | 1.697 | 1.631 |
| Standard deviation $\sigma(\sigma_\phi)$ (degrees), | 0.241 | 0.180 | 0.177 | 0.126 |
| $\sigma_{\dot{\phi}}$ (degr./s) | 5.008 | 3.498 | 2.697 | 2.317 |
| Standard deviation $\sigma(\sigma_{\dot{\phi}})$ (degr./s) | 0.755 | 0.722 | 0.538 | 0.313 |

Disturbance task

Table II.7 Error signal roll angle, roll rate and control signal.

| Configurations | C | CP | CPR | CPS | CM | CPM | P | M | PM |
|--|-------|-------|-------|-------|-------|-------|-------|-------|-------|
| σ_ϕ (degrees) | 1.943 | 1.637 | 1.854 | 1.781 | 0.778 | 0.702 | 2.668 | 0.988 | 0.998 |
| Standard deviation, $\sigma(\sigma_\phi)$ (degrees) | 0.258 | 0.135 | 0.203 | 0.144 | 0.093 | 0.083 | 0.449 | 0.180 | 0.218 |
| $\sigma_{\dot{\phi}}$ (degr./s) | 3.672 | 3.300 | 3.526 | 3.487 | 1.759 | 1.737 | 3.509 | 2.035 | 1.840 |
| Standard deviation of $\sigma(\sigma_{\dot{\phi}})$ (degr./s) | 0.338 | 0.212 | 0.313 | 0.320 | 0.210 | 0.128 | 0.604 | 0.315 | 0.307 |
| σ_{s_a} (degr./s) | 3.728 | 3.708 | 3.700 | 3.837 | 2.811 | 2.837 | 3.588 | 2.882 | 2.660 |
| Standard deviation of $\sigma(\sigma_{s_a})$ (degr./s) | 0.412 | 0.346 | 0.413 | 0.442 | 0.129 | 0.247 | 0.685 | 0.293 | 0.347 |

II.3.2 Dynamic behavior

Target following task

Table II.8 Mean subject's frequency response $H_p(\omega)$ and the uncertainties for the display configurations of the target following task

Table II.8a Central display, C

| ω (rad/s) | $ H_p $ | Phase (degrees) | $\sigma H_p $ | σ_{phase} (degrees) |
|---------------------|---------|--------------------|---------------|--------------------------------------|
| 0.153 | 0.075 | 56.21 | 0.10 | 180.00 |
| 0.230 | 0.089 | 20.23 | 0.14 | 180.00 |
| 0.383 | 0.149 | 33.42 | 0.22 | 180.00 |
| 0.537 | 0.302 | 45.17 | 0.47 | 180.00 |
| 0.997 | 0.641 | 16.43 | 0.16 | 14.04 |
| 1.457 | 0.967 | 18.01 | 0.27 | 15.39 |
| 2.378 | 1.320 | 19.56 | 0.18 | 7.84 |
| 4.065 | 2.325 | 1.60 | 0.36 | 8.75 |
| 7.440 | 4.901 | -64.28 | 2.07 | 22.95 |
| 13.576 | 4.345 | -198.10 | 2.37 | 28.62 |

Table II.8b Central and peripheral displays, CP

| ω (rad/s) | $ H_p $ | Phase (degrees) | $\sigma H_p $ | σ_{phase} (degrees) |
|---------------------|---------|--------------------|---------------|--------------------------------------|
| 0.153 | 0.074 | 149.78 | 0.120 | 180.00 |
| 0.230 | 0.096 | 136.02 | 0.121 | 180.00 |
| 0.383 | 0.148 | 60.71 | 0.317 | 180.00 |
| 0.537 | 0.262 | 75.90 | 0.433 | 180.00 |
| 0.997 | 0.640 | 48.31 | 0.346 | 28.36 |
| 1.457 | 1.017 | 47.90 | 0.418 | 22.38 |
| 2.378 | 1.287 | 31.46 | 0.320 | 13.94 |
| 4.065 | 2.111 | 5.52 | 0.515 | 13.71 |
| 7.440 | 3.672 | -71.75 | 2.169 | 30.57 |
| 13.576 | 3.518 | -197.85 | 2.846 | 38.97 |

Table II.8 Mean subject's frequency response $H_p(\omega)$ and the uncertainties for the display configurations of the target following task (continued).

Table II.8c Central display and motion, CM.

| ω (rad/s) | $ H_p $ | Phase (degrees) | $\sigma H_p $ | σ , phase (degrees) |
|---------------------|---------|--------------------|----------------|-------------------------------|
| 0.153 | 0.042 | 79.25 | 0.055 | 180.000 |
| 0.230 | 0.064 | 115.78 | 0.068 | 180.000 |
| 0.383 | 0.092 | 86.58 | 0.128 | 180.000 |
| 0.537 | 0.164 | 109.80 | 0.134 | 39.19 |
| 0.997 | 0.415 | 105.78 | 0.214 | 27.28 |
| 1.457 | 0.712 | 83.39 | 0.326 | 24.60 |
| 2.378 | 1.242 | 53.18 | 0.535 | 23.29 |
| 4.065 | 1.901 | 14.98 | 1.177 | 31.77 |
| 7.440 | 3.290 | -84.00 | 1.569 | 25.50 |
| 13.576 | 3.276 | -225.22 | 3.584 | 180.00 |

Table II.8d Central and peripheral displays and motion, CPM.

| ω (rad/s) | $ H_p $ | Phase (degrees) | $\sigma H_p $ | σ , phase (degrees) |
|---------------------|---------|--------------------|----------------|-------------------------------|
| 0.153 | 0.041 | 64.90 | 0.051 | 180.00 |
| 0.230 | 0.072 | 86.29 | 0.052 | 35.66 |
| 0.383 | 0.089 | 103.04 | 0.063 | 35.13 |
| 0.537 | 0.161 | 114.65 | 0.102 | 32.32 |
| 0.997 | 0.337 | 107.90 | 0.207 | 31.51 |
| 1.457 | 0.587 | 81.98 | 0.150 | 14.30 |
| 2.378 | 1.026 | 50.44 | 0.212 | 11.65 |
| 4.065 | 1.796 | 12.70 | 0.457 | 14.28 |
| 7.440 | 3.257 | -85.86 | 1.539 | 25.30 |
| 13.576 | 2.726 | -222.02 | 1.352 | 26.38 |

Disturbance task

Table II.9 Mean subject's frequency response $H_p(\omega)$ and the uncertainties for the display configurations of the disturbance task.

Table II.9a Central display, C

| ω (rad/s) | $ H_p $ | Phase (degrees) | $\sigma H_p $ | σ , phase (degrees) |
|---------------------|---------|--------------------|----------------|-------------------------------|
| 0.153 | 1.582 | -15.84 | 0.510 | 17.86 |
| 0.230 | 1.418 | -9.39 | 0.400 | 15.75 |
| 0.383 | 1.315 | -10.42 | 0.326 | 13.94 |
| 0.537 | 1.293 | -2.33 | 0.290 | 12.62 |
| 0.997 | 1.362 | 8.51 | 0.265 | 11.01 |
| 1.457 | 1.453 | 12.05 | 0.216 | 8.47 |
| 2.378 | 1.868 | 16.82 | 0.197 | 6.01 |
| 4.065 | 3.280 | 11.50 | 0.306 | 5.32 |
| 7.440 | 12.138 | -43.45 | 8.773 | 35.86 |
| 13.576 | 11.195 | -140.15 | 21.919 | 180.00 |

Table II.9b Central and peripheral displays, CP

| ω (rad/s) | $ H_p $ | Phase (degrees) | $\sigma H_p $ | σ , phase (degrees) |
|---------------------|---------|--------------------|----------------|-------------------------------|
| 0.153 | 1.964 | -14.28 | 0.552 | 15.69 |
| 0.230 | 1.645 | -18.97 | 0.295 | 10.17 |
| 0.383 | 1.454 | -12.16 | 0.384 | 14.79 |
| 0.537 | 1.553 | -3.02 | 0.289 | 10.55 |
| 0.997 | 1.505 | 7.06 | 0.263 | 9.92 |
| 1.457 | 1.659 | 13.69 | 0.174 | 6.00 |
| 2.378 | 2.073 | 16.76 | 0.183 | 5.04 |
| 4.065 | 3.621 | 13.78 | 0.276 | 4.36 |
| 7.440 | 11.693 | -27.92 | 6.957 | 30.75 |
| 13.576 | 14.545 | -127.70 | 21.456 | 180.00 |

Table II.9c Central display and motion, CM

| ω (rad/s) | $ H_p $ | Phase (degrees) | $\sigma H_p $ | σ , phase (degrees) |
|---------------------|---------|--------------------|----------------|-------------------------------|
| 0.153 | 4.208 | -13.11 | 2.460 | 30.31 |
| 0.230 | 4.327 | -21.03 | 2.312 | 28.12 |
| 0.383 | 4.466 | -21.42 | 3.464 | 37.80 |
| 0.537 | 4.657 | -13.08 | 1.752 | 20.62 |
| 0.997 | 3.089 | -7.94 | 0.936 | 16.85 |
| 1.457 | 2.954 | -0.60 | 0.551 | 10.57 |
| 2.378 | 3.124 | 12.37 | 0.438 | 7.99 |
| 4.065 | 4.458 | 21.21 | 0.438 | 5.62 |
| 7.440 | 8.929 | 11.68 | 1.684 | 10.68 |
| 13.576 | 38.009 | -58.98 | 44.629 | 180.00 |

Table II.9 Mean subject's frequency response $H_p(\omega)$ and the uncertainties for the display configurations of the disturbance task (continued).

Table II.9d Central and peripheral displays and motion, CPM

| ω (rad/s) | $ H_p $ | Phase (degrees) | $\sigma H_p $ | σ , phase (degrees) |
|---------------------|---------|--------------------|----------------|-------------------------------|
| 0.153 | 4.737 | -12.22 | 2.994 | 32.30 |
| 0.230 | 4.569 | -27.19 | 2.569 | 29.35 |
| 0.383 | 4.636 | -9.79 | 2.131 | 24.68 |
| 0.537 | 4.063 | -18.04 | 1.713 | 22.86 |
| 0.997 | 3.844 | -8.59 | 1.236 | 17.83 |
| 1.457 | 3.149 | -2.38 | 0.622 | 11.17 |
| 2.378 | 3.357 | 9.22 | 0.490 | 8.31 |
| 4.065 | 4.573 | 20.82 | 0.516 | 6.43 |
| 7.440 | 9.684 | 9.86 | 1.454 | 8.54 |
| 13.576 | 51.222 | -48.40 | 48.944 | 43.70 |

Table II.9e Peripheral displays, P

| ω (rad/s) | $ H_p $ | Phase (degrees) | $\sigma H_p $ | σ , phase (degrees) |
|---------------------|---------|--------------------|----------------|-------------------------------|
| 0.153 | 0.689 | -3.88 | 0.607 | 41.36 |
| 0.230 | 1.839 | -2.08 | 2.922 | 180.00 |
| 0.383 | 0.932 | 2.42 | 0.649 | 34.88 |
| 0.537 | 1.216 | 5.87 | 0.610 | 26.67 |
| 0.997 | 1.463 | 6.63 | 0.460 | 17.47 |
| 1.457 | 1.559 | 14.25 | 0.346 | 12.52 |
| 2.378 | 1.944 | 16.94 | 0.157 | 4.63 |
| 4.065 | 3.108 | 12.88 | 0.341 | 6.26 |
| 7.440 | 8.900 | -27.25 | 4.344 | 26.02 |
| 13.576 | 9.915 | -136.61 | 14.202 | 180.00 |

Table II.9f Motion, M

| ω (rad/s) | $ H_p $ | Phase (degrees) | $\sigma H_p $ | σ , phase (degrees) |
|---------------------|---------|--------------------|----------------|-------------------------------|
| 0.153 | 3.132 | 8.62 | 5.196 | 180.00 |
| 0.230 | 2.995 | 5.75 | 7.620 | 180.00 |
| 0.383 | 3.446 | -37.81 | 3.489 | 180.00 |
| 0.537 | 3.893 | -29.09 | 4.351 | 180.00 |
| 0.997 | 2.816 | -8.20 | 0.996 | 19.47 |
| 1.457 | 2.506 | -0.47 | 0.875 | 19.25 |
| 2.378 | 2.993 | 11.68 | 0.786 | 14.71 |
| 4.065 | 4.085 | 21.57 | 0.556 | 7.75 |
| 7.440 | 9.002 | 16.10 | 2.146 | 13.41 |
| 13.576 | 29.275 | -77.35 | 36.645 | 180.00 |

Table II.9. Mean subject's frequency response $H_p(\omega)$ and the uncertainties for the display configurations of the disturbance task (continued).

Table II.9g Peripheral displays and motion, PM

| ω (rad/s) | $ H_p $ | Phase (degrees) | $\sigma H_p $ | σ , phase (degrees) |
|---------------------|---------|--------------------|----------------|-------------------------------|
| 0.153 | 2.572 | -0.07 | 3.625 | 180.00 |
| 0.230 | 2.733 | -24.04 | 3.723 | 180.00 |
| 0.383 | 4.187 | -37.65 | 3.691 | 41.40 |
| 0.537 | 3.592 | -18.25 | 1.307 | 20.00 |
| 0.997 | 2.775 | -11.00 | 0.986 | 19.57 |
| 1.457 | 2.786 | 1.49 | 0.806 | 16.15 |
| 2.378 | 3.172 | 14.05 | 0.669 | 11.91 |
| 4.065 | 4.454 | 20.97 | 0.709 | 9.05 |
| 7.440 | 9.376 | 11.87 | 1.625 | 9.83 |
| 13.576 | 28.816 | -75.25 | 38.175 | 180.00 |

Table II.10 The crossover frequency and phase margin for the display configurations in the disturbance task and the target following task.

| Configuration | Crossover frequency (rad/sec) | phase margin (degrees) |
|-----------------------|-------------------------------------|---------------------------|
| Disturbance task | | |
| C | 3.235 | 16.4 |
| CP | 3.289 | 20.2 |
| CM | 4.754 | 21.5 |
| CPM | 5.033 | 20.9 |
| P | 3.025 | 17.4 |
| M | 3.886 | 21.8 |
| PM | 4.187 | 23.7 |
| Target following task | | |
| C | 2.18 | 18.7 |
| CP | 2.27 | 31.7 |
| CM | 1.86 | 74.4 |
| CPM | 1.49 | 85 |

SUMMARY

Around 1970, an important incentive was extending the application of flight simulation in flight-crew training. The motive stimulated research on the influence of motion feedback on pilot's control performance and behavior. To achieve the aim of zero flight hours type-conversion training, more flight simulation realism was required. This could be reached by the introduction of outside world displays and six degree of freedom motion systems. To reach that goal, a proper control of the motion system had to be developed. The purpose of this control is to transform the aircraft motions to simulator motions within the physical limitations of the motion system and without losing the specific effect of the motion cues to the pilot. A practical solution was found by applying 'washout filters' which were optimized by minimizing the differences between the modeled pilot's vestibular sensory outputs in real and simulated flight. Although reasonable results were obtained, it became clear that the vestibular sensory output alone was not sufficient to optimize simulator motion system control. The ultimate goal of visual and vestibular motion simulation is that a pilot's perception of aircraft motions in simulated flight are equal to those in a corresponding real flight. This can only be attained by optimizing the simulator motion system control under the condition that the perceived aircraft motions, based on the visual and vestibular cues in real and simulated flight, are equal. Such an optimization is only possible when the characteristics of the visual-vestibular motion perception process can be described in adequate details.

An engineering approach is to determine the changes in tracking performance and control behavior due to the addition of motion feedback. During the sixties and seventies, this approach was applied by several institutes which provided objective data. By fitting pilot models to the experimental data, the changes in characteristic model parameters due to the addition of motion feedback could be established. This valuable experimental work, however, did not provide the required detailed knowledge on the visual-vestibular interaction in pilot's motion perception. An extension of this research was necessary to establish the influence of the visual and vestibular motion feedback on a pilot's perception and control behavior.

Based on these considerations, it was decided to start an investigation on the contributions of the visual and the vestibular system to the perception process and the consequences for the pilot's control behavior. For this study a comparison of the specific characteristics of the visual and the vestibular system in motion perception was necessary. The tracking task was considered to be too complex to determine the differences between the visual and vestibular contribution to the perception process. As mentioned above, changes in a subject's frequency response due to motion feedback can be determined from measurements in tracking tasks. It is, however, difficult to distinguish the contributions of the individual senses to the perception process from the overall frequency response. Therefore, it was decided to evaluate the visual and vestibular perception of motion by using stimulus-response tasks with well-chosen

stimuli. An important question was, however, if the results obtained from stimulus-response tasks could be applied to the closed-loop control task.

Based on the literature about human information processing, the human operator has to be considered a single-channel information processor with limited capacity and input of multiple senses. If that model is correct, then there is no reason that it can not be applied to the closed-loop control task. Using this model, stimulus-response tasks with discrete stimuli were setup to investigate the contribution of the central or foveal visual and peripheral visual system on the perception of the aircraft attitude and angular rate. The results show that the perception of aircraft attitude from an artificial horizon is faster and more accurate than the perception of the aircraft angular rate from the artificial horizon or the peripheral visual field. Further, it was shown that the perceptions of angular rate with the central or foveal visual system and the peripheral system are different processes.

In addition to the experiments with the discrete stimuli, dynamic stimuli were applied to establish the differences between the speed and accuracy of motion perception with the visual and/or the vestibular system. From these experiments it was learned that perception accuracy is essentially independent from the senses stimulated but the reaction time is significantly decreased when the vestibular system is involved. Beside these stimulus-response experiments, a tracking task experiment was performed to obtain a data base on the influence of visual and/or vestibular motion feedback on a pilot's tracking performance and control behavior. The results of this experiment confirm those reported in the literature. The results show that both the visual system and the vestibular system have their own particular contribution to the pilot's control behavior.

The results of the stimulus-response experiments, together with the well-known characteristics of the visual and the vestibular system, provided the data to set up a descriptive multi-input single-channel information processor model. The validity of the descriptive model was evaluated with the frequency response data from tracking task data base. The model could be easily adjusted to the measured subject's frequency response from the tracking tasks by choosing a limited number of parameters.

The results of the present study contribute to an improved understanding of a pilot's motion perception and its influence on a pilot's control behavior. As already mentioned flight simulation is an important field of application for the results. The proposed descriptive model provides the opportunity to study the effects of the simulation time delays and the visual-vestibular mismatch on pilot's motion perception and control behavior. For each individual sensor, the visual and the vestibular system, the effect of the simulation process on pilot's control behavior and performance can be studied. Inversely, the descriptive model can be used to optimize the flight simulator motion system control.

SAMENVATTING

Een belangrijke aanleiding omstreeks 1970 voor het onderzoek naar de invloed van de vliegtuigbeweging op het stuurbedrag en de stuurprestatie van vliegers, was de behoefte om de toepassing van vliegtuigsimulatie ten behoeve van de training van vliegers uit te breiden. Om het beoogde doel, type-conversie training geheel met behulp van simulatie, te bereiken, was een verdere verbetering van de vliegtuig- simulatie noodzakelijk. Het realisme kon worden verbeterd door toepassing van zes graden van vrijheid bewegingssystemen en presentatie van de buitenwereld met behulp van displays. De belangrijkste reden voor het terugkoppelen van de vliegtuigbeweging, was het verbeteren van de trainingseffectiviteit. Om dat doel te bereiken, diende een correcte sturing van de simulatorbeweging te worden ontwikkeld. Het doel van deze sturing is de werkelijke vliegtuigbeweging te transformeren naar de simulatorbeweging binnen de limitaties van het bewegingssysteem en zonder het specifieke effect van de bewegingsstimulatie van de vlieger te verliezen. Een praktische oplossing werd gevonden door de toepassing van 'washout filters'. Deze filters werden geoptimaliseerd om het kleinst mogelijke verschil tussen het uitgangssignaal van het evenwichtsorgaan in de werkelijke en de overeenkomstige gesimuleerde vlucht te verkrijgen. Hoewel hiermee redelijke resultaten werden bereikt, werd het al snel duidelijk dat het uitgangssignaal van het evenwichtsorgaan alleen niet de juiste basis was voor het optimaliseren van de bewegingssturing van simulatoren. Het uiteindelijke doel van bewegingssimulatie is, dat de waarneming van de vliegtuig-beweging door de vlieger in de gesimuleerde vlucht gelijk is aan die in de werkelijke vlucht. Dit kan alleen worden bereikt, indien de bewegingssturing wordt geoptimaliseerd onder de voorwaarde dat de waargenomen vliegtuigbewegingen, gebaseerd op de visuele en de vestibulaire stimulatie, in de werkelijke en gesimuleerde vlucht gelijk zijn. Een dergelijke optimalisatie is alleen mogelijk, indien de karakteristieke eigen-schappen van het visueel-vestibulair waarnemingsproces voldoende gedetailleerd kunnen worden beschreven.

Een ingenieursaanpak om de kennis van de invloed van bewegingsterugkoppeling op het stuurbedrag van de vlieger uit te breiden, is de veranderingen, ten gevolge van bewegingsterugkoppeling, in het stuurbedrag en de stuurprestaties te bepalen. In de zestiger en zeventiger jaren zijn met deze methode, door een aantal onderzoeksinstellingen, objectieve gegevens verkregen. De veranderingen, ten gevolge van bewegings-terugkoppeling, van de karakteristieke vliegermodelparameters konden worden bepaald door deze modellen aan de gemeten beschrijvende functies aan te passen. Dit waardevolle experimentele onderzoek leverde echter geen gedetailleerde kennis over de visueel-vestibulaire interactie in de bewegingswaarneming op. Daarom was een voortzetting en uitbreiding van dit onderzoek nodig, om de invloed van visuele en vestibulaire bewegingsterugkoppeling op het waarnemings- en stuurbedrag van de vlieger vast te stellen.

Op basis van deze overwegingen werd besloten een onderzoek in te stellen naar de bijdrage van het visuele en het vestibulaire systeem aan het bewegingswaarnemingsproces en de gevolgen daarvan voor het stuurgedrag. Voor dit onderzoek was een vergelijking van de specifieke eigenschappen van het visuele en het vestibulaire systeem noodzakelijk. De stuurtaak werd te gecompliceerd bevonden om de bijdrage van het visuele en het vestibulaire systeem aan de bewegingswaarneming te bepalen. Daarom werd besloten om de visuele en vestibulaire waarneming van de beweging te evalueren met behulp van goed gekozen stimuli, in stimulus-response taken. Een belangrijke vraag daarbij was, of de resultaten van het stimulus-response onderzoek konden worden toegepast in de gesloten regelkring.

De mens kan, volgens de literatuur over de menselijke informatieverwerking, worden beschouwd als één-kanaals-informatieverwerker met meerdere sensorische ingangen en beperkte capaciteit. Indien dat model juist is, dan is er geen reden te veronderstellen dat dat model niet zou gelden voor stuurtaken in de gesloten regelkring. Gebaseerd op dit model, werden stimulus-response experimenten met discrete stimuli ontworpen, om de bijdrage van het centrale of foveale visuele en perifeer-visuele systeem tot de waarneming van de vliegtuigstand en standsverandering te onderzoeken. De resultaten lieten zien dat de waarneming van de vliegtuigstand, de rolhoek, aanzienlijk sneller en nauwkeuriger is dan die van de standsverandering, de rolsnelheid. Tevens bleek dat de waarneming van de standsverandering met het centraal visuele systeem en met het perifeer visuele systeem, verschillende processen zijn.

In aanvulling op de experimenten met discrete stimuli, werden dynamische bewegingsstimuli toegepast, om de verschillen tussen waarnemingssnelheid en nauwkeurigheid van het visuele en het vestibulaire systeem te onderzoeken. Deze experimenten leerden, dat de waarnemingsnauwkeurigheid onafhankelijk is van de gestimuleerde sensoren, maar dat de reactiesnelheid aanzienlijk afneemt indien het vestibulaire systeem bij de waarneming is betrokken. Naast deze stimulus-response experimenten, werd een stuurtaakexperiment uitgevoerd om een gegevensbestand over de invloed van de visuele en/of vestibulaire bewegingsterugkoppeling op het stuurgedrag en de stuurprestatie te verkrijgen. De resultaten van dit experiment kwamen overeen met die uit de literatuur en lieten zien dat zowel het visuele als het vestibulaire systeem ieder een specifieke invloed hebben op het stuurgedrag van de vlieger.

De resultaten van de stimulus-response experimenten, samen met de bekende eigenschappen van het visuele en het vestibulaire systeem, maakten het opzetten van een beschrijvend model mogelijk. Dit model werd geëvalueerd met behulp van de gemeten beschrijvende functies van het stuurtaakexperiment. Het model kon voor diverse taakvariabelen eenvoudig aan de beschrijvende functie worden aangepast door de keuze van een beperkt aantal weegfactoren.

De resultaten van deze studie dragen bij tot een beter begrip van de bewegingswaarneming door de vlieger en de invloed daarvan op zijn stuurgedrag. Een belangrijk toepassingsgebied van de verkregen kennis is vliegtuigsimulatie. Het voorgestelde beschrijvende model van de vlieger biedt de mogelijkheid de effecten van het simulatieproces op het stuurgedrag van de vlieger te evalueren. Voor iedere sensor in het visuele en het vestibulaire systeem kan de invloed van het simulatie- proces op het stuurgedrag van de vlieger worden onderzocht. Omgekeerd kan het beschrijvende model worden toegepast bij het optimaliseren van de sturing van het simulatorbewegingssysteem.

ACKNOWLEDGEMENTS

The research, reported in this thesis, was performed at the Faculty of Aerospace Engineering of the Delft University of Technology. The research was funded from the research budget of the Disciplinary Group for Stability and Control. Besides the funding, the support of many colleagues was indispensable and I would like to thank them for their help, in particular:

The technicians Henk Kluiters and Adri Tak and the pilot subjects Roel Kuil, Poppe de Lange and, Ruud Roggekamp. Adri Tak was always motivated for the maintenance of the analog computer, to search for electric noise sources, to solve problems with the simulator-motion system, and even to keep the 8-channel trace recorder operational. The subjects, for their motivation to train to a high level of performance and to maintain that performance throughout the experiments.

Steve Hulshof and the people of Editech for carefully reading the manuscript and their advice for the use of the English language.

My supervisors Professor Henk Stassen and Professor Fred Abbink for their positive attitude and support in writing this thesis.

CURRICULUM VITAE

Ruud Hosman was born in Utrecht, The Netherlands, on April 17, 1939. After secondary school, he attended the course for Aeronautical Engineering at the "Hogere Technische School" in Haarlem, from 1955 till 1959 and got his Bse-degree in Aeronautical Engineering. From 1959 till 1961 he fulfilled his military service as a technical officer in the Royal Netherlands Air Force. He started his study in Aeronautical Engineering at the Faculty of Aerospace Engineering at the Delft University of Technology in 1961 and obtained his MSc. degree in 1967, cum laude. During his study in Delft he followed the professional pilot training at the Governmental Pilot Training School at Groningen Airport from 1965 till 1966.

He joined the Disciplinary Group for Aircraft Stability and Control of the Faculty of Aerospace Engineering at the Delft University of Technology in 1965, the first two years as a student-assistant and after graduation in 1967 as a staff member. Initially he was involved with research on flight-test techniques. Since 1975, his research has been primarily directed to Man-Machine Systems in Aerospace. The main research topics have been: the influence of aircraft motions on a pilot's perception and control behavior, the measurement of the pilot's workload with subjective rating scales and physiological measurements, display formats for 2D and 3D presentations on the Electronic Flight Instrument System, EFIS, the influence of manipulator dynamic characteristics on pilot's control behavior, and the neuro-muscular dynamics of the pilot's arm. For the two last research topics, he developed an electro-hydraulic servo-controlled side stick as a research tool. In 1987 he became "Universitair Hoofddocent" (associate professor).

From September through December 1988 he was a visiting scientist at the Man-Vehicle Laboratory, Department of Aeronautics and Astronautics, Massachusetts Institute of Technology, Cambridge, MA.

From 1975 till 1993 he was part-time first officer on the Boeing 737-200 and 300 at Transavia Airlines.

He was a member of the Scientific Committee of the Faculty of Aerospace Engineering from 1983 till 1985, and the Faculty Council of the Faculty of Aerospace Engineering from 1985 till 1993.

He has been a member of the Sub-Committee for Flight Characteristics and Operations of the Scientific Committee of the National Aerospace Laboratory, NLR, Amsterdam since 1973.

From 1990 till 1993 he was directly involved with the specification, selection, and procurement of the joint National Aerospace Laboratory, NLR, and Delft University of Technology laboratory aircraft, a Cessna Citation II. He has been an active pilot on this aircraft since 1993.

He is presently involved with the development of flight-simulator motion-system control algorithms to optimize pilot's aircraft motion perception in simulation.